Leibniz-Institut
für
Oberflächenmodifizierung e. V.

BIENNIAL REPORT 2010/2011

Executive Board

Director:

Prof. Dr. Dr. h.c. Bernd Rauschenbach

Tel.: +49 341 235-2308 Fax.: +49 341 235-2313
E-mail: bernd.rauschenbach@iom-leipzig.de

Address

Permoserstrasse 15

D-04303 Leipzig (postal address)
D-04318 Leipzig (address for dispatch)

WWW

http://www.iom-leipzig.de

Members of the Board of Trustees

Freistaat Sachsen, Minister für Wissenschaft und Kunst
vertreten durch Frau ROR'in Cathrin Liebner

Bundesrepublik Deutschland, Bundesminister für Bildung und Forschung
vertreten durch Herrn MinR Dr. Herbert Zeisel

Verein des Leibniz-Instituts für Oberflächenmodifizierung e. V.
vertreten durch Prof. Dr. Rüdiger Szargan
Universität Leipzig, Wilhelm-Ostwald-Institut für Physikalische und Theoretische Chemie

Members of the Scientific Advisory Board

Dr.-Ing. Markus Roth (Chairman)
Osram GmbH, Business Unit UV/IR, Wipperfürth

Prof. Dr. Andre Anders
University of California and Lawrence Berkeley National Laboratory, Plasma Application Group, USA

Prof. Dr. Klaus-Dieter Asmus
Adam-Mickiewicz-University Poznan, Poland

Dr. K.-F. Beckstette
Carl-Zeiss Oberkochen

Dr. Kurt Dietliker
ETH Zürich and BASF Schweiz AG, Switzerland

Prof. Dr. Roger Gläser
Universität Leipzig, Fakultät für Chemie und Mineralogie

Prof. Dr. Marius Grundmann
Universität Leipzig, Fakultät für Physik und Geowissenschaften

Prof. Dr. A. Tünnermann
Institut für Angewandte Physik der Universität Jena und
Fraunhofer Institut für Angewandte Optik und Feinmechanik, Jena

Organisation of the Institute

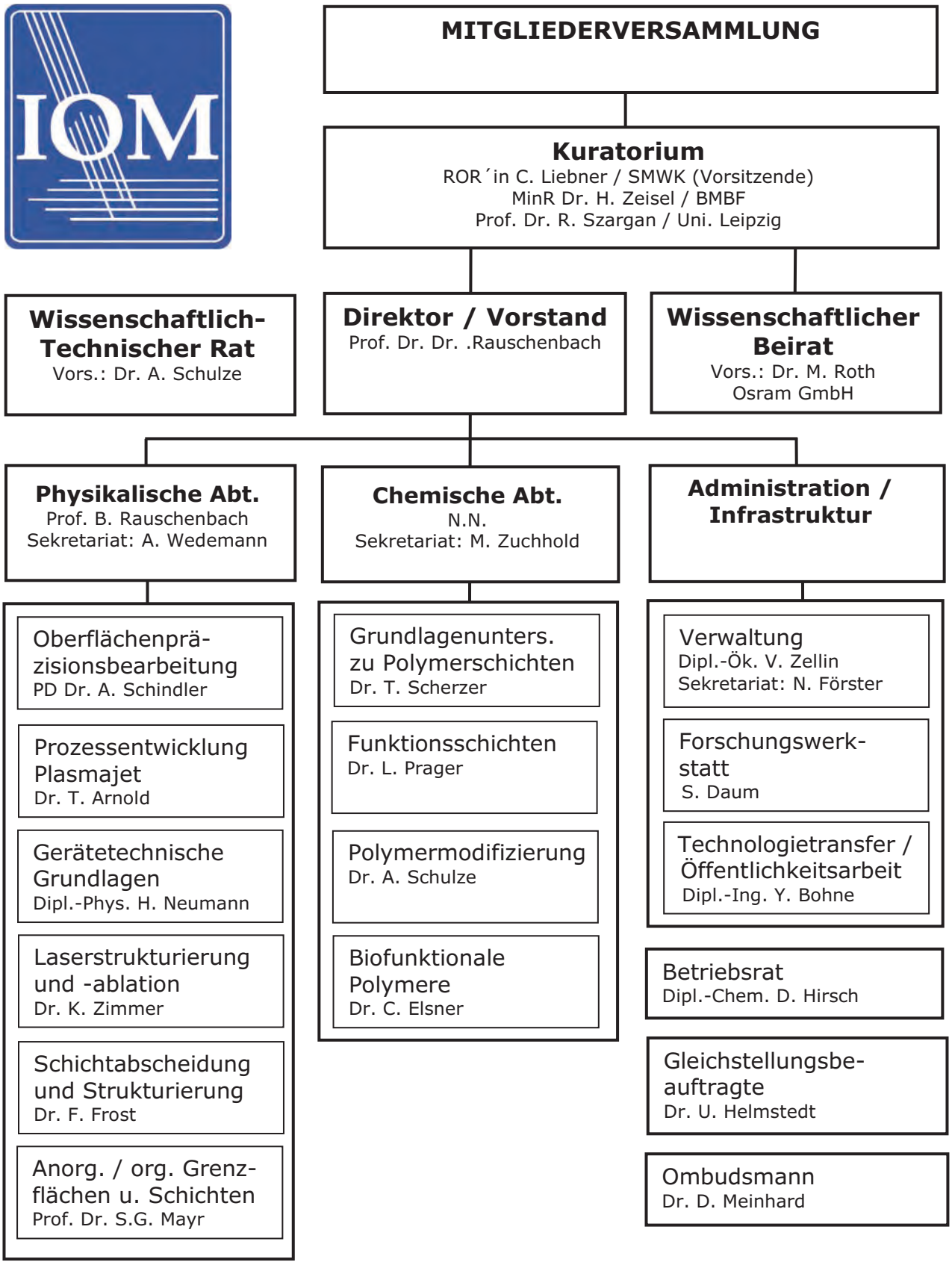

Contents

Preface

The Leibniz Institute of Surface Modification (IOM), a member of the Leibniz Association, combines basic research and application-oriented studies in the fields of surfaces and thin films modified by low-energy ion bombardment, laser and electron irradiation and plasma treatment.

Research and development areas of the Institute are

- Ion and plasma assisted ultra-precision shaping and smoothing
- Micro- and nanodimensional structuring and structure transfer
- Thin film deposition and nanostructures
- Fundamental principles of polymeric coatings
- Manufacture of functional coatings
- Functional nano- and microstructured systems

In its research, the IOM puts strong emphasis on collaborations with industry, small and medium enterprises, universities, and other research laboratories. The IOM also participates in joint projects directly funded by industry or Federal Agencies such as the BMBF or by the Free State of Saxony. Among extensive research other activities, the participation in DFG research units, the excellence competition and main focus programs should be mentioned. The successful cooperation with chemical, optical, and semiconductor industry was continued.

In this biennial report the IOM presents its scientific activities and major achievements in the years 2010 and 2011. In this context, the report presented here gives a comprehensive summary of our results. In the first part, overviews on selected projects are given, arranged according to the structure of the IOM research program. These overviews are supplemented by feature articles on selected topical highlights. Finally, the appendices give a full list of publications, talks, teaching activities, and other achievements of the IOM staff.

The Institute would like to thank all friends and organisations who supported its progress in the last two years. Special thank is due to our Board of Trustees and Scientific Advisory Board. Our partners from industry and other research institutes play an essential role for the IOM. The Board of the Institute would like to thank all members and guests of the institute for their active and excellent contributions to a successful development

Leipzig, January 2012

Prof. B. Rauschenbach

The institute aims with the audit at the creating sustainability of the existing offers and the development of further measures to the compatibility of career and family.
The offer presents a balance between official business and employee-interests.
They should strengthen the work-contentment and motivation of the co-workers with it as well as should make possible the development of their achievement potential.

The certificate to the audit "berufund-familie" was handed out over to Ms V. Zellin from the IOM in March 2011.

Every year the IOM Leipzig honours the best scientific and/or technological work with the research award and the best thesis with a doctorate award.

Institute awards in 2010
Dr. Thomas. Arnold (research award)
Dr. Rajendar Bandari (doctorate award)
Dr. Marisa Mäder (doctorate award)

Institute awards in 2011
Dr. Sergej Naumov (research award)
Dr. Johanna Lutz (doctorate award)

Scientific and Technology Results

Reports

Selected Results

Laser processing for CIGS thin film photovoltaics

K. Zimmer, M. Ehrhardt, A. Wehrmann, H. Schulte-Huxel

Introduction

High-efficient solar cell modules are the key for further development of photovoltaics as one component of the alternative energy generating system that must be competitive with conventional or other green energy sources. To qualify photovoltaic generators for these applications both the technical specifications as well as the economical requirements must be fulfilled. Currently a number of very different technical developments are encouraged to achieve this goal. Among them laser processing is one topic, whereby laser application in photovoltaics are ranging from laser scribing, laser drilling, and laser texturing to laser recrystallisation, local doping, and local contact formation.

Scaling-up issues of copper-indium-gallium-selenide ($Cu(In,Ga)Se_2$, CIGS) thin-film solar cell (TFSC) production and the reduction of production costs below $1/Wp are essential requirements for the future development of the entire fabrication process of CIGS modules. To this end, laser processing is a key technology to address this issues [1].

Thin-film solar modules

The electrical interconnection technique for the phovoltaic module is essential for the module fabrication separate solar cells as well as for integrated approaches. Traditionally, single, entirely processed solar cells are connected for module fabrication by making use of, e.g., metal ribbons or conductive adhesives. Furthermore, other interconnection methods known from rigid solar cell or electronics, such as soldering, welding, and wire bonding, are under investigation for flexible TFSC. However, the unique properties of the materials used for the CIGS solar cell stack as well as of the polyimide (PI) substrate prevent a simple adaption of these technologies to flexible TFSC. For instance, since the substrate of the CIGS TFSC is a non-conductive polyimide, conventional ways for interconnections, such as bonded stripes to the top and bottom (back-contact) of another cell are ruled out. Therefore, the choice of employed technolog for flexible CIGS TFSC is limited and specific interconnection techniques are mandatory.

Integrated interconnection techniques are beneficial for thin-film solar cells as a cost-effective approach but still challenging to achieve. Due to the different fabrication flow of monolithic integrated interconnection (MII) and external integrated interconnection (EII), see figure 1, as well as the different interconnection techniques, specific optimized laser scribing parameters and processes are required [2-6]. The alternative approach of increasing the effective area of solar modules can be realized by shingling of solar cells like for a roof [7].

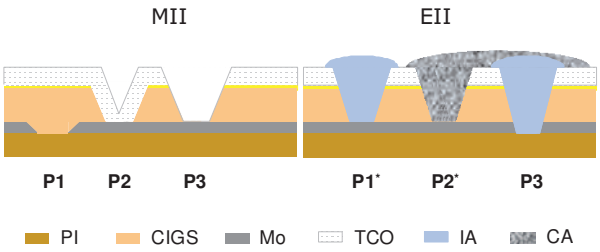

Figure 1: Sketches of monolithic integrated interconnection (MII) and external integrated interconnection (EII) with the scribes P1, P2, and P3. The asterisks denote the different stages for scribing within the fabrication process. At EII all scribing are done after thin film deposition. IA /CA: Insulating / conductive adhesive.

Laser for CIGS TFSC interconnection

Besides their high quality, the efficiency of flexible CIGS solar cells, which was recently reported by EMPA to be 18.7% [8] is much lower, on module level. On the other hand, the record of a monolithic integrated, flexible CIGS solar cell module is 15.9% with an aperture area of 75.7 cm² [2]. In contrast, this flexible module is made by mechanical scribing of P2 and P3 onto a thin (300 µm) ceramic substrate; hence the industrial challenge of CIGS TFSC on polyimide is not addressed.

Photolithography for patterning of CIGS TFSC works well [3] but cannot be employed for large area module fabrication [9]. Currently mechanical tools are still in use to scribe CIGS TFSC for module fabrication. Especially for selective scribing of thermal sensitive films, such as CIGS (P2) and the TCO film (P3), these technologies are useful due to the less damage of the TFSC. However, the process suffers from tool degradation and features limitations in the precision and speed of the process.

Different approaches for the development of laser scribing processes in CIGS solar module

fabrication by monolithic integrated interconnection are known. The scribing of the molybdenum film (P1) by laser is well accepted [2-4]. However, ns-Nd:YAG laser may produce cracks in the molybdenum that have to be avoided.

Since P2 is a connective scribe – according to Ref. [3] – it is not necessary to remove the CIGS completely. In consequence, a micro-weld process was developed, that enables the electrical interconnection by laser-induced modification of the CIGS. Therefore, a better quality interface especially near the front contact can be achieved by depositing the TCO film without CIGS scribing [4]. The fabrication of CIGS modules with a reasonable efficiency made by laser scribing has been reported [5, 9]. Within a close collaboration with industrial partners the most prospective approaches of laser utilization for the fabrication of CIGS thin-film solar modules were investigated.

Laser ablation for back side contacts

A suitable technique for solar module fabrication is the shingle technique that is also called roof-tile method [7]. For this approach single solar cells are arranged like a shingle roof cladding, in which the front and back contact, overlap and are connected with a conductive material. This approach is straightforwardly applicable for TFSC on conductive substrates such as copper or stainless steel foils. For CIGS TFSC on insulation polyimide substrates, that offer a number of benefits for application, the back contact needs to be exposed prior interconnection of the TFSC in the manner of shingles. The main benefit of the shingle technique, confirmed by the sketch in figure 2, is the large effective area of the module.

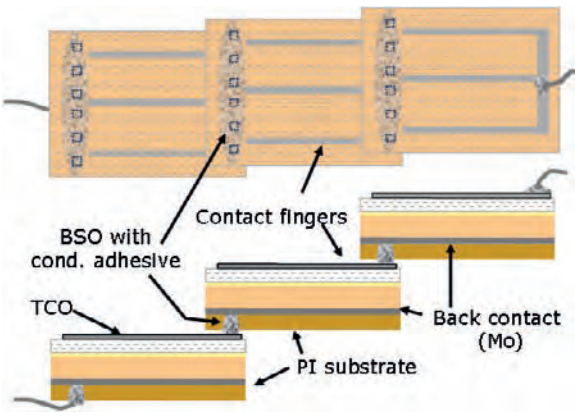

Figure 2: Schematically sketch of the shingle technique for CIGS TFSC on polyimide.

For the development of shingled solar cell modules a back side opening process (BSO) was developed that is based on the ablation of the polyimide substrate [10] with UV laser (λ =248 nm, tp = 20 ns). This BSO process suits the requirement of a gentle selective laser ablation of the polymer substrate and is characterized by: (i) the complete ablation of the polyimide substrate, (ii) an almost clean surface of the exposed metal film, and (iii) an undamaged CIGS TFSC. The basic approach of the developed laser process is to perform laser ablation in several steps with specific parameters that fit the needs to the process at different stages of the substrate ablation. This implies that not until high laser fluence (~ 800 mJ/cm²) is reached, the bulk of the PI substrate is ablated whereas near the interface the laser fluence is reduced to avoid thin-film damage due to melting or disruption.

The result of an exposed molybdenum back contact fabricated with an optimized BSO process is shown in figure 3. The size of a single exposed area is determined by the laser spot size; within the optimization of the BSO process exposed areas of up to 800 x 75 µm² were achieved.

For the fabrication of complete modules a conductive adhesive was applied to the exposed back contact to perform both the electrical interconnection as well as the mechanical joining of the serial interconnected solar cells. The contact resistance of such laser-exposed back side openings with a size of 0.1 x 0.1 mm² are slightly above the contact resistance of large-area contacts. This effect might be the result of the confinement of the conductive adhesive with the micrometer-sized silver flakes.

Shingled modules from 32 x 38 cm^2 CIGS thin film solar cells were fabricated using this

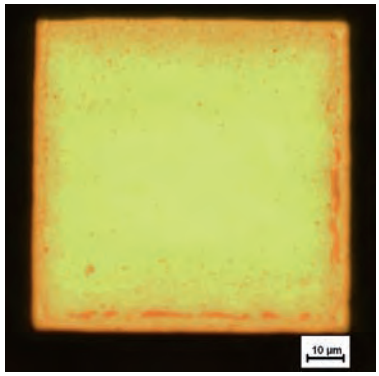

Figure 3: Optical micrograph of exposed molybdenum back contact fabricated with an optimized BSO process.

innovative BSO process. The measured V-C curve at a solar simulator proved the operability of all solar cells of the shingled CIGS solar module with a reasonable efficiency.

Laser scribing of CIGS for solar modules in a role-to-role process

The mechanical tools for scribing of CIGS TFSC provide evidence that laser scribing of such thin-film stacks is still challenging for the current laser technology. One reason is the demand on the functional evaluation of the laser scribing process in relation of laser parameters and the methodology for the optimization of the laser scribing in relation to the module performance. Thus, in addition to geometrically demands, such as scribing width etc., the electrical characteristic of the thin solar films, including shunts and contact resistance, are of fundamentl relevance for the solar module characteristics.

The requirements on the laser scribing process for external integrated interconnections are even more challenging compared to the scribing process for the integrated monolithic interconnection as the damage of the TFSC must be avoided for all scribes from P1* to P3.

Quasi in situ I-V measurements of CIGS TFSC

An experimental set-up shown in figure 4 was developed enabling quasi in situ measurements at laser scribing. This allows the collection of reliable and quick information on the changes of the solar cell characteristics by the laser scribes. Together with the capabilities of the laser scribing workstation now the scribe geometry, the optical image of the scribe as well as the electronic properties extracted from the I-V curves can be evaluated quasi in situ for the assessment of the laser – thin film interactions as well as for the laser scribe optimization of TFSC.

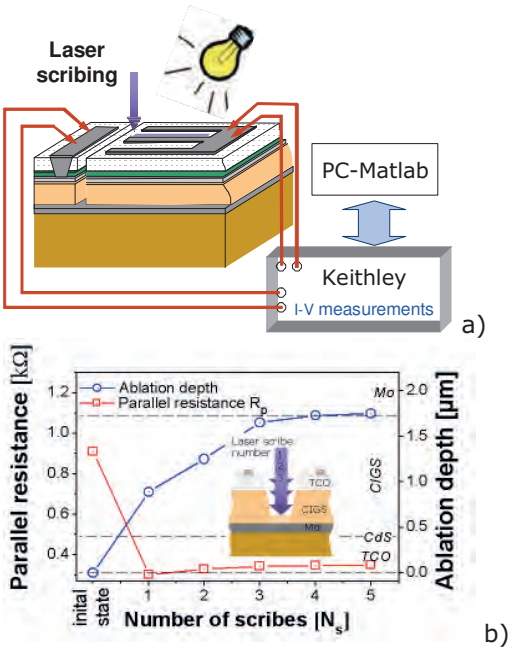

Figure 4: Quasi in situ measurements of CIGS TFSC for the optimization of the scribing process with ultrashort pulse laser (tp ~ 150 fs). a) Experimental set-up, b) Parallel resistance during sequential laser scribing with a laser fluence of 0.786 J/cm² and a pulse overlap of 77%.

The sequential scribing of CIGS TFSC with ultrashort laser pulses (λ = 775 nm, t_p = 150 fs) cause a sudden drop of the parallel resistance due to shunt formation as shown in figure 4 b). Surprisingly this happens during the first scribe that results in a laser ablation depth of nearly one micron but does not remove the CIGS completely. However, further scribes do not change the Rp substantially because the observable Rp rise is caused by the recovery of the laser damaged cell areas of the first scribe.

Images of the edges from the laser scribes by optical microscopy and SEM show differences in the noticeable modifications: The modified region outside the molten CIGS is only observable in the optical image (see figure 5) whereas in the SEM the TCO film seems to be intact.

I-V characteristics together with the optically visible damage at laser fluences below the ablation threshold suggest that the defect mechanism is probably due to the destruction of the pn junction at the CIGS/TCO interface [11]. This damage mechanism can be understood in the following manner: Due to the Gaussian intensity distribution of the laser focus and the found laser damage threshold fluences – for 775 nm 150 fs laser pulses intensities of 0.55 J/cm² and 0.25 J/cm² are measured for TCO and CIGS, respectively – the energy density at the shoulder of the laser spot is below the ablation threshold of the TCO but above the

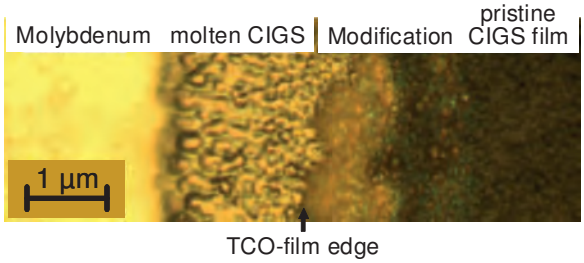

Figure 5: Optical micrograph of the edge region from a laser scribe with the characteristic features.

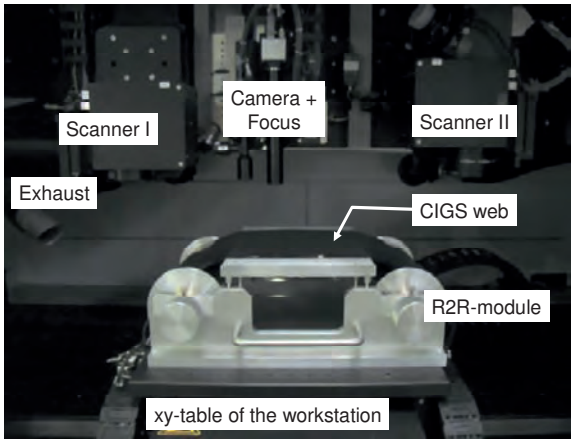

Figure 6: Optical image of the R2R tool mounted onto the laser workstation's stages.

damage threshold of the strong absorbing CIGS and CdS films. Hence, the damage of the interface without ablation of the TCO can be explained.

CIGS modules in a role-to-role process

With the aim to establish a consistent role-to-role (R2R) process for the demonstration of external integrated interconnections of CIGS TFSC on polyimide for module fabrication, a manual R2R module for laser scribing has been developed. This R2R module mounted into the picosecond laser workstation and used for laser scribing is shown in figure 6. Due to the incorporation of the module in the laser workstation the full functionality including image reorganization, laser processing, and autofocus is available. These features can be combined to a fully automated process flow enabling a full CNC control of laser scribing of CIGS thin solar stack material for the fabrication of P1*, P2*, and P3 scribes with different processing parameters. A relative precision and an overlay accuracy to external markers of better than 5 µm and 10 µm has been measured within the R2R module area of 20 x 20 cm², respectively.

The compete EII process for CIGS module fabrication comprises (i) the deposition of the complete stack of CIGS SC material, (ii) the performing of the laser scribing with ultrashort laser pulses, and (iii) the external integrated interconnection by screen printing of a silver-containing conductive adhesive. The benefits of this technology are the separation of the thin-film deposition and the laser scribing, whereby both the thin-film deposition and the laser scribing can be optimised without interference, the less demands on the scribing procedure concerning the requested accuracy, and the opportunity of utilization the same process for

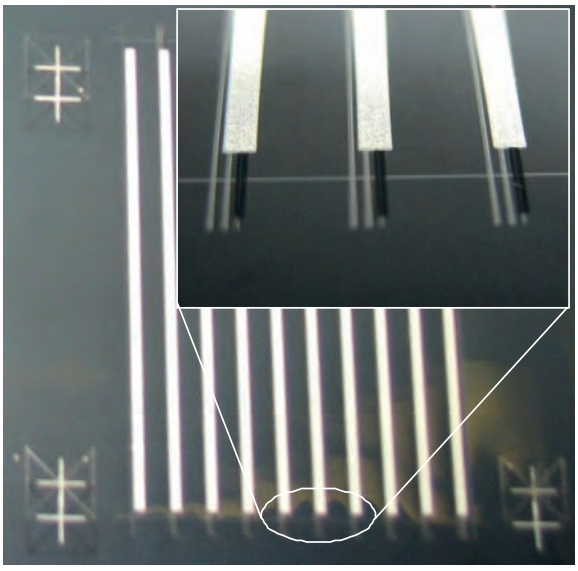

Figure 7: Images of a CIGS module made by EII using the R2R laser scribing process.

CIGS thin-film deposition as used for CIGS solar cell fabrication.

Laser-scribed CIGS thin-film modules, seen in figure 7, with output voltages of ~ 4.5 V and an efficiency of approx. 10% were fabricated. The rather extended interconnection area is due to the limited precision of the screen printing and holds the potential for further increase of the module efficiency in the future.

The results of this work are based on a collaboration with Ch. Scheit and A. Brau (Solarion AG, Leipzig).

Literature

[1] N. G. Dhere, Solar Energy Materials and Solar Cells 95 (2011) 277.
[2] Shogo Ishizuka et al., Solar Energy Materials and Solar Cells 94 (2010) 2052.
[3] F. Kessler, D. Herrmann, M. Powalla, Thin Solid Films 480 (2005) 491.
[4] P. O. Westin, U. Zimmermann, et al., Solar Energy Materials and Solar Cells 95 (2011) 1062.
[5] S. Wiedeman et al., presented at the Photovoltaic Specialists Conference, 2002. Conference Record of the Twenty-Ninth IEEE, 2002.
[6] Sae Chae Jeoung et al., Opt. Express 19 (2011) 16730.
[7] M. Winkler et al., Thin Solid Films 387 (2001) 86.
[8] Ayodhya N. Tiwari, http://www.empa.ch/plugin/template/empa/*/79159 (2011).
[9] Johan Wennerberg, PhD Thesis, Uppsala University, 2002.
[10] K. Zimmer et al., Appl. Surf. Sci. 255 (2009) 9869.
[11] A. Wehrmann, H. Schulte-Huxel, M. Ehrhardt, et al., in Proc. of SPIE 7921 (2011) 79210T.

Atomic particle beam techniques - progress in ultra-precision surface finishing

A. Schindler, F. Pietag, A. Nickel, H. Paetzelt, T. Arnold, G. Böhm, T. Hänsel

Introduction

In last two years in ultra-precision surface machining IOM focused on techniques to solve deterministic correction of mid spatial frequency roughness (MSFR) surface figure errors using both methods - ion beam figuring and atmospheric plasma jet machining (APJM). Amplitudes of those surface errors are in the sub-10 nm peak to valley (PV) range. Besides a reduction of the Gaussian shape tool size down to 500 µm full width of half maximum (FWHM) of the ion beam and the plasma jet the beam and jet powers had also to be adjusted accordingly to provide for the necessarily high long term stability of the respective removal functions. Other problems in such high spatial resolution deterministic surface shape correction arise from the alignment of the tool and the workpiece together with the measured error topology of it. The alignment accuracy has to be below 10 µm in x and y. Especially for large workpieces thermal expansion duo to the tool power will be a problem. With the low power pulsed microwave cold plasma jet with jet temperatures as low as 30°C developed for such dedicated surface processing including for thermal sensitive materials it was possible to start research in the new field of plasma medicine for dentistry application.

Ion Beam Figuring (IBF)

Ion beam figuring (IBF) for ultra precision surface finishing is well established in high end optics fabrication for lithography, space and beam-line optics and advanced optical instruments, respectively [1, 2]. IBF standard technology uses a constant and stable ion beam that moves computer controlled across the entire optic via a meander like scanning with variable scan line velocity according to the local dwell time necessary for the specified removal of material at the certain place. The beam tool size has to be adjusted according to the spatial surface error size processing. One serious disadvantage of this method is the continuous and constant beam and the limitations in maximum speed and acceleration/deceleration of the mechanical multi axes motion system. This causes wasting of material removal at least in that part of the surface where no material should be removed (absolute minimum of the surface figure). Further additional surface error can be arise in cases of steep gradients and small surface feature sizes of the surface topology where the beam can not follow the very small dwell times due to the limitations of the dynamics of the motion system.

The new solution uses a pulsed ion beam instead of a direct current (dc) one combined

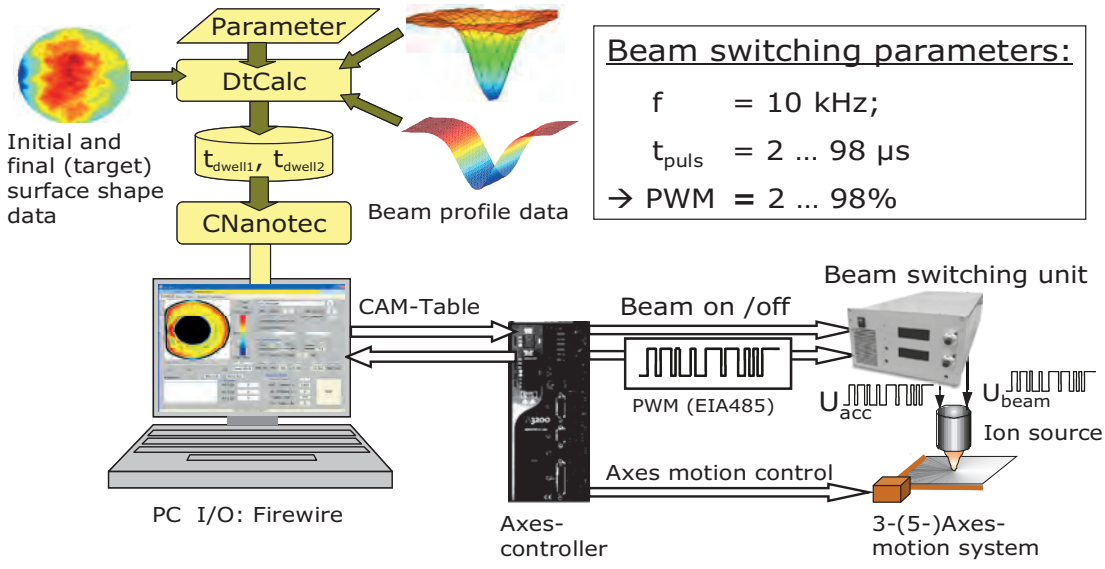

Figure 1: Scheme of the motion synchronized PWM ion beam controlled ion beam figuring technique.

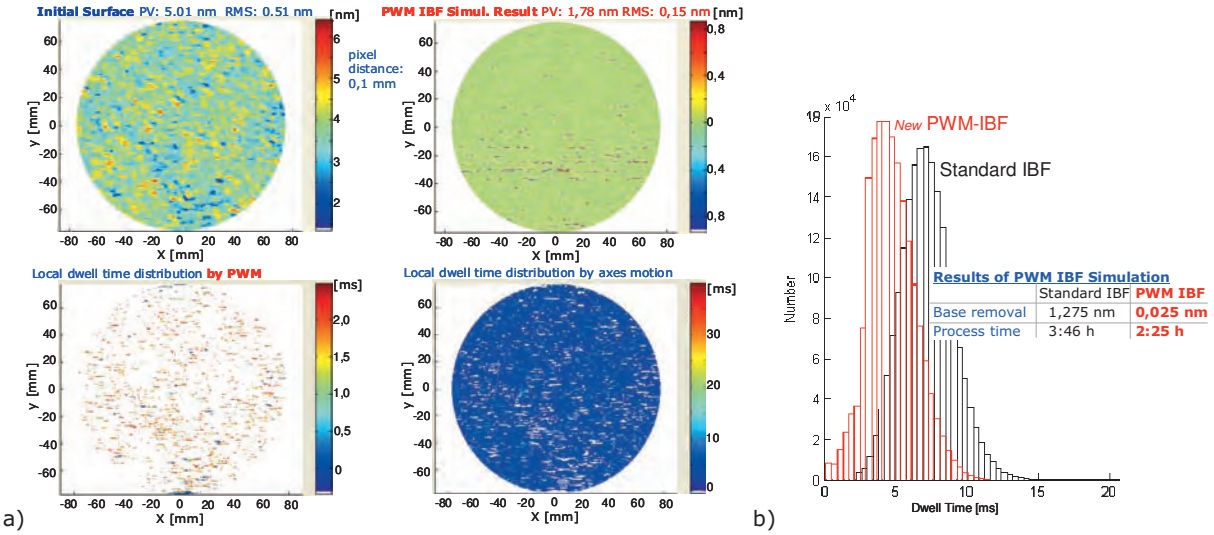

Figure 2: a) Upper row: IBF simulation of a ∅160 mm lens with MSFR sub-nm error features using new PWM technique, left: interferogram before IBF, right: residual error map as a result of the IBF simulation, bottom row: calculated local dwell time distributions of the PWM action only (left) and of the axes velocity (right); b) histograms of the calculated dwell times for the standard IBF with dc beam (black) and new PWM ion beam IBF (red).

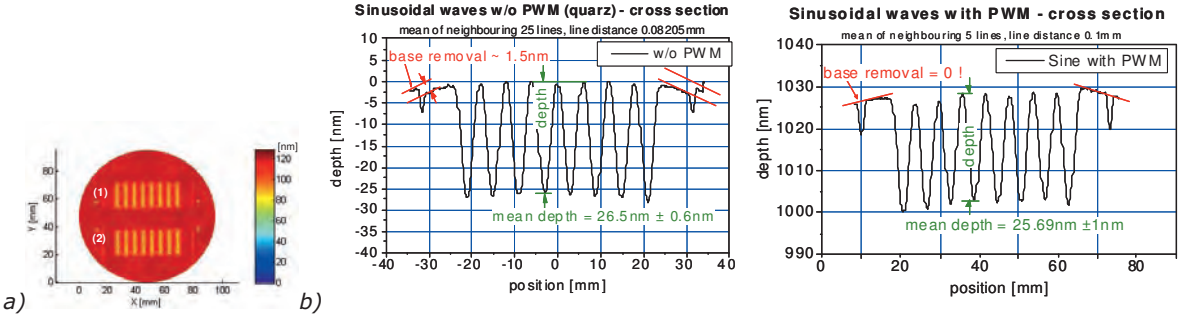

Figure 3: a) Interferogram of sinusoidal structures etched by standard IBF (1) and PWM IBF (2) into a quartz plate; b) cuts of both profiles from a), showing the strong reduction of the base removal in PWM case.

with pulse width modulation (PWM) for variation of the mean beam power. PWM signal is controlled by the motion control of the multi-axes system that moves the ion beam (source) across the surface to be figured extend the limited dwell time scale by the mechanical motion system by two orders of magnitude to lower values. Fig. 1 shows the scheme of the new technique. New IBF processing software ("DtCalc") has been developed using two dwell times instead of one as before. The first is the very same as for the standard IBF technique where the velocity of the motion system is controlled and the second is the additional new one which controls the PWM of the ion beam as follows. For calculated dwell times lower than an adjustable minimum dwell time value (dependent on the maximum speed of the mechanical motion system) the motion system moves further with a constant velocity corresponding to this value and automatically at the very same time the PWM control starts to lower the average beam power that takes effect to reduce the dwell time further. Thus the PWM beam control allows extend the dwell time range by two orders of magnitude. Two hardware components have been added to a standard IBF facility, (i) an intelligent axis controller with a fast processor unit and a fast data transfer for controlling of the standard axes of the motion system and the virtual "PWM axis" and (ii) a beam switching unit for the pulse powering of the beam and accelerator voltages of the RF (13.56 MHz) ion source.

Fig. 2 shows results of the simulation for the new ion beam figuring PWM technique of a lens surface dominated by MSFR error characteristics with effect of strong reduction of the base removal and the processing time compared to the state of the art IBF. Fig. 3 shows experimental test results of IBF processing of sine-like nanostructures in SiO_2 thin film by the standard and by the new PWM techniques, respectively.

A new IBF PWM technique has been demonstrated with main advantages of strong reductions of the wasting „base removal" and of the

IBF processing time, respectively further lowering the wear of the axes system and enabling precision figuring of separate areas of surfaces.

Atmospheric Plasma Jet Machining

Atmospheric Plasma Jet Machining (APJM) with reactive gas components has a great technological potential for the ultra-precision modification and figuring of optical surfaces. High rate and sub-surface damage free processing are the main advantages of the method. Figuring with sub-mm lateral resolution and sub-nm depth accuracy has been achieved for different optical materials using fine focused atmospheric plasma jets with sub-millimeter FWHM tool size. As an example, results for fused silica are shown.

Two microwave (2.45 GHz) powered atmospheric plasma jet sources have been developed to perform APJM of silicon based optical materials [3, 4]. System I operates in dc-mode up to 600 W while system II is in a pulsed mode with an adjustable average output power of 3 to 10 W. Ar/He-plasma is used for both systems with NF_3, SF_6 or CF_4 as fluorine containing reactive gas and O_2/N_2 as additional gases. Typical total flow is less than 10 slm for system I and less than 5 slm for system II. Both systems were optimized to achieve a rotationally symmetric removal function with a near Gaussian shape (FWHM size of ~0.7 mm) and material removal rates of 0.001 to 0.003 mm^3min^{-1} for fused silica. System II operates in contact mode with the plasma jet touching the surface (Fig. 4) while system I uses the reactive plasma species of the plasma jet afterglow for the etching process. We used both systems mounted on 5-axes CNC machines allowing the treatment of large work pieces with sizes of up to 500 mm in diameter. Deterministic surface shaping is performed by the same dwell time algorithm and processing software as for standard IBF described above. Details on dwell time calculation based on MATLAB©-programs can be found in [1]. Most important

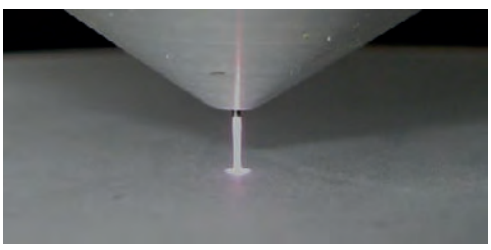

Figure 4: Pulsed microwave (2.45 GHz) powered APJM (system II) during fine correction.

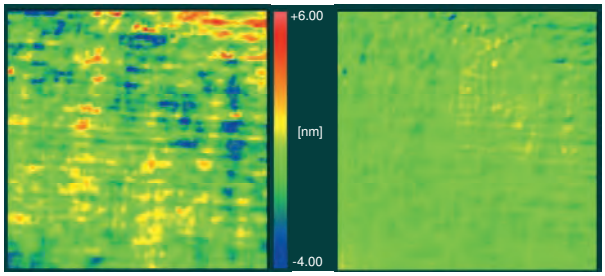

Figure 5: Sub-mm spatial surface error correction of a 160 mm ∅ SiO_2 lens by APJM. Surface error maps of 200 x 200 pixel (pixel size 150 µm x 150 µm) are shown: before APJM PV 9.13 nm, RMS 1.09 nm (left); after APJM PV 5.23 nm and RMS 0.39 nm (right).

preconditions for ultra precision large area figuring are (i) a very long term stable plasma jet removal function and (ii) a most accurate APJM process simulation calculation for determining the dwell time distribution. The first one was achieved by optimization of the process parameter sets and the source configurations, the second by extended measurements of the tool working function by etching of foot-prints, line profiles and meander-like scanned areas. APJM tests of samples (up to 150 mm ∅) with both systems showed substantial reduction of the mid spatial figure errors by 50% and more. Fig. 5 shows the interferograms of a 30 x 30 mm part of a fused silica lens before and after APJM using system II. Average scan velocity was 6 mms^{-1}, scan line distance 150 µm and the processing time 17 min.

For the first time we have demonstrated APJM deterministic fine correction of nanometric mid spatial frequency surface figure errors for optical finishing technology. Since there are almost no geometric restrictions for the contactless plasma jet tool there exist nearly no limits for the optical surface correction and design. This opens a very interesting and powerful new technology.

The results of this work are based in collaboration with K. Nomura, Nikon Corp. Sagamihara, Japan and M. Weiser, N. Kaier, Carl Zeiss SMT GmbH Oberkochen, Germany.

Literature

[1] T. Hänsel, F. Frost, A. Nickel, A. Schindler, Vakuum in Forschung und Praxis, 19 (2007), 24-30.
[2] M. Weiser, Nucl. Instr. Meth. B, 267 (2009), 1390-1393.
[3] T. Arnold, G. Boehm, I. Eichentopf, M. Janietz, J. Meister, A. Schindler, Vakuum in Forschung und Praxis, 22/4 (2010), 10-16.
[4] T. Arnold, G. Böhm, R. Fechner, J. Meister, A. Nickel, F. Frost, T. Hänsel, and A. Schindler, A., Nucl. Instr. Meth. A, 616 (2010), 147-156.

Ion beam assisted synthesis and characterization of ferromagnetic shape memory alloys for medical applications

Y. Ma, A. Arabi-Hashemi, A. Graumann, A.M. Jakob, I. Claussen, T. Edler, S.G. Mayr

Introduction

Ferromagnetic shape memory alloys (FSMA) are very promising materials for various kinds of future applications. Compared to conventional shape memory alloys, FSMAs are fast switchable by a moderate external magnetic field at constant temperature. Such as in Ni-Mn-Ga systems [1], as shown in Fig. 1, high strains due to easy moveable martensitic twin variants (Fig. 1b) can be induced via magneto elastic coupling [2]. So far, the maximum strain values up to 10% have been reported for Ni_2MnGa single crystals [3], while the maximum strain of 5% can be yielded in $Fe_{70}Pd_{30}$ single crystals [4]. However, $Fe_{70}Pd_{30}$ has better mechanical properties as it is more ductile after martensitic transformation and does not tend to fracture formation [5].

Superior straining characteristics at applied external magnetic fields enable a high potential for applications such as actuators, sensors, valves and switches. Especially thin film FSMA are highly promising for developing miniaturized low power switching devices applicable in micro mechanics and medicine. This requires more detailed knowledge of their mechanical properties – especially at the micro and nano scale. Previous investigations, however, only focused on determining mechanical characteristics of large bulk samples. Measuring techniques utilized for this purpose are not suitable for our requirements. By means of contact resonance atomic force microscopy (CR-AFM), one can overcome this lack in order to get a deeper understanding in nano mechanical processes behind the FSM effect.

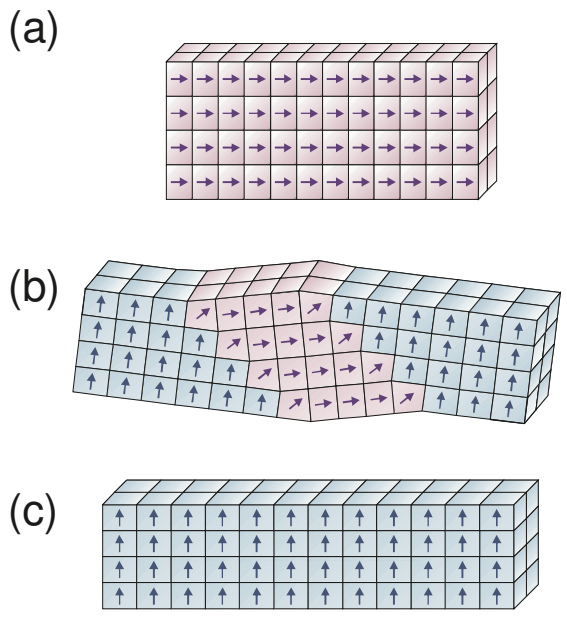

Figure 1: Scheme of shape changing process at different stages for Ni-Mn-Ga ((a) → (b) → (c) and vice versa). An external magnetic field induces reorientation of twin variants due to aligning magnetic moments.

Additionally, to gain more information on phase transition conditions of $Fe_{70}Pd_{30}$, superconducting quantum interference device (SQUID) as well as temperature dependent X-ray diffraction (XRD) measurements were performed.

External controllability at constant temperatures and sufficiently high strains makes ferromagnetic shape memory alloys also excellent candidates for biomedical actuation, such as surgical implant material. However the biocompatibility and *in vivo* behaviour of this material must be well confirmed before it can be safely used as an implant material. Ni_2MnGa is not a suitable material for such kind of applications due to its nickel content which is poisonous at higher concentrations. For $Fe_{70}Pd_{30}$ biocompatibility pro-perties have been examined with *in vitro* assessments in cooperation with the Soft Matter Physics Division (Physik der weichen Materie) of the University Leipzig [6].

Experimental

Iron-Palladium thin films are synthesized by physical vapour deposition by means of electron beam evaporators in optional presence of energetic ion beams. Utilizing two separately rate controlled evaporation sources for Fe and Pd allows a very precise adjustment of the film composition of At-% Fe 70 and At-% Pd 30 (Fig. 2).

High crystalline quality is achieved while hetero epitaxial growth of $Fe_{70}Pd_{30}$ on MgO (100) substrates is carried out under ultra high vacuum (UHV) conditions with a base pressure of less than 10^{-9} mbar. In addition, the substrate is kept at 850 °C to provide good diffusivity of the deposited atoms on the surface, which is also enhance by bombardment with energetic

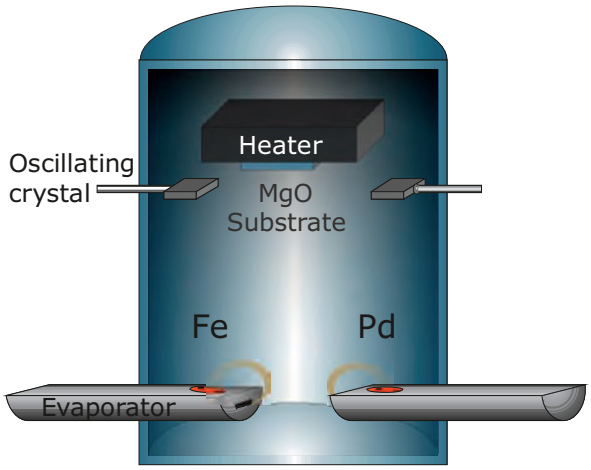

Fig. 2: Schematic of the evaporation chamber.

ions. Thin film single crystallinity is confirmed by high resolution transmission electron microscopy (TEM, Fig. 3) [7, 8] and pole figure measurements published in previous literature [9, 10].

Fe and Pd are deposited with a total deposition rate of around 1,5 A/s. Typically 500 nm thickness films are prepared.

That $Fe_{70}Pd_{30}$ is not stable at room temperature is an additional reason for deposition at high temperature. Using a liquid nitrogen shield supports on the one hand the ion getter pumps and on the other hand it ensures a quick cooling down after epitaxial thin film growth. Therefore, $Fe_{70}Pd_{30}$ films reach a metastable state at room temperature without decomposing into its stable phases alpha-Fe and $Fe_{50}Pd_{50}$ [11].

In order to eliminate the substrate constraints in functionalization and application purposes, these films must be lifted off from the MgO substrate.

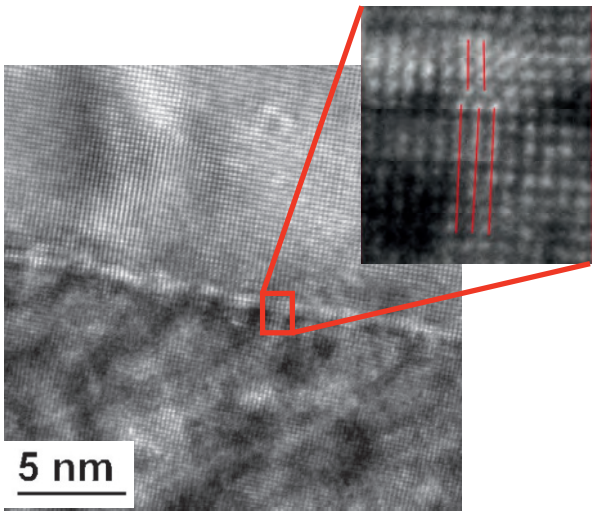

Figure 3: TEM characterization of the MgO/ Fe-Pd interface.

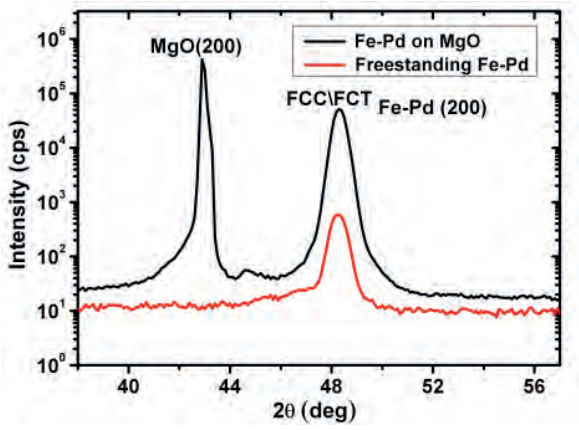

Fig. 4: XRD spectra before and after lift-off.

Our results show, freestanding thin films can be readily prepared by chemically dissolving the MgO with a $NaHCO_3$ solution. Meanwhile, the crystal structure, phase and composition are kept intact after lift off which is confirmed by EDX and XRD measurements (Fig. 4). An alternative lift off method is etching the MgO substrate using an EDTA solution [9].

Ni_2MnGa thin films were epitaxially grown by DC-magnetron-sputtering of a pre-alloyed target. The base pressure is below 10^{-6} mbar while during the process pressure is kept at 10^{-3} mbar with flowing Argon. The MgO substrate is held at 600°C during deposition. After 35 min of sputtering at a mean power of 50W the substrate heater is switched off. An approximately 400 nm thick thin film is obtained which has the orthorhombic 7M phase after subsequently cooldown.

Mechanical properties of Ni-Mn-Ga thin films

CR-AFM measurements were performed on Ni-Mn-Ga samples to gain information on indentation modulus *M* at the nano scale. Compared to theoretical predictions based on Density Functional Theory (DFT) calculations, experimentally observed values are significantly reduced, indicating movement of twin variants (see Fig. 1) due to stresses applied by the scanning probe. This behaviour could be accompanied by intermartensitic phase transitions. Further investigations are necessary to get a deeper understanding. Moreover, mechanical contrast imaging revealed variations of *M* up to 10% near boundaries between twin variants. We therefore suggest that movement of existing twin variants during straining is preferred over generating boundaries within single twin variants.

Magnetic properties of Fe-Pd

Attempts to investigate the phase transformation temperature in substrate-attached and freestanding Fe-Pd thin films were successful with temperature dependent magnetization measurements (200 K to 400 K; temperature sweep rate approx. 2 K/min). By collaboration with Prof. Esquinazi from the Division of Superconductivity and Magnetism of the Faculty of Physics and Earth Sciences of the University of Leipzig, these measurements were performed by a SQUID magnetometer MPMS-7 from Quantum Design in presence of an in-plane external magnetic field.

Fig. 5 shows the absolute and relative (normalized to 200 K) temperature dependent magnetization of martensitic Fe-Pd films attached on substrate measured in a magnetic field of 300 Oe; arrows mark the direction of temperature variation. It is clearly visible that magnetization almost reversibly increases as a function of temperature up to ≈326 K, while following a Curie-Weiss behavior We interpret this reversible phase transformation in terms of the favorable martensite variants. As the easy axis of magnetization is established to coincide with the longer a axis in Fe-Pd system [12], shape anisotropy of the film enforces in plane magnetization. Furthermore, the external magnetic field is too weak to enforce reorientation, only half of the variants will have their magnetization directed parallel to the applied magnetic field deep in the martensite state. This behavior changes dramatically during the martensite -> austenite transition, where both variants equivalently become cubic with one of their three easy axes (and thus magnetization) directed along the externally applied field. While magnetic domain structure changes favoring alignment of magnetization along the external field, this is reflected by an increasing magnetization. From the location of maximum magnetizations, which reveal a slight hysteresis, the martensite start temperature (Ms) and austenite finish temperature (Af) are determined by the tangential method to be 324 K and 326 K, respectively. Consequently, the phase transformation temperature is confirmed by XRD (T) and SQUID independently to occur at about 326 K for the martensitic Fe-Pd thin films attached on MgO substrates.

Additionally, the same procedure of temperature dependent magnetization measurements has been performed on austenitic and martensitic freestanding Fe-Pd thin films. The martensite

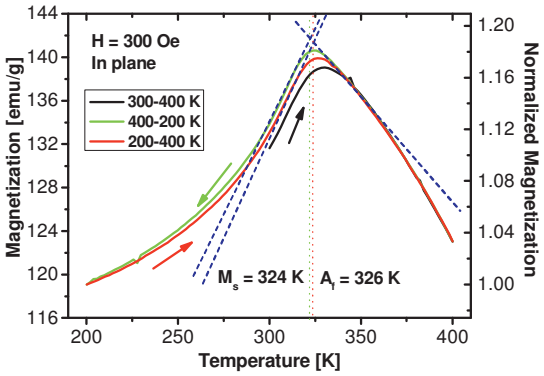

Fig. 5: Temperature dependent magnetization measurements on martensitic Fe-Pd film on MgO (100) substrate.

variants selection is observed from the M(T) curves measured at a magnetic field of only some tens of Oe. These findings pave the way for application of Fe-Pd based membranes in miniaturized devices.

Biocompatibility

At the present state our work focused on *in vitro* biocompatibility assessments of single crystalline $Fe_{70}Pd_{30}$ FSMA films grown on MgO (100) single crystal substrates. As the first step, a simulated body fluid (SBF) approach to mimic the nominal ion concentrations in human blood plasma, as proposed by Kokubo and Takadama [13], was employed at the IOM. The SEM images of the morphological changes on the surface of Fe-Pd films during SBF test showed that bonelike apatites with granular microstructure formed after soaking in SBF, these findings clearly indicate, that $Fe_{70}Pd_{30}$ film can, in fact, induce materials aggregation from the SBF on its surface, which is very important for bone-bonding between the live tissues and implants. Moreover, the Ca/P ratio of 1.32 was determined from the EDX spectra. Fe and Pd concentrations within SBF before and after specimen removal were measured with inductively coupled plasma optical emission spectroscopy (ICP-OES). The results indicate that Fe concentration increased, while the concentration of Pd did not change during the test.

As the second step, viability cell tests were performed to investigate the interactions of NIH 3T3 embryonic mouse fibroblast cells with the sample material. This work was conducted by Dr. Zink from the Soft Matter Physics Division of the University of Leipzig.

Fig. 6 presents the optical morphological features of NIH 3T3 cells after 65 h growing on a 500 nm $Fe_{70}Pd_{30}$ film and staining with calcein acetoxymethylester (AM) and propidium

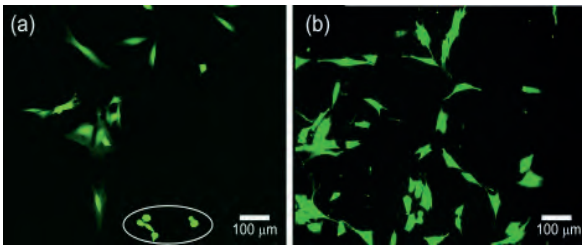

Figure 6: Optical morphological features of green fluorescent mouse fibroblast cells from calcein staining on the 500 nm FePd film (a) and plastic culture dish(b). Cells in the white circle had a red fluorescent core from PI which signal is too weak to overshine the calcein fluorescence.

iodide (PI). It turned out that cells adhered and proliferated on the surface of the film, some samples exhibited a lower cell density compared to the cells on the surface of the surrounding culture dish. Additionally, cells on the film were slightly smaller than cells on the culture dish. It turned out that after staining with calcein AM and PI, cells on the film surface fluoresced in green. Only a few red cell cores were determined, whereas these cells also exhibited a strong green calcein signal and adhered to the film surface. This behavior indicates that these cells were not apoptotic but pathologically transformed. In contrast, only viable cells fluorescing in green were obtained in the surrounding culture dish without any red fluorescing cores.

Anyway, these results suggested that $Fe_{70}Pd_{30}$ films are biocompatible with little restrictions. Therefore*, in vivo* mouse test are planed to further test the biocompatibility of $Fe_{70}Pd_{30}$ films. Additionally, film coatings will be employed to improve biocompatibility.

Conclusion

In summary, single crystalline $Fe_{70}Pd_{30}$ and Ni_2MnGa thin film shape memory alloys were synthesized using electron beam evaporation and magnetron sputtering, respectively. Regarding nano mechanical characterization of Ni_2MnGa, CR-AFM revealed the important role of twin boundaries for the FSM effect. Further CR-AFM investigations will deal with comparable observations of $Fe_{70}Pd_{30}$ thin films.

Furthermore, magnetic properties of $Fe_{70}Pd_{30}$ were examined with SQUID measurements. The austenite-martensite transition temperature was determined at about 326 K, which is also confirmed with XRD (T) measurements.

The *in vitro* tests show the biocompatibility of $Fe_{70}Pd_{30}$ with little restrictions. Bonelike apatites with granular microstructure formed on it after soaking in simulated body fluid which makes it an interesting candidate for a wide range of medical purposes. Key future work will be focused on film surface modification for improving the biocompatibility of $Fe_{70}Pd_{30}$ films.

Acknowledgements

This project is funded in parts by the German Federal Ministry of Education and Research (BMBF, PTJ-BIO, 0313909), the Leipzig Graduate School of Natural Sciences "Building with Molecules and Nano Objects" (BuildMoNa) the DFG as well as the SMWK/ESF.

The results of this work originated in cooperation with M. Zink A. Setzer and P. Esquinazi, University of Leipzig, Germany.

Literature

[1] G. J. Mahnke, M. Seibt, S.G. Mayr, Phys. Rev. B 78 (2008) 012101.
[2] R. D. James, M. Wuttig, Philos. Mag. A 77 (1998) 1273.
[3] A. Sozinov, A. A. Likhachev, N. Lanska, K. Ullakko, Appl. Phys. Lett. 80 (2002) 1746.
[4] T. Kakeshita, T. Fukuda, Mater. Sci. Forum 394 (2002) 531.
[5] J. Cui, T. W. Shield, R. D. James, Acta Mater. 52 (2004) 35.
[6] Y. Ma, M. Zink, S.G. Mayr, Appl. Phys. Lett. 96 (2010) 213703.
[7] T. Edler, J. Buschbeck, C. Mickel, S. Fähler, S.G. Mayr, New J. Phys. 10 (2008) 063007.
[8] L. Kühnemund, T. Edler, I. Kock, M. Seibt, S.G. Mayr, New. J. Phys. 11 (2009) 113054.
[9] T. Edler, S.G. Mayr, Adv. Mater. 22 (2010) 4969.
[10] T. Edler, S. Hamann, A. Ludwig, S.G. Mayr, Scripta Mater. 64 (2011) 89.
[11] I. Kock, T. Edler, S.G. Mayr, J. App. Phys. 103 (2008) 046108.
[12] J. Cui, R. D. James, IEEE Transactions on magnetics 37 (2001) 2675.
[13] T. Kokubo, H. Takadama, Biomaterials 27 (2006) 2907.

Development of a new rotogravure printing technology

Y. Bohne, U. Helmstedt, A. Freyer, M. Naumann, B. Rauschenbach

Introduction

Rotogravure printing is a type of direct printing for which the image is engraved onto a cylinder. It combines cost-efficient production of prints in high numbers of copies with best quality and easy-to-handle printing. These advantages are opposed by a complex and time-consuming image carrier production. It comprises electrodeposition of various metal layers partially with highly toxic galvanic baths to provide the printing surface as well as digital electromechanical engraving of the image with a diamond stylus.

To improve the technology recently different studies focused on laser imaging, but have not yet been realized technically. In the majority of cases a direct laser engraving of the cylinder's surface is discussed. Replacement by alternatives to metal, e.g. ceramics or polymers were in discussion, each with different laser ablation mechanisms, interpreted as thermal or non thermal ablation. Various laser sources – such as cw-, pulsed- or UV-Excimer-lasers – were used, respectively.

Combining IOM's expertise in UV-curable nanocomposite materials and laser ablation techniques seemed a promising way to realize these ideas technically. One has to keep in mind the technical requirements arising from a printing cylinder of about 4 metres length, which rotates with a regular speed of 10 m/s.

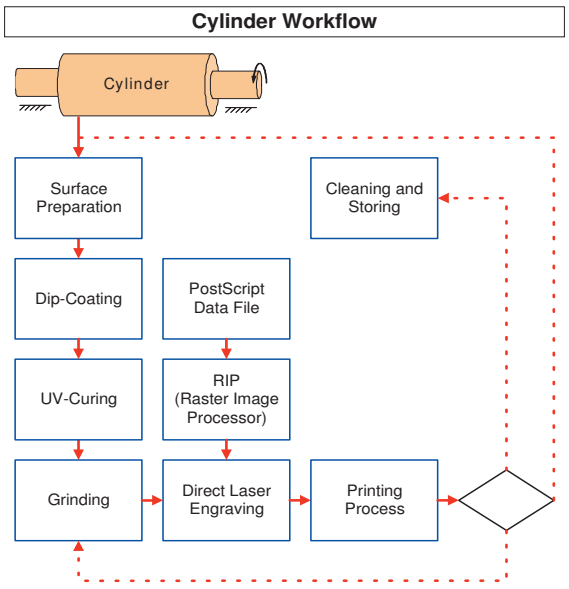

Figure 1: Cylinder workflow in the new rotogravure printing technology.

Here, it is reported about a successful development of the following technology on a laboratory scale ([1], figure 1): The cylinder is coated with a nanocomposite in a dip-coating process followed by UV-curing. High-quality grinding provides the dimensional accuracy and surface roughness required for the printing process. An ultra-short pulse UV-laser is used to engrave cells which in combination with the nanocomposites surface gave satisfying results for the printed image. After the printing process the cylinder can be prepared for the next writing step either by a new grinding process or by refilling the engraved images followed by a new dimensional grinding.

Three fields had to be worked on, which are discussed in their order within the technology chain:

1. Coating material

A hard, scratch- and solvent-resistant polymeric material had to be found which provides sufficient adhesion to the companies printing cylinder's surface. After curing it had to be processable to the needed surface accuracy and roughness as well as engravable by the laser efficiently and without remaining ablation products. Upscaling for real-machine tests had to be managed.

2. Printing cylinder preparation

An efficient and technologically feasible process for applying the nanocomposite layer onto the companies printing cylinders was needed. For this purpose the technology was developed in laboratory scale for cylinders of about 30 cms lengths. A technology was sought to achieve the required dimensional accuracy and roughness of the printing surface without defects.

3. Laser imaging

An efficient way to engrave the image into the nanocomposite surface which results in printed images of the required rotogravure quality needed to be developed. The latter could be verified by test prints on a laboratory printing unit, provided by the industrial partner.

Material Development

Up to now the polymer materials tested in the literature for image carrier coating (thermoplastic polymers, elastomers, resins, waxes and others) do not meet the above mentioned criteria. Organic-inorganic nanocomposites possess properties to fulfil these specific demands. In the scope of this project an UV-curable nanocomposite was developed, which is based on radicalically UV-curable acrylates and filled with aluminiummaleate nanoparticles (ALMAL). UV-curable compositions have the advantage of being free of solvents. This fact and the abolishment of the handling of galvanic baths would lead to a safer working environment for the employees.

Adhesion and solvent resistance

At the beginning of the project six different acrylate formulations were identified out of a large number of commercial available UV-curable acrylates, which showed both, acceptable solvent resistance and adhesion on the cylinder's surface. Those two properties are contrary qualities. A high degree of cross-linking yields high solvent resistance but low adhesion due to high volume contraction during curing. Above mentioned six formulations exhibited an acceptable compromise.

Performance in the laser process

Engraving of the image into the coating has to be highly efficient and precise. Therefore the influence of nanoparticle fillers on the laser process was tested. Nanoparticles with different chemical composition and surface modification [2], were dispersed in selected formulations. The resulting coatings were tested in a model laser process. The efficiency of laser ablation for the different materials is shown in figure 2 and

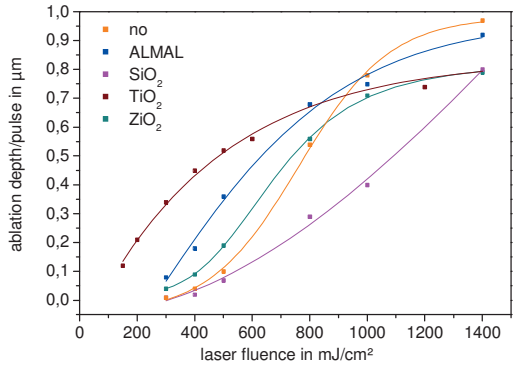

Figure 2: Ablation depth per pulse in nanocomposite materials with different inorganic fillers.

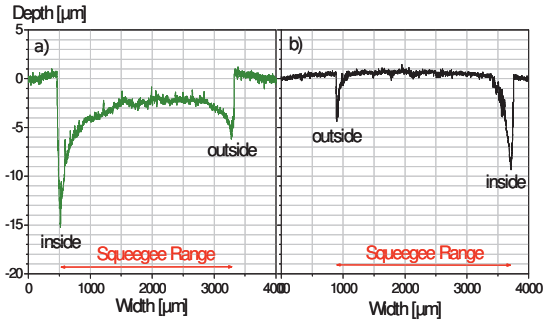

Figure 3: Wear marks measured with profilometer: a) without protective coating, b) with protective coating.

identifies formulations with ALMAL and TiO_2 nanoparticle fillers to perform best. According to the other relevant criteria, ALMAL coatings were identified as superior within the process.

Barrier coating

As could be shown by stress tests in the laboratory printing unit (see next chapter) the material meets the abrasion and solvent resistance criteria on the laboratory scale. To be prepared for an eventual failure in real scale machines preliminary tests for a barrier coating for the image carrier were performed. A layer of SiO_x was deposited on the surface of the grinded nanocomposite by UV-induced conversion of polysilazanes [3]. Mechanical studies showed a noticeable reduction of abrasion (Figure 3).

Printing cylinder preparation

Coating

For the manufacture of recyclable cylinders laboratory-scale printing cylinders were coated with composite material using a custom-built coating machine combining coating and UV-curing pro-cesses, both executed in rotation mode (Fig. 4).

The coating technology was chosen due to the high viscosity of the coating material. It comprises dip-coating with a coating blade to ensure consistent layer thickness adjustment and homogeneous distribution of the material

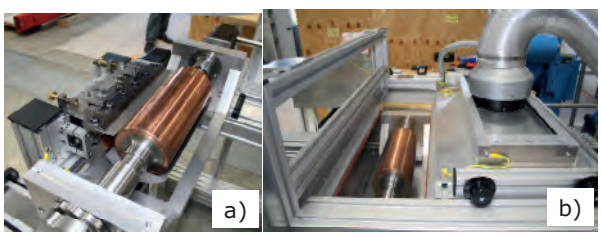

Figure 4: Custom-built coating machine for preparation of a recyclable cylinder with part a) coating process and part b) UV-curing arranged in rotation.

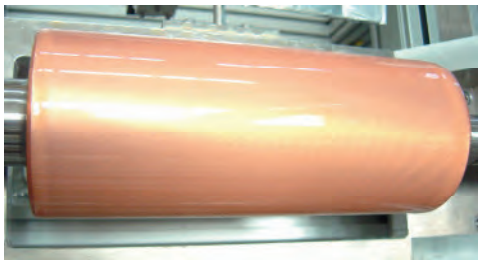

Figure 5: Laboratory-scale printing cylinder after coating and UV-curing using composite material.

during the coating process.

For layer deposition the dipped cylinder rotates on its axis resulting in formation of smooth surfaces with marginal roughness after UV-curing (Fig. 5). The thickness of the deposited composite layers upon the printing cylinders varied between 100 to 300 µm.

Surface processing

After the coating process a surface finish of the coating is required to eliminate irregularities in thickness, to produce a plane-parallel surface and to exhibit the characteristic surface roughness for printing.

Utilisation of a cylindrical grinding machine affords the generation of plane surfaces (± 10 µm) with roughness ≤ 1 µm necessary for printing surfaces that do not tone if no image is engraved.

The stability of a coated printing cylinder regarding mechanical stress during handling and printing is heavily determined by sufficient adhesion between the cylinder's surface and the coating material. To support adhesion by chemical modification of the coating material a mechanical pre-treatment of the cylinder's surface was developed. The stability of coated and polished cylinders tested in a laboratory printing unit (Fig. 6) indicated optimal results using a surface roughness of $R_z \geq 10$ µm for the uncoated cylinder.

A 15 h long-term test could affirm the suitable abrasion resistance of the material. Only marginal roping was observed on the surface.

Recycling

Another technological step is the recycling of the coated cylinder after print. Different recycling processes were proven to be acceptable options for the process. Re-coating of surface after printing was tested using an already coated and polished cylinder after print. During the second coating process a homogeneous distribution of uncured compound on the UV-cured layer could be observed as a result of good wettability of

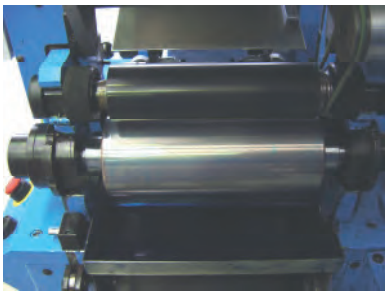

Figure 6: Long-term test (15 h) of a coated and polished cylinder in a laboratory printing unit (MOSER HS-157) using cyan ink.

the cleaned surface. The two-layer cylinders were subsequently grinded and tested in the laboratory printing unit with the result that no failure or layer separation was observed.

Laser Imaging

Laser ablation of polymers uses an intense absorption of those materials in the ultraviolet region. Using laser fluences near the ablation threshold chemical bonds can be broken photochemically without thermal damage [4]. Based on this well known ablation-mechanism the formulated polymers were investigated.

Material testing

To test the developed materials firstly plane coated samples (film-thickness approx. 100 µm) have been studied using UV laser radiation (λ = 248 nm, t_p = 20 ns). Both, laser fluence and pulse number were varied. Ablation depths up to 0.6 µm/pulse could be achieved. Heat affected damage such as cracks, burr or deformation was not detected. Carbon related ablation products – deposited at the surroundings of cells – could be easily removed. To provide insight into the interaction of the engraved surface with ink, printability was tested for a grey scale wedge (depth and diameter of cells vary). Hence, varying laser spot sizes (20-100 µm) were used to expose simple pyramidal stepped cells. A test print showed satisfying preliminary results.

Direct laser ablation of gravure cells

Large dimensions as well as high resolutions of gravure print forms require an efficient engraving process. Concerning this, high pulse repetition rates are crucial for large scale micro structuring [5].

For this purpose an industrial ultra-short pulse UV laser was applied (λ = 355 nm, t_p= 10 ps, f_{rep} = 1 MHz), whose reduced pulse duration leads to less heat diffusion into the polymer [6]. The picosecond-workstation was adapted to the requirements for the imaging of the laboratory-

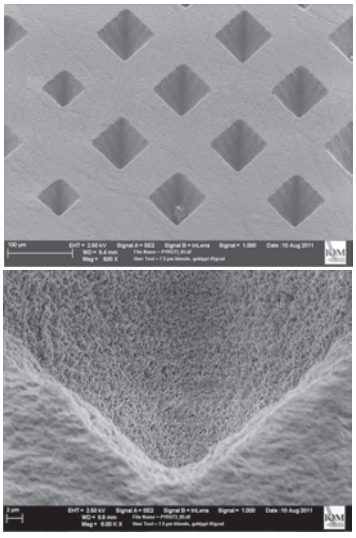

Figure 7: SEM-micrograph of pyramidal shaped cells (perspective 45° tilted), structured by ultra-short pulse UV laser (laser fluence 3.5 J/cm², pulse overlap 75%); a) section of the wedge, b) edge of a cell.

scale cylinders suitable for the coating machine and the laboratory printing unit. The pulse-defined programming of the workstation enables each geometrical cell shape by overlapping several laser pulses (spot diameter about 15 µm). Typical cell volumes produced were between 2 x 10^3 and 300 x 10^3 µm³.

Provided cylinders have been structured by fluences in the range from 3 J/cm² to 7 J/cm² without any thermal damage or debris. Process-related ablation particles were completely removed by exhaustion (see figure 7).

To engrave rotogravure characteristic printed wedges coated cylinders were structured using pyramidal, cylindrical, prismatic, elliptic and conic cell geometries in five gradations. The result for all imaged areas – 5 cm² per wedge – showed excellent ink transfer to the paper as confirmed by the printout in figure 8.

To scale up the technology optimized parameters were fixed. Regarding process performance on real scale further characteristics – such as engraving efficiency, repeatability and an 8-bit grey scale – will have to be taken into account in further investigation.

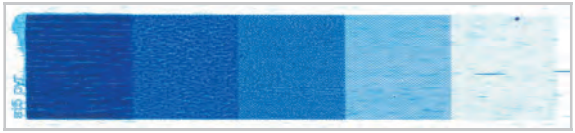

Figure 8: Optical-micrograph of a wedge (pyramidal cells, 5-tone grey scale), printed by a laboratory printing unit, using cyan ink and HWC-paper.

Conclusion

In the laboratory scale the full technology chain has been developed and showed to work in a reproducible manner:

Application of an abrasion-resistant and laser-engravable nanocomposite layer makes galvanic process steps redundant, releases no volatile organic solvents and therefore will reduce environmental management costs. A dip-coating technology could be established which results in layers of about 200 µm thickness, which are UV-curable and processable to result in dimensionally accurate and printable surfaces. The developed laser engraving technology is competitive to state-of-the-art electro-mechanical engraving of images regarding accuracy.

For first tests on real production cylinders the material was produced in a 10 kg scale by subcontractors (Convertex Chemie GmbH and Cetelon Nanotechnik GmbH). Prinovis Ltd. & Co. KG could upscale the dip-coating and surface processing. The first coated production cylinder passed the first dry stress test in the real printing machine successfully.

In addition to these promising results the developed laser-imaging process opens up new possibilities concerning shape-variability of the printing cells. This will lead to higher printing standards and could open up new markets for rotogravure printing.

The results of this work are based in collaboration with C. Jahn-Wolf, O. Krämer, A. Schenk, W. Berthold, Prinovis Ltd. & Co. KG, Dresden.

The authors thank the Sächsische Aufbaubank (SAB) for funding.

Literature

[1] Y. Bohne, C. Elsner, B. Rauschenbach, C. Jahn; EP 2 151 324 A3.
[2] F. Bauer, V. Sauerland, H. Ernst, H.J. Gläsel, S. Naumov, R. Mehnert; Macromolecular Chemistry and Physics 204 (2003) 375.
[3] L. Prager, A. Dierdorf, H. Liebe, S. Naumov, S. Stojanovic, R. Heller, L. Wennrich, M. R. Buchmeiser, Chemistry – A European Journal 13 (2007) 8522.
[4] D. Bäuerle; Laser Processing and Chemistry, Springer Berlin Heidelberg, 3rd rev. (2000).
[5] G. Hennig, K.H. Selbmann, S. Brüning; LTJ, No.3, 5, (2008) 52.
[6] A. Serafetinides, M.I. Makropoulo, C.D. Skordoulis, A.K. Kar; Applied Surface Science 180 (2001) 42.

Quantum-chemical modelling of primary processes

S. Naumov

Introduction

For a better understanding of ongoing reactions, the reactivity and other properties of intermediates must be known. Here, quantum chemical calculations can be of a considerable help. Polymerisation reactions, for example, may be induced upon electron- and photo-excitation or by free radicals. Ad initio, density functional theory and other calculations allow us to compute molecular geometries and energies of excited states and of intermediates such as neutral radicals, radical cations and radical anions. The interpretation of ESR spectra that may have been obtained in the course of the reaction can be assisted by calculating the coupling constants of such intermediates. With the increasing complexity of the systems that are investigated, programs capable of dealing with larger molecules at high level of theory at reasonable computation times, e.g., Jaguar (Schrödinger), have to be introduced. Often quantum-chemical calculations are carried out in the gas phase. This may lead to erroneous results when the reaction has been carried out in highly polar solvents such as water, especially in the cases of charged molecules. Hence, solvent polarity has always been taken into account in the simulations to be reported.

Experimental

Reactions of excited states

The initiation mechanism of the VUV-induced conversion of polyorganosilazanes into methyl–Si–O–Si networks was studied by means of model disilazane compounds. Quantum-chemical calculation of the various potential decay routes, starting from excited state both singlet and triplet (Fig. 1) allowed rationalizing the experimental observations [1].

Even though the smallest dissociation Gibbs free energy was calculated for the Si–CH3 bond cleavage, Si–NH bond scission is found to be the preferred photochemically induced reaction pathway in condensed media, which can be rationalised by the favourable change of electron distribution along the Si–NH–Si bonds upon excitation.

Quantum-chemical calculation of the various potential decay routes of acrylate formulations, starting from excited triplet state formed after short-wavelength vacuum UV (VUV) irradiation. The short-wavelength VUV irradiation of acrylates results in radical formation and self-initiation of the photopolymerization, i.e. photoinitiator-free curing of acrylates [2]. The UV-Vis excitation spectra were calculated at TD DFT method und shows very reasonable agreement with experiment (Fig. 2).

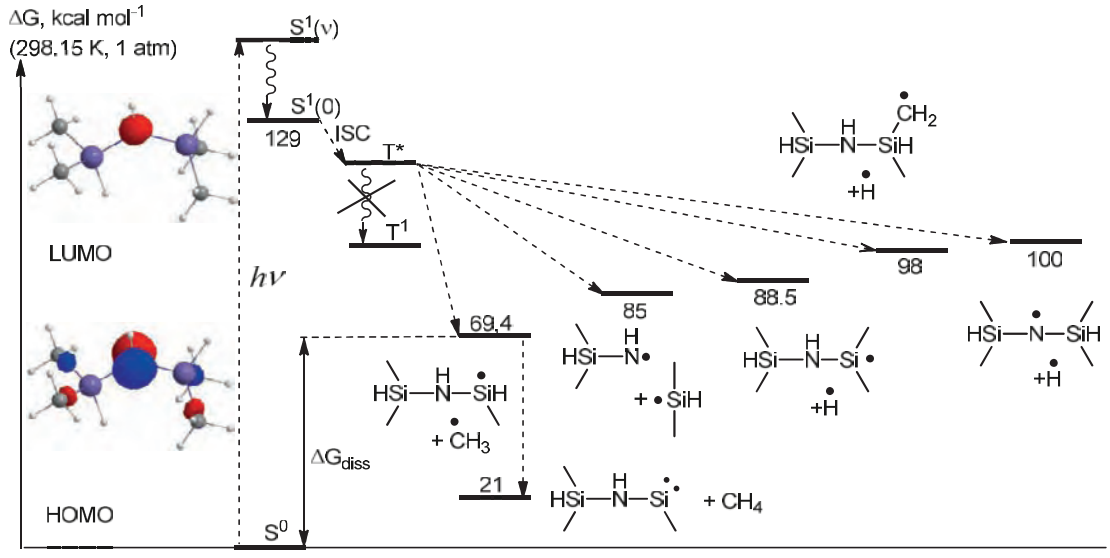

Figure 1: Quantum chemical calculations on the photolytic excitation of 1,1,3,3-tetramethyldisilazane (TMDSz) and possible fragmentation pathways.

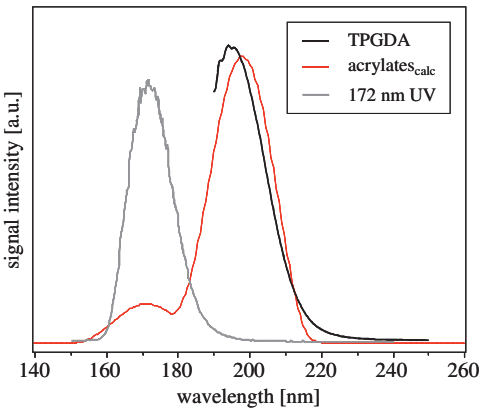

Figure 2: Comparison of the UV spectrum of tripropylene glycol diacrylate (TPGDA) and a DFT calculated spectrum of an acrylate with the emission spectrum of the monochromatic 172 nm excimer lamp.

After photoexcitation, the first excited singlet state of 1- and 2-thio-naphthols decay by radiationless internal conversion and intersystem crossing with pronounced S-H photodissociation. Fluorescence as a deactivation channel plays a minor role.

To understand the influence of a structural variation between the parentthiophenol and its larger aromatic thionaphthol moiety on theirfirst excited singlet states deactivation, the excited state energy properties (singlet and triplet) of 1- and 2-NpSH and their corresponding structures as well as those of the parent thiophenol were calculated using DFT method at the B3LYP/6-31+G(d,p) level [3]. From the comparison between the molecular orbitals of different aromatic thiols given in Figure 3 one can observe that the extended aromatic moiety of thionaphthols increases the π-electron delocalization and consequently lowers significantly the excited-state energies. Consequently, increasing π-electron delocalization ought to stabilize the S1 electronic state of thionaphthols (nanosecond time scale) and cause a remarkable spectral red shift (about 50-60 nm) of their fluorescence in comparison with those of the parent thiophenol molecule (ArSH(S1) in subpicosecond time scale). These data are in line with our steady-state experimental results.

Formation and properties of free radicals

The $^{\bullet}OH$ radical, the solvated electron, e_{aq}^{-}, and the hydrogen atom, $^{\bullet}H$, are the primary radicals in the radiolysis of water. In basic solution, $^{\bullet}OH$ is present as $O^{\bullet-}$ [pK_a($^{\bullet}OH$) = 11.8]. Of these, only $^{\bullet}OH$ does not react with O_2. The reason for this has now been elucidated by quantum

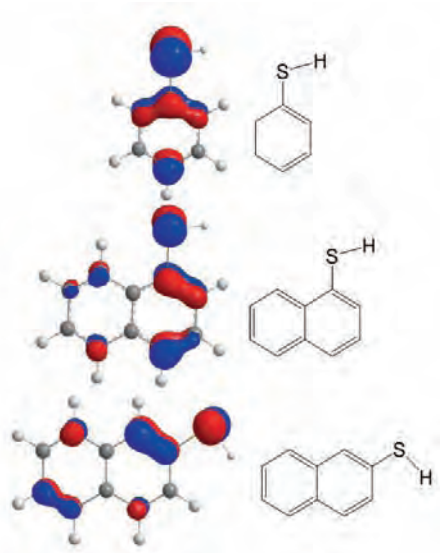

Figure 3: Electron-density distribution of the molecular orbitals for thiophenol and 1- and 2-thionaphthols in the most stable structure.

mechanical calculations, and based on the thermo-dynamic cycle (Fig. 4) the pK_a value of $HO_3^{\bullet}$ could be established at –2.0 [4].

Although O_2 is widely used a scavenger of free radicals, a fast and irreversible reaction occurs only with a very limited number of free-radical types, notably the abundant group of carbon-centered free radicals. This is in contrast to ozone, which reacts with most free radicals, including oxygen- nitrogen, and most halogen-centred free radicals [5]. For the calculations of the standard Gibbs free energies of these reactions, the above mentions Jaguar program has been used with advantage.

The $^{\bullet}OH$ radical is also generated in the reaction of ozone with OH^{-} and with HO_2^{-}. The present mechanistic concept has been revised base on thermokinetic and quantum-chemical calculations [6, 7]. In a pulse radiolysis study with -OH-, -CH_3-, or -NH_2-substituted indole chalcones and hydroxy benzenoid chalcones involving $^{\bullet}OH$ and other oxidizing radicals, the observed intermediates by optical detection were characterized by quantum-chemical calculation of the spectra of various conceivable intermediates [8]. A experimental and quantum

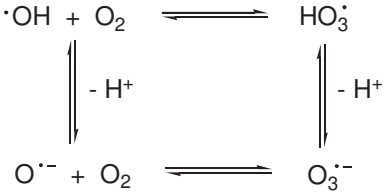

Figure 4: Thermodynamic cycle involving O_2, $^{\bullet}OH/O^{\bullet-}$ and $HO_3^{\bullet}/O_3^{\bullet-}$

chemical study has been performed on the reactivity, formation and properties of transients generated in the reaction of selected organic selenides with $^{\bullet}OH$, $O^{\bullet-}$, e_{aq}^{-} and $^{\bullet}H$ in aqueous solution [9].

In case of the neutral adduct radical $Me_2Se^{\bullet}OH$ the con-version into the three-electron bonded dimer species, $Me_2Se^{\cdot}.SeMe_2$ proceeds, in part, via the molecular $(Me_2Se^{\cdot}.OH_2)^{+}$ radical cation. DFT calculations also revealed a generally higher thermodynamic stability of the Se-centered radicals relative to the S-centered ones.

Properties of radical cations and electron transfer reactions in condensed media have been reviewed [10-12]. As main arguments resulting from the quantum-chemical considerations the following points might be derived: -bending motions around the Ar-XH axis (where X = O, S, Se, N) result in a continuous change of the molecular structure. This concerns the electron distributions as well as the geometry of the molecule. Within the Born-Oppenheimer approximation the molecular geometry remains stiff during the time required for electron relaxation and he very fast (instantaneous) electron jump. The hetero atoms carry lone electron pairs and are thus potential electron donors. In the planar structure, due to the strong resonance with the π-electron of the aromatic ring, the n-electrons are shifted from the hetero atom to the aromatic moiety. Hence, the (HOMO) molecular orbital in the planar structure is strongly delocalized over the whole molecule. Rotation around the Ar□XH axis disturbs this coupling between ring and lone electron pairs. Therefore, the molecular orbital in the perpendicular structure assumes n-symmetry and is almost entirely localized at the hetero atom (Fig. 5). The consequences emerging from all the above show up in the initial products of the FET involving the two border line conformer structures, namely, the planar and the perpendicular (twisted) ones.

General chemical kinetics

In many aspects, $^{\bullet}OH$ radicals and ozone have similar properties. They are both strongly electro-philic, and in their reactions with aromatic compounds they both form adducts. The logarithm of adduct formation relates to the (calculated) standard Gibbs free energy of adduct formation (Fig. 5) [13].

A similar correlation with the HOMO (Fig. 6) is the quantum-chemical basis of this dramatic substituent effect.

Also for other ozone reactions, quantum-chemical calculations were essential for understanding mechanistic details [14, 15]. In one case [15], the program indicated the path taken during structure optimization. Prior to

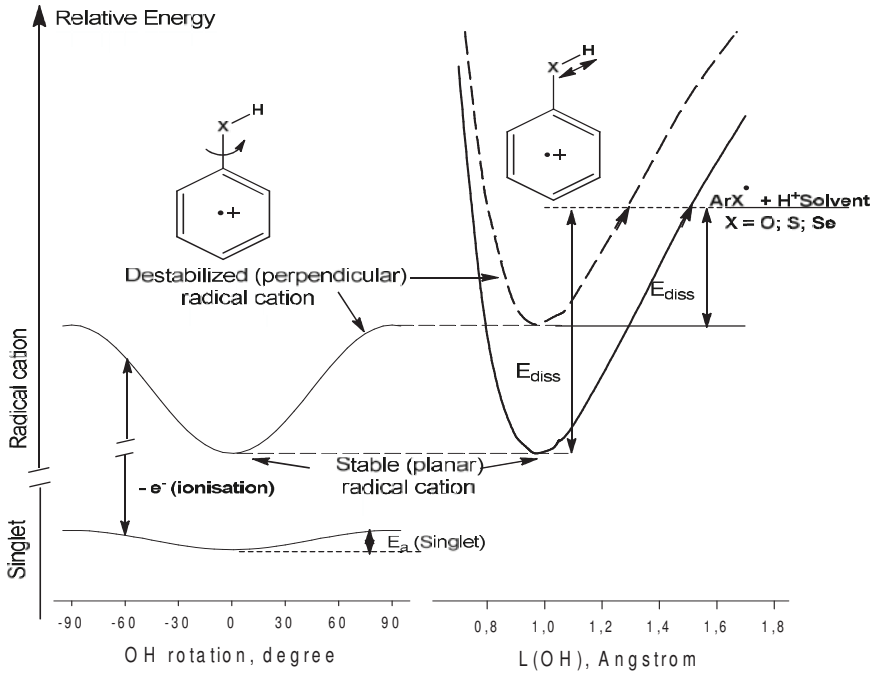

Figure 5: Potential diagrams describing the energetic situation of phenol as donor in the ground state and for the different conformer radical cations. The left part shows the potentials dependent on the rotation angle, and the right part illustrates energy changes dependent on the bond length (L) of Ar-OH.

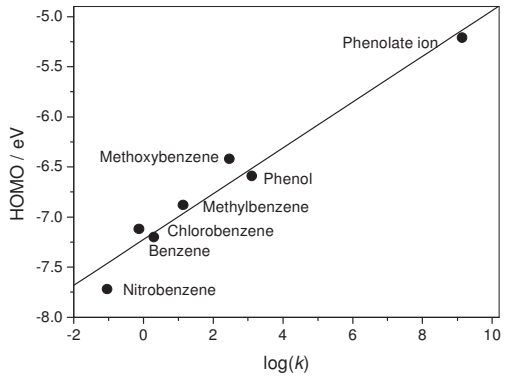

Figure 5: Correlation of the logarithm of the rate constant with the energy of the HOMO.

this, the reaction even had not been considered.

For the quantum chemical study of the systems containing the heavy atoms and the transition metals complexes, new hybrid meta exchange-correlation functional (M06, M06-2X etc) with the basis sets, which uses different models of the relativistic effective core potentials (LACVP, Lanl2DZ etc.) for the inner core electrons and treats the outer core and valence electrons with a 4s/4p/2d/2f basis set, will be applied.

Mass and energy spectra of negative and positive ions in magnetron sputtering discharges have been investigated with an energy-dispersive mass spectrometer. A variety of target metal (Cu, In, and W) containing negative and positive molecular ions were found in the discharge. Calculations of bond dissociation energies were required for understanding plasma processes [16, 17]. These energies were correlated to the electron affinity and the bond strength of the molecules which have been calculated by density functional theory. The occurrence of the different ions is explained in the context of their bond strengths obtained from DFT calculations.

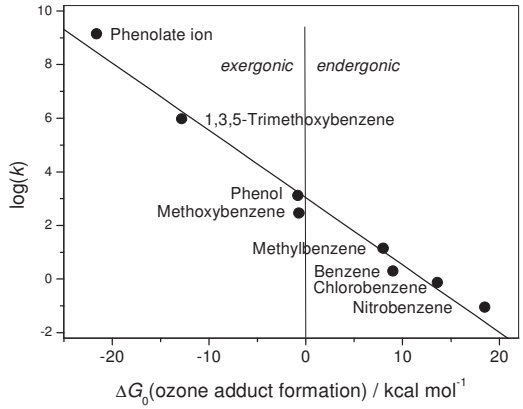

Figure 6: Correlation of the calculated standard Gibbs free energies with the logarithms of experimental rate constants of the reactions of ozone with some aromatic compounds in aqueous solution.

The synthesis and characterization of water-soluble dispersions of Ag nanoparticles by the reduction of $AgNO_3$ using tryptophan under alkaline synthesis conditions are reported [18]. The binding of thryptophan to silver nanoparticles was studied both experimental and by quantum chemical calculations. Our results suggest that the replacement of the BH_4 – ions adsorbed on the nanoparticle surface by tryptophan destabilizes the particles and further caused aggregation. A mechanism is proposed for the formation of silver nanoparticles by tryptophan. The Ag nanoparticles were characterized by UV–vis absorption, dynamic light scattering and transmission electron microscopy techniques.

Literature

[1] W. Knolle, L. Wennrich, S. Naumov, K. Czihal, L. Prager, D. Decker, M.R. Buchmeiser, Phys. Chem. Chem. Phys. 12 (2010) 2380.
[2] F. Bauer, U. Decker, S. Naumov, C. Riedel, Progr. Org. Coatings 69 (2010) 287.
[3] Y.M. Riyad, S. Naumov, B. Abel, R. Hermann, J. Phys. Chem. A 115 (2011) 718.
[4] S. Naumov, C. von Sonntag, J. Phys. Org. Chem. 24 (2011) 600.
[5] S. Naumov, C. von Sonntag, Environ. Sci. Technol. 45 (2011) 9195.
[6] G. Merényi, J. Lind, S. Naumov, C. von Sonntag, Chemistry – Eur. J. 10 (2010) 1372.
[7] G. Merenyi, J. Lind, S. Naumov, C. von Sonntag, Environ. Sci. Technol. 44 (2010) 3507.
[8] P. Gaikwad, K. I. Priyadarsini, S. Naumov, B. S. M. Rao, J. Phys. Chem. A 114 (2010) 7877.
[9] Th. Tobien, M. Bonifačić, S. Naumov, K.-D. Asmus, Phys. Chem. Chem. Phys 12 (2010) 6750.
[10 O. Brede, S. Naumov, In: Recent Trends in Radiation Chemistry, J. F. Wishart, B.S.M. Rao (Eds.) World Scientific Publishing, Singapore (2010) pp. 411.
[11] O. Brede, S. Naumo, Chem Soc Rev 39 (2010) 3057.
[12] O. Brede, S. Naumov, In: Charged Particle and Photon Interactions with Matter - Recent Advances, Applications, and Interface, Y. Hatano, Y. Katsumura, A. Mozumder (Eds.), (2010), Taylor & Francis, Boca Raton, pp. 237.
[13] S. Naumov, C. von Sonntag, Ozone: Sci. Eng. 32 (2010) 61.
[14] S. Naumov, G. Mark, A. Jarocki, C. von Sonntag, Ozone: Sci. Eng. 32, (2010) 430.
[15] G. Mark, S. Naumov, C. von Sonntag, Ozone: Sci Eng 33 (2011) 37.
[16] Th. Welzel, S. Naumov, K. Ellmer, J. Appl. Phys. 109 (2011) 073302.
[17] Th. Welzel, S. Naumov, K. Ellmer, J. Appl. Phys. 109 (2011) 073303.
[18] J. A. Jacob, S. Naumov, T. Mukherjee, S. Kapoor, Colloid Surf. B: Biointerfaces 87 (2011) 498.

Membrane hydrophilization using electron beam and plasma techniques

A. Schulze, A. Boulares-Pender, M. Went, I. Thomas, B. Marquardt, A. Prager

Introduction

Today, micro- and ultrafiltration membranes are predominantly fabricated from synthetic membrane materials such as polyethersulfone (PES), polyvinylidene fluoride (PVDF), polysulfone (PSf), or polyacrylonitrile (PAN). The diversity of applications requires the modification of the polymer in order to avoid any fouling of the hydrophobic membrane surfaces or to achieve a functionalized membrane.

Here, we present two different methods using electron beam irradiation (EB) [1-3] and combined plasma and EB treatment for permanent hydrophilization of polymer membranes. No catalysts, photoinitiators, organic solvents or other toxic reagents were used, and no additional synthetic or purification steps are required.

Electron Beam Modification

Membrane modification was performed by dipping the membrane into an aqueous solution of one of the functional molecules 1-15 (Figure 1) followed by EB irradiation (dose: 30-300 kGy). The modified membrane was rinsed with water for 1.5 h and subsequently dried at 20-100 °C.

Results

Modification of hydrophobic polymer membranes (PES, PVDF, PSf, PAN) with one of the reagents 1-15 resulted in considerably improved water wettability which was observed by water contact angle measurements (Figure 2).

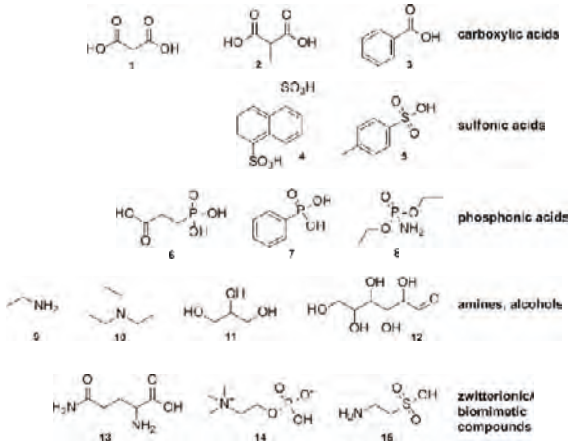

Figure 1: Functional molecules used for the EB-based membrane modification.

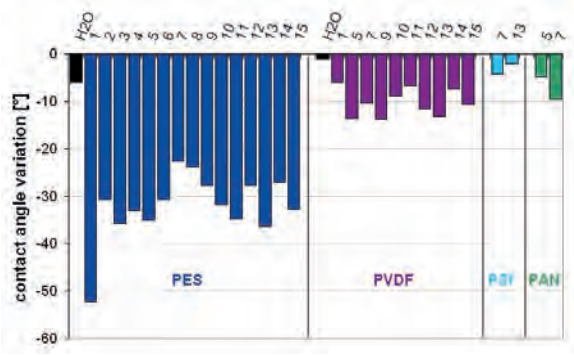

Figure 2: Change of water contact angles after modification of PES (homemade), PVDF, PSf, and PAN (commercial pre-hydrophilized) membranes with molecules 1-15. The water contact angles of the unmodified membranes are: PES: 76°; PVDF: 67°, PSf: 62°; PAN: 52°.

Water contact angles of homemade pure PES membranes resulted in contact angle changes > 20° after modification. Commercial pre-hydrophilized PVDF, PSf, and PAN membranes could also be improved in water wettability but since the respective starting contact angle was already small the effect was not as strong compared to the pure PES membrane.

Fouling tests were performed by filtration of BSA solution (1 g/l in PBS buffer at pH 7.0) through the membrane followed by back-washing with pure water. This treatment was repeated several times resulting in significantly decreased flux in the case of the unmodified PVDF membrane (Figure 3). Modification with several of the small molecules resulted in improved antifouling membrane properties. Especially after modification with molecules 12, 14, and 15 (glucose, phosphocholine, taurine) a strong positive impact on the resulting membrane performance was observed.

This effect was also confirmed by SEM measurements after 5 filtration cycles (Figure 4). Here, it can clearly be seen that the unmodified PVDF membrane is completely covered by a fouling layer of BSA, and the former pore structure is rarely observable (Figure 4 top). When the same treatment is applied on a membrane modified with glucose 12, the membrane pore structure is open and

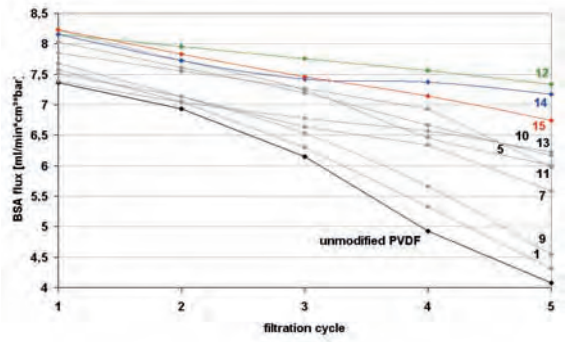

Figure 3: Fouling properties after treatment with BSA solution of an unmodified PVDF membrane and after modification with different small molecules.

nearly no filter cake has been formed (Figure 4 bottom).

Membrane performance in terms of pure water flux was characterized for selected modifications by dead end filtration using pure water. Here, the modified PES membranes show a higher flux (e.g., +25% after modification with 13) than the unmodified. Similar results were obtained for the modified PVDF membranes. The flux generally increased, e.g. 16 % after modification with 1 compared to the unmodified PVDF membrane. The increase in flux can be correlated to the improved wettability of the hydrophilic membrane surface, whereby contact angles decrease at the same time.

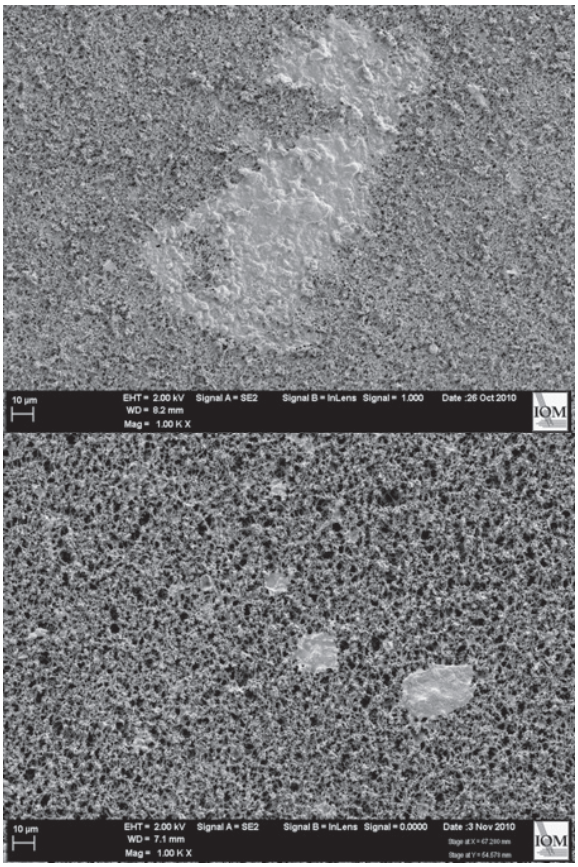

Figure 4: SEM pictures of PVDF membranes after fouling treatment with BSA solution: unmodified membrane (top) and membrane modified with 12 (bottom).

To demonstrate the stability of the modification, selected modified PES membranes were exposed to a continuous Soxhlet extraction for 7 days in boiling water. Albumin adsorption was measured before and after extraction and was found to be comparable within the limits of experimental error (Table 1). Similar results were found for the corresponding contact angles before and after Soxhlet extraction.

Table 1: Protein adsorption [µg/cm²] before and after soxhlet extraction in boiling water (7 d).

	PES	PVDF	
reagent	**14**	**1**	**12**
before extraction	3.61	1.87	0.86
after extraction	3.68	1.79	0.91

However, due to the low concentration of the functional groups in the final modified membrane, it was not feasible so far to unambiguously identify the exact connectivity of the functional molecules to the membranes. The high stability of the modification indicates a permanent membrane functionalization, i.e. that covalent bonds are formed between the polymer backbone and the functional molecules.

XPS analysis showed that the electron beam-based treatment did not result in any changes in the PES structure and no additional S-based signals were observed. This result was additionally confirmed by bubble point and MWCO measurements before and after irradiation confirming that the pore size was not enlarged by decomposition of the membrane polymer.

Conclusion

We successfully modified different types of polymer membranes (PES, PVDF, PSf, PAN) soaked in aqueous solutions of functional molecules and treated by EB. Furthermore, we have shown that the modification method seems to be generally applicable on different types of polymer membranes. With selected functional molecules, this simple modification procedure resulted in significantly improved water wettability as well as reduced fouling behaviour. The procedure guarantees for a permanent functionalization of the membrane polymer that neither requires the use of catalysts/photoinitiators nor of other toxic reagents. Further experiments are currently in

progress to shed light on the mechanism, i.e. the reactive intermediates.

Combined Plasma and Electron Beam Treatment

Plasma modification is a powerful method for hydrophilization of polymer surfaces. However, after common plasma treatment hydrophobic recovery is very often observed leading to increasing contact angles within several days or even weeks.

In the present study, plasma modification was "fixed" by subsequent electron beam (EB) irradiation due to cross-linking of the polymer chains to prevent potential hydrophobic recovery. Plasma gases O_2, N_2, Ar and binary mixtures thereof were used. The membranes were soaked in water few minutes after plasma treatment and then exposed to EB irradiation. The modified membranes were characterized by contact angle measurements, whereby the surface composition after surface treatments was investigated by X-ray photoelectron spectrometry (XPS).

Results

Polyvinylidene fluoride (PVDF) flat sheet membranes were exposed to either gas plasma treatment, EB treatment, or both treatments successively, i.e. gas plasma followed by EB irradiation. The techniques used in this study have the following effect on the filtration properties of the membranes: we observed an increase up to 15-20% in water flux according to the surface treatment and the nature of the polymer membrane. For bubble point values no drastic changes were observed, except for oxygen containing plasma treated PVDF membranes, where an increase in bubble point is observed. For these samples the changes in bubble point values can be symptomatic of a modification of the pore size; however the SEM images did not reveal a difference in the pore size as it can be observed on selected images presented on Figure 5.

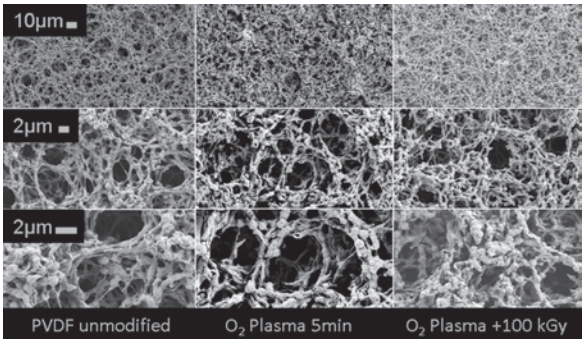

Figure 5: SEM images of PVDF membrane samples: unmodified (left), oxygen plasma treated (middle) and oxygen plasma followed by electron beam exposure (right).

Table 2: Water and diiodomethane (DIM) contact angles of the modified PVDF membrane.

	Contact Angle		Surface Energy	Contributions	
	Water [°]	DIM [°]	[mN/m²]	Disp.	Polar
PVDF	138.3	77.8	22.1	18.6	3.5
EB	128.6	67.8	26.8	24.1	2.7
N_2	137.5	90.4	14.0	12.5	1.5
N_2-EB	110.8	80.9	17.2	17.0	0.1
N_2/Ar	137.3	94.4	11.9	10.8	1.1
N_2/Ar-EB	126.5	77.7	19.8	18.7	1.1
Ar	132.9	100.0	8.9	8.7	0.2
Ar-EB	129.6	89.3	13.6	13.0	0.6
O_2/Ar	126.0	101.3	8.2	8.2	0.6
O_2/Ar-EB	102.2	85.0	16.7	15.0	1.7
O_2	65.1	82.8	37.0	16.1	20.9
O_2-EB	68.9	71.0	36.1	22.3	13.8
O_2/N_2	127.4	72.6	23.3	21.4	1.9
O_2/N_2-EB	116.8	77.4	19.0	18.9	0.1

Table 2 presents the contact angles with water and diiodomethane (DIM), as well as mean values of the total surface free energy, as a function of the PVDF membrane surface treatments. If the EB irradiation treatment alone can be employed to reduce the water contact angle, such procedure would be more efficient when the irradiation is carried out after plasma treatment. Even though, this treatment does not induce a meaningful change in the surface polarity due to cross-linking of PVDF chains upon exposure to EB irradiation. Here a chain rearrangement is generated during processing rather than a chemical surface modification.

A more significant reduction in contact angle is observed after treatment with oxygen plasma or with a combination of nitrogen and oxygen gas plasma. With oxygen plasma alone, the polar contribution to the surface energy is greatly increased; this is generally attributed to the presence of polar functions at the surface upon plasma treatment, but it also show that only oxygen containing plasma treatments are efficient enough to produce chemical changes at the surface of the PVDF membrane. Since other treatments do not lead to–significant increase of the polar contribution to the surface energy, it would indicate that the modification is more structural (etching) than chemical. Furthermore, the additional electron beam treatment always

tends to lower the water contact angle and in some cases the polar contribution of the surface energy; this can be explained by the formation of CH_2-CH_2 bond via a radical mechanism, which is still of hydrophobic nature, thus the modified surface will tend to have similar properties to that of a polyolefin.

X-ray photoelectron spectroscopy (XPS) was used in this work to investigate the changes occurring at the surface of the membranes upon gas plasma and EB treatments. The resulting data (not presented) show an increase in oxygen content after all surface treatments and we observe also an increase with the additional EB irradiation after plasma treatment when compared to plasma treatment alone. The C1s deconvolution results (Figure 6) show that the EB irradiation alone, while it increases the oxygen content to 3 at.-%, does not produce obvious oxidation species as for plasma surface treatment, such as hydroxyl or acid functions, at the surface, thus the 3 at.-% oxygen could be attributed to oxygen intake from air upon treatment. On the C1s deconvolution level the increase in oxygen content, after plasma treatment and combined plasma and EB treatments, is underlined by the relative increase of the 287.5 eV and 288.5 eV assigned to C-O and C-Ox peaks (C-Ox = R-C-O; R-C=O; with R=C, O, etc.), which is definitely due to the action of the gas plasma, but seems to be also enhanced by the electron beam irradiation after plasma.

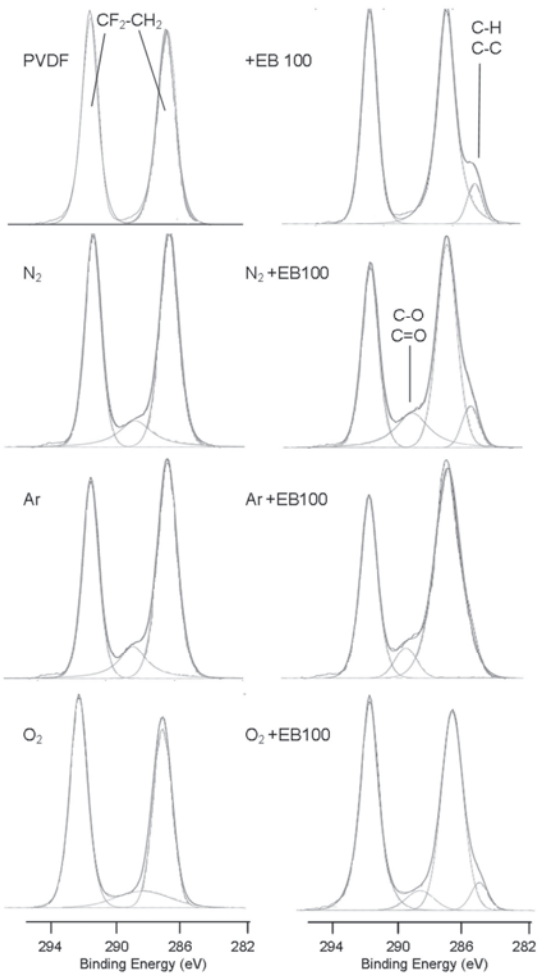

Figure 6: High resolution C1s XPS spectra of pristine PVDF, plasma treated only (left: N_2, Ar and O_2) and plasma treated plus EB irradiated (+EB100) PVDF membrane samples.

More interestingly, a peak at 284.9 eV always appears after EB irradiation and has been assigned to a C-C/C-H bond of a CH_2-CH_2 chain segment. Figure 6 presents the C1s deconvolutions while this 284.9 eV peak was obtained on most EB irradiated samples located on the right side of Figure 6. This peak confirms the cross-linking of the PVDF through the formation of a CH_2-CH_2 bond during EB irradiation.

Conclusion

The study of the effect of EB and plasma surface treatments on PVDF membrane has shown that only oxygen based plasma treatment were efficient enough to increase the wettability and polarity of the PVDF membrane surface.

PVDF membrane polymer chains can be cross-linked by EB irradiation as it was demonstrated by XPS studies. The combination of plasma treatment and EB irradiation appears to be an efficient method for the hydrophilization of the membrane surface and as well as the generation of a cross-linked polymer network. Thus, hydrophobic recovery can be avoided when both methods are combined which is the focus of current investigations.

Literature

[1] A. Schulze, B. Marquardt, S. Kaczmarek, R. Schubert, A. Prager, M. R. Buchmeiser, Macromol. Rapid Commun. 31 (2010) 467.
[2] A. Schulze, B. Marquardt, S. Kaczmarek, R. Schubert, M. R. Buchmeiser, DE 10 2009 036 947 A1.
[3] A. Schulze, B. Marquardt, M. Went, A. Prager, M.R. Buchmeiser, Water Sci. Technol. (2011) accepted.

In-line monitoring of the thickness of thin printed layers by near-infrared reflection spectroscopy: An innovative method for process control

T. Scherzer, G. Mirschel, O. Savchuk

Introduction

Transparent varnishes play an important role in printing technology. The thickness of printed layers may be influenced by numerous factors. Besides the chemical and physical properties of the used inks or varnishes, it depends on various technical parameters related to the printing process. However, there was no suitable analytical method so far, which allowed in-line measurements of the coating weight or the thickness of such layers during printing at a printing press.

In the past, near-infrared (NIR) spectroscopy has been used at IOM for monitoring of the thickness and the conversion of UV-curable coatings with a thickness of about 5 to 50 µm [1]. On the basis of these investigations, a new method was developed, which can be used for process control in printing technology, i.e. for the analysis of layers with a thickness of about 0.5 to 5 µm.

Experimental

Investigations were carried out with a NIR reflection spectrometer, which was developed for process control. It consists of a spectrometer unit and a separate probe head, which can be integrated into complex technical systems such as a printing press. Quantitative analysis of the spectral data was carried out with sophisticated chemometric methods. The application of such methods requires complex calibration procedures. Moreover, it has to be ensured that measurements during calibration in the laboratory and during in-line monitoring are carried out under identical conditions. In order to simulate the mounting of the probe head above an impression cylinder of the printing press, a special reflector was developed, which exactly mimics a segment of this cylinder with respect to curvature and material (Fig. 1).

Figure 1: NIR probe head with the metal reflector developed for calibration measurements.

UV-curable varnishes

Fig. 2 shows an example of a calibration curve for a UV-curable clear varnish based on an acrylate formulation. Calibration samples with different thicknesses were printed with a laboratory-scale printing machine, and reference data were obtained by gravimetry.

Before calibrations were used for in-line monitoring, their performance was tested with independent test samples, which were not included in the calibration process. The error of the predictions from application of the calibration in Fig. 2, for example, was found to be less than 90 mg m^{-2}.

For in-line monitoring, the probe head was mounted above an impression cylinder of a sheet fed offset printing press at SID (see Figs. 3 and 4). Great care was directed towards the precise alignment of the probe head in order to ensure identical measurement conditions to those used during calibration in the laboratory, which is essential for correct predictions during process control.

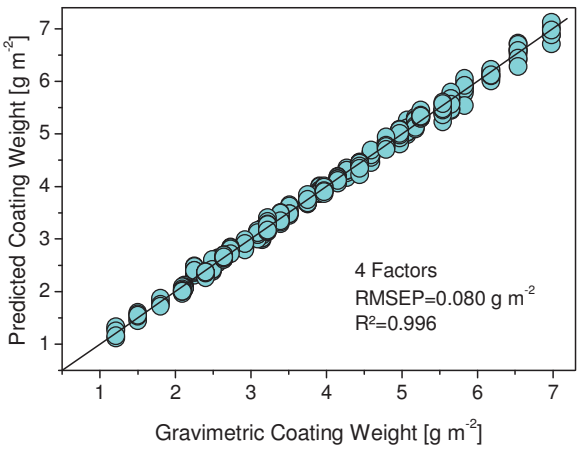

Figure 2: PLS calibration curve for the coating weight of layers of a UV-curable varnish based on a urethane acrylate printed on paper.

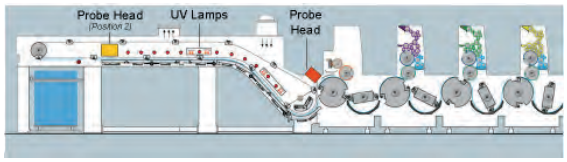

Figure 3: Scheme of the offset printing press with the current and the future position of the probe head.

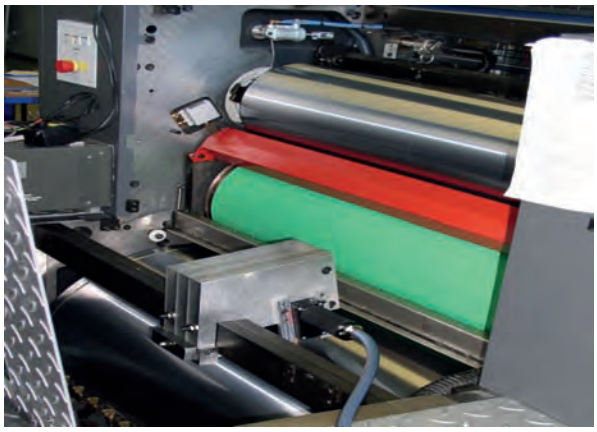

Figure 4: NIR probe head mounted above the impression cylinder of the coating unit of a sheet fed offset printing press.

During printing, spectra were recorded at a rate of 30 s^{-1}. Hence, at least 3 spectra were taken per sheet. In order to apply layers with different coating weights, the speed of the duct roller and the relative opening of the ink keys, which both control the amount of varnish on the printing plate, were varied (labeled as *Speed* and *Opening* in all in-line monitoring plots). Fig. 5 shows the result of a typical in-line monitoring experiment. The comparison with reference data clearly shows that the coating weight of the printed layers can be determined with an error of about 150 mg m^{-2} only [2].

Oil-based varnishes and the effect of different gloss levels

Oil-based varnishes are still the most widely used chemical system in printing technology. Therefore, detailed studies were carried out on such systems as well. The varnishes cure by reaction with atmospheric oxygen, which means that a well-defined time regime has to be maintained during calibration. This allows a similar precision during in-line monitoring like for UV-curable lacquer systems [3].

In order to obtain specific design effects during printing, clear varnish layers may be applied with different degrees of gloss. Unfortunately, the gloss level was found to strongly affect the NIR measurements, which led to a dramatic decrease of the precision. This effect is demonstrated in Fig. 6. The coating weight of matte printed layers was determined either with the specific calibration which had been developed for this varnish or with the calibration model of a high-gloss varnish. Whereas correct results were found in the former case, a considerable offsetwas obtained in the latter one.

In order to overcome the detrimental effect of the surface roughness on the prediction performance, the variation of the gloss has to be included into the calibration model. Accordingly, PLS calibration models were developed, which contain spectra of samples with different gloss levels [4]. Fig. 7 shows the results of the test of the prediction performance of a universal calibration model. The error (RMSEP) was found to be 160 mg m^{-2}. The results prove that the interfering effect of the gloss on the precision of the predictions can be completely suppressed,

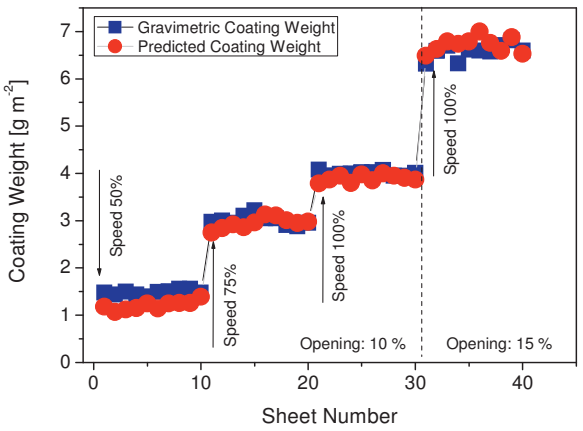

Figure 5: In-line monitoring of the coating weight of layers of a UV varnish printed on paper. For comparison, coating weights determined by gravimetry are shown.

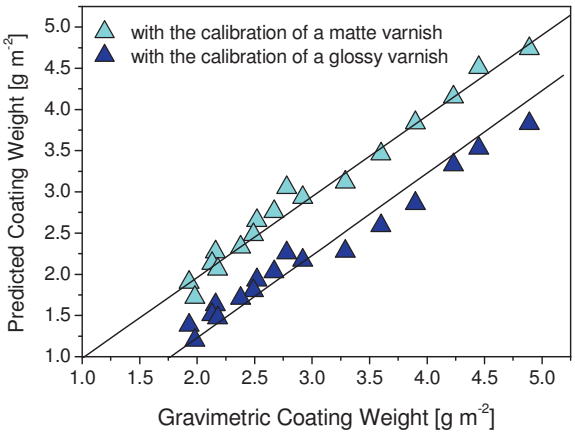

Figure 6: Prediction of the coating weight of printed layers of a matte oil-based varnish using the calibration model for a glossy lacquer or the appropriate calibration for the matte lacquer, respectively.

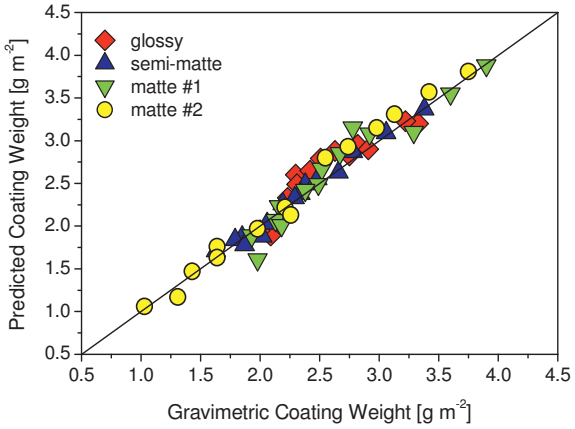

Figure 7: Prediction of the coating weight of test samples of printed layers with different degrees of gloss using a universal calibration model.

when the variation of the gloss is included in the design of the model.

In addition to the lab-scale investigations, the universal calibration models were also tested at the printing press, i.e. the coating weight of various clear printed varnish layers with different gloss levels was determined by in-line monitoring. The record of a typical printing trial is shown in Fig. 8.

It is obvious that a close correlation between the predictions from NIR spectra and the reference data from gravimetry was achieved. The error was found to be 150 mg m^{-2} [4]. Similar results were also obtained during in-line monitoring of lacquers with other gloss levels.

Dispersion varnishes

In addition to UV-curable acrylate formulations and oil-based lacquers, dispersion varnishes represent a third group of materials, which are widely used in printing technology. They are characterized by extremely fast drying and a very thin thickness of the applied layers, which particularly makes calibration a very challenging task. Nevertheless, it could be shown that the coating weight of such layers can be determined with rather high precision [3], which is demonstrated in Fig. 9.

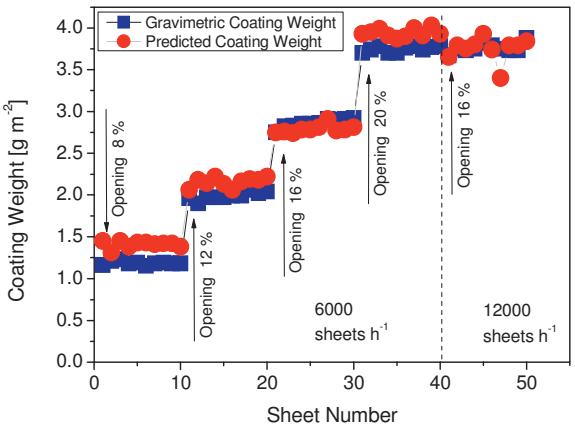

Figure 8: In-line monitoring of the coating weight of layers of a semi-matte varnish on paper. Coating weights from gravimetry are given for comparison.

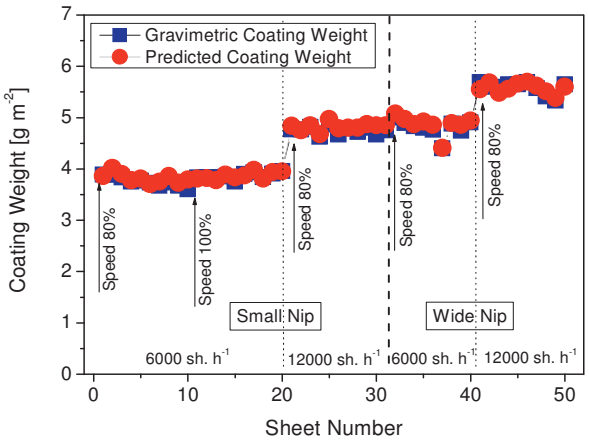

Figure 9: In-line monitoring of the coating weight of layers of a dispersion varnish printed on paper. Gravimetric reference data are shown for comparison.

Universal and multistage calibrations for varnishes with different compositions

In general, each calibration is dedicated to a special problem, i.e. a certain combination of a specific substrate and a specific varnish. Examples for calibrations, which were developed for chemically different classes of varnishes (acrylate, dispersion and oil-based systems) were shown above. However, in coating and printing technology, a huge range of formulations is used, which only differ in the specific composition. For example, UV-curable lacquers may be prepared on the basis of different acrylate monomers and oligomers. For time and cost reasons, it is impossible to develop a dedicated calibration model for each specific varnish formulation.

For this reason, we developed various strategies, which allow the characterization of coatings based on as many different lacquer formulations as possible. Two approaches will be introduced here: the use of universal and multistage calibration models, respectively. The principle of both methods will be discussed for acrylate formulations based on different oligomers.

The general procedure for the development of a universal calibration model is comparable to the method described for varnishes with different degrees of gloss, i.e. the different varnishes are

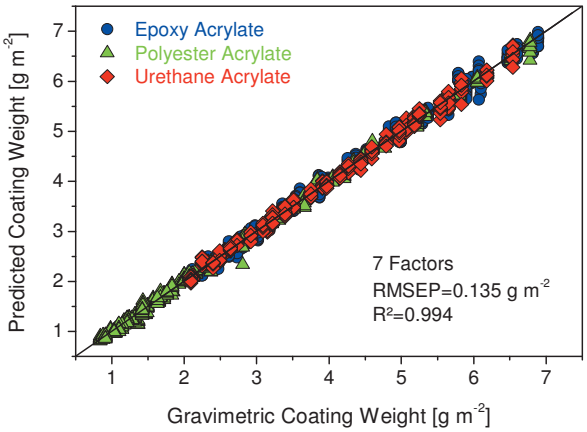

Figure 10: Universal calibration model for the coating weight of layers of different clear acrylate varnishes.

included in a joint calibration. An example for varnishes based on different acrylate oligomers is shown in Fig. 10.

Fig. 11 compares the predictions for the coating weight of layers of a formulation based on a urethane acrylate, which were obtained either by application of the universal calibration (Fig. 10) or the single calibration model, which had been developed for this specific varnish only. Both data sets show excellent correlation with the off-line data from gravimetry, which clearly demonstrates the power of this approach.

In the first step of multistage calibration procedure a qualitative analysis of the spectrum is carried out, i.e. the spectrum is assigned to one of the included single calibration models, which is then used for quantitative analysis. The test of this procedure with different varnishes in the laboratory (Fig. 12) and during in-line monitoring of the coating weight at the printing press (Fig. 13) proves the reliability of this approach.

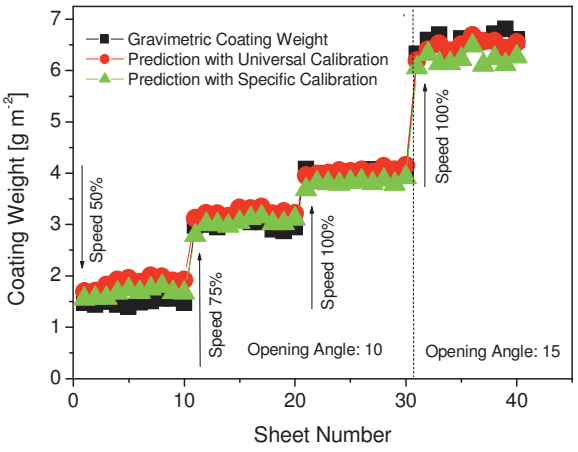

Figure 11: In-line monitoring of the coating weight of layers of a urethane acrylate varnish using the specific calibration for this varnish or the universal calibration model, respectively.

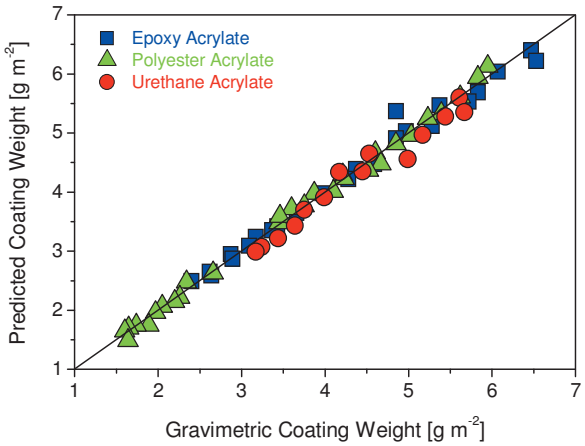

Figure 12: Prediction of the coating weight of printed layers of different acrylate varnishes using a multistage calibration procedure.

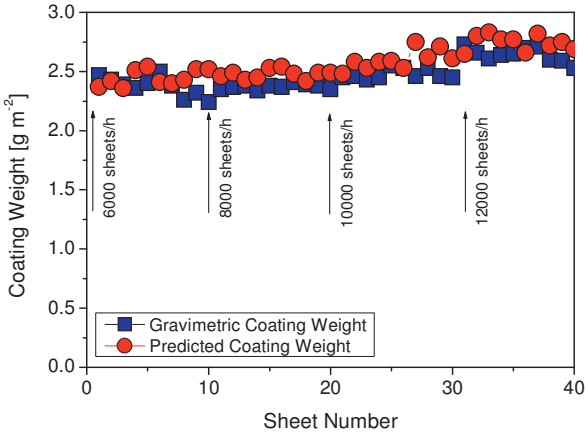

Figure 13: In-line monitoring of the coating weight of layers of an epoxy acrylate at different printing speeds using a multistage calibration procedure.

The results of this work originated in cooperation with B. Genest (Sächsisches Institut für die Druckindustrie GmbH, Leipzig).

Literature

[1] G. Mirschel, K. Heymann, T. Scherzer, Anal. Chem. 82 (2010), 8088.
[2] T. Scherzer, G. Mirschel, O. Savchuk, K. Heymann, B. Genest, Proc. RadTech Europe Conf., Basel, 2011.
[3] G. Mirschel, K. Heymann, O. Savchuk, T. Scherzer, B. Genest, Appl. Spectrosc., submitted.
[4] G. Mirschel, O. Savchuk, T. Scherzer, B. Genest, Anal. Bioanal. Chem., 2011, submitted.

Early stages of GaN film growth by ion-beam assisted epitaxy

J.W. Gerlach, L. Neumann, B. Rauschenbach

While many results of thin film epitaxy generally depend on the first few nanometers of deposited film material, the very first stages of film growth such as nucleation, island formation, coalescence of islands, etc. are of particular interest. In order to investigate the crucial early stages of hyperthermal ion-beam assisted epitaxial film growth, the IBA-MBE system at the IOM was extended by an UHV-SPM system, comprising scanning tunnelling microscopy (STM) and atomic force microscopy (AFM) options. In this way, the surface topography of samples can be recorded before, during and after the deposition process by interrupting the process and transferring the sample *in vacuo* to the SPM chamber.

Ultra-thin epitaxial GaN films were deposited directly on bare, super-polished 6H-SiC(0001) substrates, i.e. without any buffer layer, at a fixed substrate temperature of 700°C [1]. The nitrogen ion to gallium atom flux ratio (I/A ratio) was altered in the range from 0.9 to 3.2 by variation of the Ga deposition rate at a constant flux of hyperthermal nitrogen ions towards the sample. The total coverage with GaN was kept constant to achieve an average film thickness of 10 nm (≈ 40 GaN monolayers).

The influence of ion-beam irradiation during thin film epitaxy was studied by *in situ* monitoring during film growth by reflection high-energy electron diffraction (RHEED) in combination with *in vacuo* STM. Dependent on the I/A ratio the growth mode is found to be three-dimensional (I/A high) or two-dimensional (1.6 > I/A > 1.0) (Fig. 1). Too Ga-rich growth (I/A ≤ 1.0) leads to significant grain coarsening. The coverage of the SiC substrate with GaN, as estimated by using photoelectron spectra of film-related and substrate-related core-level electron lines (Fig. 2, left; Fig. 3) [1], is highest for the two-dimensionally grown films, indicating a high degree of coalescence, and decreases consistently for the films that exhibit grain coarsening. Azimuthal x-ray diffraction (XRD) scans show that the two-dimensionally grown films consist of a mixture of hexagonal and cubic polytypes (Fig. 2, right) that easily switch between each other during growth by stacking fault formation. However, as the full widths at half maximum (FWHM) of the XRD rocking curves are equally small for all the two-dimensionally grown films in the observed I/A ratio range (Fig. 3), the crystallite tilt distribution, representing the crystalline film quality, is evidently unaffected by coarsening or polytypism. Contrary, the FWHM is significantly broader for the three-dimensionally grown, hexagonal GaN films obtained at the highest I/A ratio.

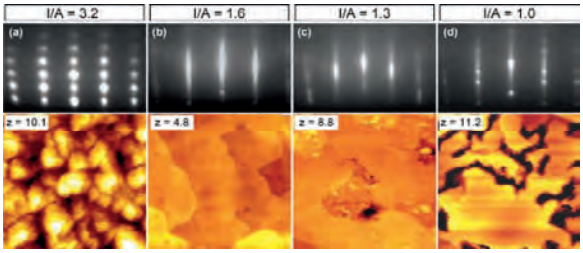

Figure 1: RHEED patterns (top) and corresponding surface topography obtained by STM (bottom) of GaN films deposited at different I/A ratios (scan range: 200 x 200 nm²; z-range given in nm).

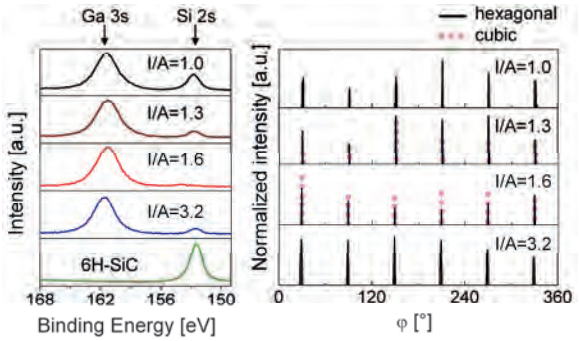

Figure 2: XPS spectra (left) and azimuthal XRD scans (right) of GaN films deposited at different I/A ratios.

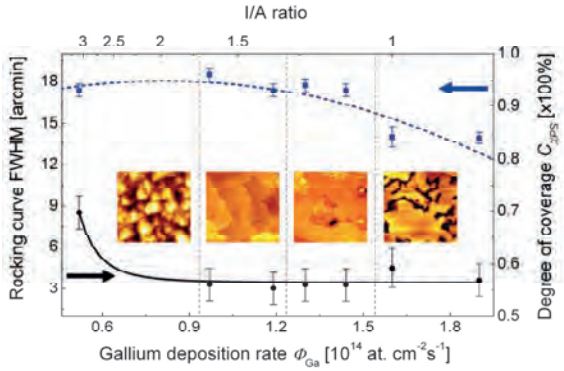

Figure 3: GaN(0002) XRD rocking curve FWHM (black) and degree of coverage of the substrate with GaN (blue) as a function of Ga deposition rate and I/A ratio.

Literature

[1] Neumann, J.W. Gerlach, B. Rauschenbach, Thin Solid Films. (accepted)

Self-organized patterning on Si by ion sputtering with simultaneous metal incorporation

F. Frost, M. Cornejo, M. Teichmann, B. Ziberi, D. Hirsch

Within a sub-project of the DFG research unit FOR 845 [1] this study focuses on the self-organized pattern formation on Si(001) by low-energy ion erosion without and with simultaneous incorporation of metal atoms, using a broad-beam ion source [2].

In the erosion facility used for this study, Fe atoms, together with other metals in lower concentrations, are sputtered from a stainless steel plate lining situated between the extraction system and the sample holder, and reach the sample together with the ions. The flux of Fe atoms onto the substrate can be controlled by the ion beam divergence, which in turn is determined mainly by the acceleration voltage and ion energy.

Si surfaces bombarded with low-energy ions without Fe incorporation (or very low Fe flux) show no pattern formation at incidence angles lower than ~ 65°. At higher incidence angles (θ = 65 - 85°) perpendicular-mode ripples were formed first. As the fluence is increased, isolated protuberances oriented parallel to the beam direction evolved. Their density on the surface increased with the fluence until they covered the entire surface. The faceting of these features underlines that gradient dependent sputtering is responsible for the formation of the structures.

The evolution of the surface topography under ion erosion with Fe incorporation (with relatively high Fe flux) is different. Especially at low angles, the evolution of the surface topography is affected. At this incidence angle range, ripples, dots or smooth surface were observed depending on the erosion conditions and the Fe flux. The ripples, which are perpendicular to the ion beam direction and have a wavelength between 40 nm and 70 nm and amplitude up to 10 nm, are of special interest due to their high regularity. With respect to the position of the Fe atoms in the samples, according to SIMS depth profile measurements, most of the Fe atoms are in the first 3 or 4 nm, and by HRTEM and EELS it was determined that they are situated mainly at the crest of the ripples.

In general, it was observed that when the concentration of Fe on the sample in the steady state was below ~ 0.5 × 10^{15} at cm^{-2} no pattern evolved while when it was above ~ 1 × 10^{15} at cm^{-2} nanostructures were formed.

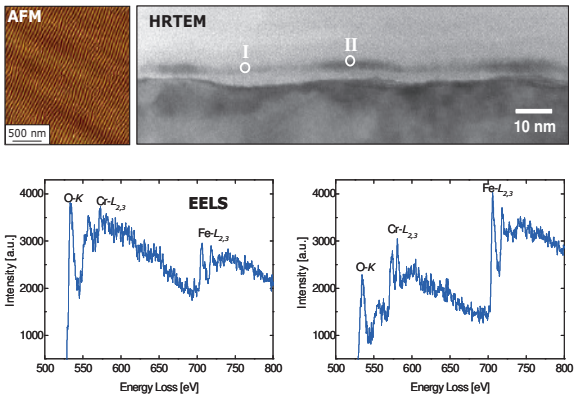

Figure 1: AFM and HRTEM images of a Kr^+ eroded Si surface (E_{ion}=1.5 keV, θ=20°, fluence 8.7×10^{18} cm^{-2}). The EELS spectra correspond to the positions I and II indicated in the HRTEM image. It is clearly seen that the concentration of Fe and Cr is higher at the crests of the ripples (dark region) than at the valley.

Concerning the specific role of the Fe atoms one possibility could be the formation of iron silicides and their rearrangement by self-organization. In turn, the non uniform distribution of the Fe atoms on the surface may generate sputter protected areas, like in the case of seed cone formation, which would lead to local differences in the sputter rate and height fluctuations on the surface. Overall the investigations correlate very well with results obtained in a co-deposition setup by using a fine focus, nearly parallel ion beam which is scanned across the surface [3, 4].

The results of this work originated in cooperation with Th. Michely, S. Macko, M. Engler (Universität zu Köln) and T. Höche, Fraunhofer-Institut für Werkstoffmechanik (IWM) Halle.

This project is funded by the Deutsche Forschungsgemeinschaft.

Literature

[1] www.iom-leipzig.de/FOR845
[2] M. Cornejo, Ph. D Thesis, Univ. Saarbrücken, 2011.
[3] S. Macko, F. Frost, B. Ziberi, D. Förster, Th. Michely, Nanotechnology 21 (2010) 085301.
[4] S. Macko, F. Frost, M. Engler, D. Hirsch, T. Höche, J. Grenzer Th. Michely, New J. Phys. 13, 073017 (2011).

Advanced electron microscopy in material science at IOM

A. Lotnyk, B. Rauschenbach

Electron microscopes (EMs), like transmission electron microscope (TEM) and scanning electron microscope (SEM), are powerful instruments in material science allowing the understanding of property-microstructure relations of functional materials links down to atomistic levels. Since the optimization of material properties can only be derived from a precise knowledge about defects and inhomogeneities on the atomic scale, particular point of the research plant is on the investigation of structure and composition with atomic resolution using advanced imaging TEM techniques as well as state of the art electron and X-ray spectroscopy techniques. In the last few decades, the performance of the TEM has improved slowly but steadily and the resolution limit has decreased from 1 nm to around 70 pm [1].

Recently, the facilities of IOM Leipzig are extended to two EMs, viz. a state of the art Cs-probe corrected analytical scanning TEM (STEM) (see Figure 1a) and environmental SEM (ESEM) (see Figure 1b). The both instrumentals are a part of new established laboratory (Leipziger nanoAnalitykum-LENA). The EMs as well as the laboratory have been acquired through financial support from the Free State of Saxon and the European Union.

The central instrument of the "Electron Microscopy" laboratory is a FEI Titan^3 G2 60-300 Cs-probe corrected analytical STEM equipped with a post-column Gatan Quantum SE/963P Imaging Energy Filter and with FEI ChemiSTEM^{TM} technology including a Super-X EDX System with four EDX SDD detectors and a novel, ultra-stable high-brightness X-FEG electron source. The ChemiSTEM technology provides superior element sensitivity allowing to detect very low concentrations of elements (well below 1 wt%) and it has advanced performance in EDX spectroscopy and fast EDX elemental mapping [2]. The Titan has an ultra high resolution of 70 pm in STEM imaging mode at 300 kV acceleration voltage. The microscope is also aligned at 80 kV acceleration voltage and can be used for investigations of e.g. beam sensitive samples. The microscope will be primary used for atomic resolution imaging and chemical analysis of nanostructures and interfaces. Software packages for state-of-the art image simulation, digital image processing, spectra data analyses and exit wave reconstruction from focal series support the evaluation and processing of the experimental results. Furthermore, a conventional Hitachi 8100 STEM for preliminary sample inspections as well as laboratories for conventional and advanced (using focused ion beam system) TEM specimen preparation are also available.

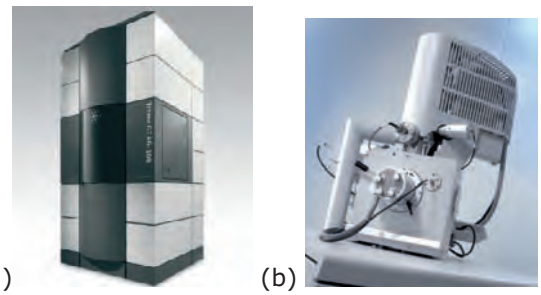

(a) (b)

Figure 1: (a) FEI Titan^3 G2 60-300 and (b) FEI Quanta 250 ESEM.

The FEI Quanta 250 FEG ESEM offers new possibilities compared to normal SEM and enables the investigation of nonconductive, hydrated or oily samples without preceding preparation steps [3]. This is achieved by the presence of a gas, in most cases water vapour, in the microscope chamber. The ESEM can be operated in three different imaging modes - high vacuum, low vacuum and ESEM. The relative humidity in the chamber can be varied by choosing appropriate parameters for pressure and temperature. The potential of in situ investigation of different processes is presented by e.g. changing the vapour pressure in the chamber to perform hydration/ dehydration experiments [4].

The main research projects of the new research group aim at the understanding of microstructure-property relationships of functional materials. Particular emphasis is put on the application of advanced TEM techniques in materials and surface science. Special interest is devoted to study the real structure of thin film systems, interfaces and nanomaterials at the atomic scale.

Literature

[1] K.W. Urban, Science 321 (2008) 506.
[2] P. Schlossmacher, D.O. Klenov, B. Freitag, H.S. von Harrach, Microscopy Today 18 (2010) 14.
[3] E. Stabentheiner, A. Zankel, P. Pölt, Protoplasma 246 (2010) 89.
[4] D. Stokes, Principles and Practice of VP-ESEM (2008), published by: John Wiley & Sons, Inc.

Numerically controlled local plasma jet oxidation of silicon

H. Paetzelt, G. Böhm, T. Arnold

Surface machining with nanometre accuracy of optical materials such as fused silica, SiC, ULE and silicon is still a challenging task. Especially, local shape modification with tool diameters in the range of a few millimetre to sub millimetre, in combination with computer controlled surface scanning machines is investigated [1].

Numerically controlled local plasma jet oxidation method comprises two processing steps to achieve material removal. A silicon oxide layer is generated on the silicon surface by oxygen radicals provided by the plasma jet, which is then removed by HF wet etching. The main advantages of this method compared to ion beam figuring and chemical plasma jet machining can be summarized as follows: Firstly, the silicon surface is protected from material contaminations during the process, since the new surface occurring after wet etching is the former interface between the newly generated silicon oxide and the silicon base material. Secondly, the employment of fluorine containing precursor gases like tetrafluoromethane (CF_4) or sulfurhexafluoride (SF_6) can be avoided. These gases are normally used in plasma dry etching methods possibly leading to SiO_xF_y residual layers. The plasma jet presented here uses argon and oxygen as gas supply, which are much easier to handle and even more cost efficient. Removing the generated silicon oxide film by wet chemical etching like HF treatment is a commonly used and well established method.

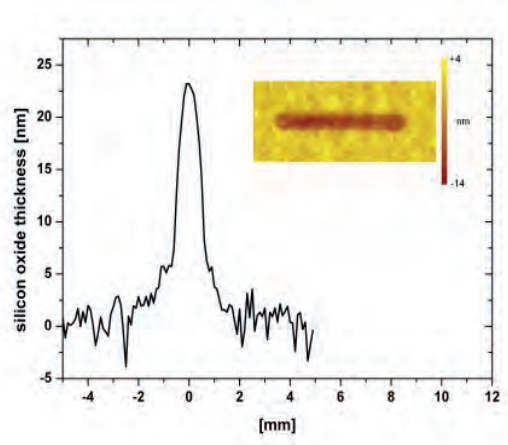

Figure 1: Thin film reflectometry thickness measurement of line oxidation (scan velocity 1 mm/s, 8 overlaying line scans). Interferometric measurement after HF etching (embedded).

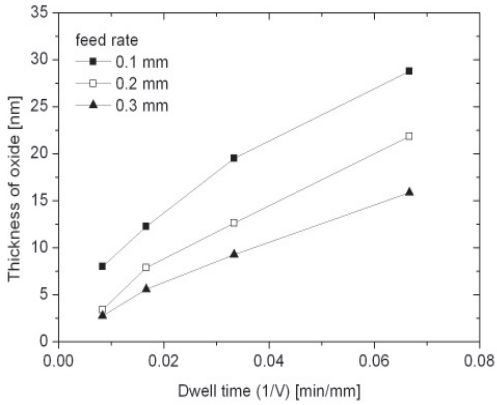

Figure 2: Silicon-oxide layer thickness vs. dwell time for different feed rates. Thin film reflectometry was used for the film thickness measurement of a plasma jet oxidized area of 5 x 5 mm² in Si wafer.

The atmospheric-pressure plasma jet source is based on a cross-shaped coaxial wave guide system powered by microwave at a frequency of 2.45 GHz. The argon and oxygen gas supply was held constant to 0.4 slm and 2 slm, respectively. All oxidation experiments have been made on Si-Mat polished silicon wafers with an orientation of (100) and a thickness of 525 µm. The oxide-layer thickness was measured using optical thin film profiler (see figure 1). The optical constant index of refraction n was determined using spectroscopic ellipsometry to be 1.446, which is near the value of thermal oxidized SiO_2 (n = 1.4571). The plasma jet produces a near Gaussian shaped oxidized profile with a size of 1.1 mm FWHM. Figure 2 shows the relationship between the silicon-oxide layer thickness of oxidized areas of 5 x 5 mm^2 and the dwell-time. The nearly linear relationship allows computer controlled surface modification and machining using local plasmajet oxidation of silicon as a high accuracy surface error correction method.

Literature

[1] T. Arnold, et. al., Vakuum in Forschung und Praxis 44 (2010) 10.

In-situ temperature distribution measurement on electric propulsion thruster

C. Bundesmann, F. Scholze, H. Neumann

Future space missions make high demands on the propulsion system. Electric propulsion (EP) thrusters are very promising candidates. Before flying into space, any thruster has to pass extensive test procedures. Therefore, an advanced diagnostic system for in-situ characterization of EP thrusters was realised [1, 2]. The system uses a high-precision five-axis positioning system and five diagnostic tools: a triangular laser head for surface profiling, a telemicroscope for high-resolution optical imaging, a pyrometer for thermal characterization, a Faraday cup for current density mapping, and an energy selective mass spectrometer for ion energy and beam pollution characterization.

Exemplarily, Figure 1 presents measurements of the accelerator grid surface temperature of a gridded ion thruster RIT-22 (Astrium ST) while firing [3]. Figure 1(a) shows a sketch of the experimental setup. Pyrometer line scans across the diameter of the thruster are performed. The pyrometer detects the integrated radiation intensity I of the test object in the spectral range from 2.0 µm to 2.8 µm.

The experimental pyrometer line scan data (Figure 1(b)) are modulated by interference-like structure, because the pyrometer measures always a mixture of radiation emitted by the grid surface and by the background (through the grid holes). The diameter of the measurement spot can be calculated and, hence, the fraction of the measurement spot area *F(y)*, which covers the grid, is modelled in dependence of the spot position *y*. By comparing any neighbouring pairs of minima and maxima of the area fraction curve with those of the pyrometer line scan curves the grid surface temperature is obtained by solving the following system of equations:

$$F_{\max}(y)I_{grid}(y)+[1-F_{\max}(y)]I_{back}(y)=I_{\max}(y),$$

$$F_{\min}(y)I_{grid}(y)+[1-F_{\min}(y)]I_{back}(y)=I_{\min}(y).$$

In Figure (1c) the extracted grid surface temperatures are plotted. These measured temperature data allow for a validation of the RIT 22 thermal modelling.

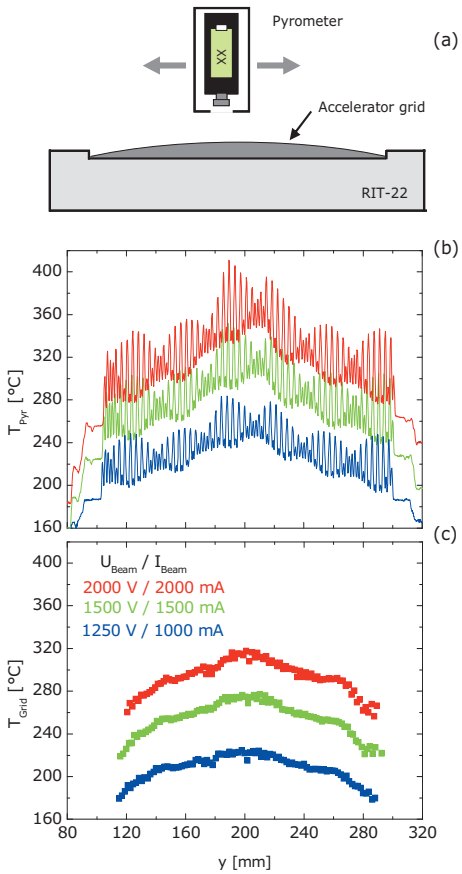

Figure 1: (a) Sketch of the experimental setup with pyrometer and top part of thruster. (b) Experimental pyrometer line scan data for different thruster operation parameters. (c) Accelerator grid surface temperature extracted from experimental data in (c).

Future activities are focused on minimizing the size of the in-situ diagnostics.

The results of this work are based on a collaboration with H.J. Leiter (Astrium Space Transportation), Moeckmuehl, Germany and F. Scortecci (Aerospazio Tecnologie s.r.l.), Siena, Italy.

Literature

[1] C. Bundesmann, M. Tartz, F. Scholze, et al.; Rev. Sci. Instrum. 81, 046106 (2010).
[2] C. Bundesmann, M. Tartz, F. Scholze, et al.; Proc. 31st Int. Electric Propulsion Conf., 2009, IEPC-2009-160.
[3] C. Bundesmann, M. Tartz, F. Scholze, et al., F. Scortecci; J. Propul. Power 27, 532-537 (2011).

Time dependent decomposition of metastable expanded austenite phases in FeCrNi and CoCr alloys

S. Mändl, D. Manova, J.W. Gerlach

Nitriding of stainless steel by energetic ions is a well-established laboratory technology, which is now ready to be employed by industry. The obtained layers of expanded austenite exhibit very high hardness and wear resistance, while maintaining the excellent corrosion resistance of the base material. However, this phase with an unusually large lattice expansion is metastable with a lifetime of around 100 hours at a temperature of 400 °C before developing CrN precipitates [1].

Nevertheless, the formation of this expanded phase without compromising the corrosion resistance by CrN is possible at temperatures beyond 400 °C when ascertaining a correspondingly short process time [2]. In addition to austenitic stainless steel 316Ti (DIN 1.4572), a detailed investigation of this phase transition – and its effect on the nitrogen diffusion – was carried out for the CoCr alloy HS188 (which shows identical behaviour as all major alloys used for biomaterials) [3].

Fig. 1 presents the layer thickness, as measured by SIMS as a function of the processing time for both alloys at a "high" and a "low" temperature. At the lower temperature, a perfect inverse parabolic growth rate, indicating diffusion limited layer growth was obtained for implantation times between 15 and 120 minutes. It has to be pointed out that no CrN was observed for the CoCr alloy at 450 °C even after the longest processing time.

At the high temperature of 580 °C, a very

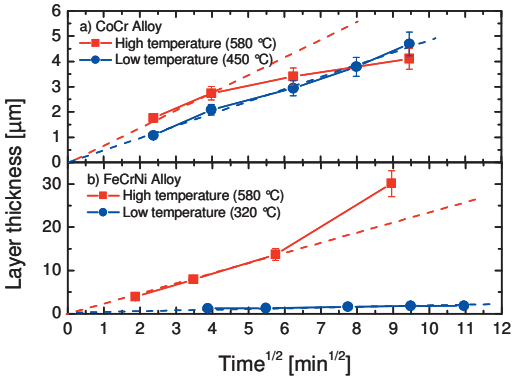

Figure 1: Evolution of layer thickness for "low temperature" and "high temperature" nitriding by plasma immersion ion implantation. Using the square root of the process time allows a direct comparison with an inverse parabolic growth rate $d \propto t^{1/2}$.

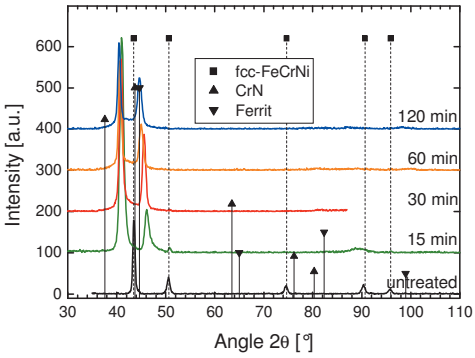

Figure 2: Phase identification by XRD for steel 316Ti as function of PIII processing time.

significant deviation of the thickness evolution is obtained for longer processing times, with the transition occurring earlier for the CoCr alloy than for the FeCrNi alloy, i.e. the austenitic stainless steel. The diffusion rate is decreasing in CoCr and increasing in steel when CrN precipitates are formed.

The differences in the relative diffusivity changes can be explained straightforward as the nitrogen diffusivity in the ferritic matrix is higher than in austenite, whereas nitrogen diffusion in Co without Cr admixtures is very low.

The corresponding XRD data for stainless steel are shown in Fig. 2. Here, the transition from expanded austenite towards CrN precipitates and a ferrite matrix occurs between 30 and 60 minutes. While no CrN is visible in the XRD data, the ferrite (110) reflection is clearly visible and different from the expanded (200) reflection.

Nevertheless, "fast and hot" processing may be viable alternative compared to long treatments at 350 – 380 °C, allowing for faster and more efficient industrial treatments. However, an exact process control is necessary to avoid CrN precipitates. Additional in-situ XRD investigations to quantify the temperature-time relationship with the aim to extract an activation energy are in progress.

Literature

[1] T. Bell, Key Engineering Materials 373 (2008) 289.
[2] D. Manova, F. Scholze, S. Mändl, H. Neumann, Surf. Coat. Technol. 205 (2011) S286.
[3] J. Lutz, Ph.D. Thesis, Univ. Leipzig, 2010.

Investigation of UV- and e-beam curing and properties of waterborne urethane acrylate nanodispersions

U. Decker, A. Prager, I. Reinhard, E. Bilz

Polyurethanes become more and more important for applications in green (waterborne) coating technologies due to their wide variability of physical and chemical properties which can additionally be modified by adding different particles, pigments and other additives.

To optimize the coatings several samples of Bayhydrol (Bayer Material Science) under different treatments were studied:

- The drying kinetics and the UV-curing were followed by real-time infrared spectroscopy at different temperatures.
- Dynamic mechanical analysis and microhardness measurements were peformed with cured (e-beam and UV) and uncured samples to get informations about crosslinking by the radiation.
- Different concentrations (0-15%) of SiO_2 nano particles (Köstrosol 03550 (Chemiewerke Bad Köstritz) unmodified and modified with Dynasilan Glyeo) were added.

The degree of conversion was quantified by measuring the acrylic double bond concentration (with IR at -810 cm^{-1}) during irradiation or on both sides of the sample.

After the drying process UV-light (1200 mW/cm^2) was applied under inert atmosphere (2 min N_2), different concentrations (0.5 %, 1%, 2% per weight of urethane) of photoinitiator Irgacure 819 (BASF) were tested. The investigations with REM show, that the sphere structure holds for the solid non- and irradiated coatings (Fig.1). Dimensions of the dispersed particles were about 150nm. The modified nanoparticles are about 60nm in size and the unmodified tend to give bigger aggregates, which results in slightly turbid coatings.

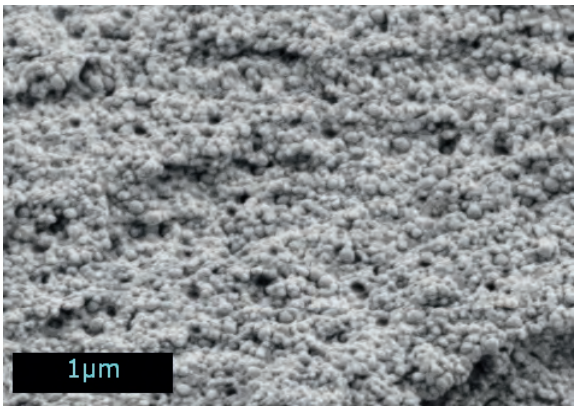

Figure 1: REM of Bayhydrol UV XP 2690+10%SiO_2 +1%IC819 UV-irradiation at 30°C.

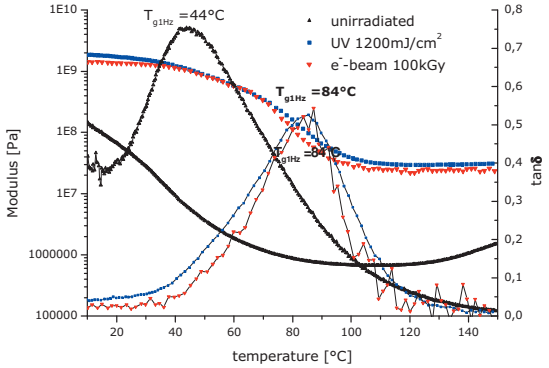

Figure 2: E-modulus and tanδ versus temperature of Bayhydrol UV 2317 unirradiated, UV-irradiated and e-beam irradiated.

The radiations treatment improves crosslinking between the dispersed particles and so the mechanical properties as E-module and micro hardness increased more than one order of magnitude.

The crosslinking is also reflected by the significant change of glass transition temperature Tg several ten degrees °C (Fig. 2).

The added nanoparticles improve also the mechanical properties, but from the current measurements it remains unclear, whether the modified particles really bonded or not to give a higher network density especially at high nanoparticle concentrations.

Also it is not quite clear, what happens in the dispersed urethane particles, because there the crosslinking will be hindered. These aspects will be in the centre of future work.

The results of this work originated in collaboration with M. Sofian B. Alias, Malaysia Nuclear Agency Bangi, Malaysia.

Wavelength dependence of the photochemical conversion of (meth)acrylates in the range of 172-222 nm (VUV-UVC)

W. Knolle, S. Naumov, K. Czihal, U. Decker, L. Prager, T. Scherzer

(Meth)acrylates can be cured directly, i.e. without the use of a conventional photoinitiator, by UVC or VUV light. This photochemical process has been studied in detail for 222 nm excitation, whereby α-scission of the carboxyl group was found to be the main pathway (quantum yield of ~ 0.3) for starting radical formation. The subsequent polymerisation kinetics is nearly the same as for conventional curing using photoinitiators, i.e. only a small depletion of C=O functionality (< 5%) upon complete conversion of C=C double bonds. In contrast, the band emission of Xe_2* (165-190 nm, λ_{max} = 172 nm) leads to a significant conversion of C=O groups [1].

In order to investigate this effect, thin layers (~ 500 nm) of lauryl (meth) acrylate as model compounds were irradiated with 172, 185 and 222 nm light directly on top of the ATR crystal. Fig. 1 shows the time dependence of typical vibrational bands assignable to the vinyl (810 cm^{-1}) and carboxyl (1188 and 1730 cm^{-1}) functionalities of the acrylates. The curves are normalized to the ~ 2900 cm^{-1} vibration of simple -CH_2, -CH_3 groups, hardly involved in photoprocesses, to account for material loss (photoablation) and/or shrinkage during polymerisation. In case of 185 nm light, the complete consumption of C=C bonds (solid black line) due to polymerisation goes along with only a slight depletion of C=O functionality (blue). The decrease of the C-O-C vibration to 40% reflects mainly the matrix hardening, as observed also in the case of PI-initiated polymerisation. After complete curing no further changes are observed. In case of 172 nm light,

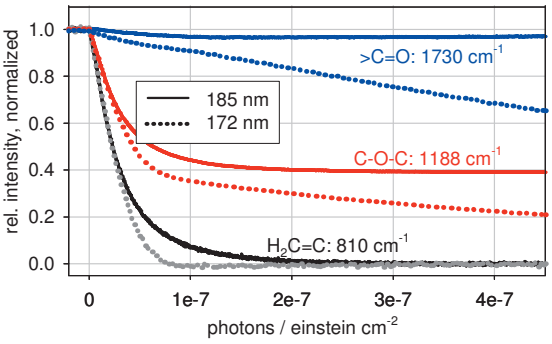

Figure 1: Time-dependence of the absorptivity of different functional groups during irradiation of lauryl acrylate with 172 and 185 nm light.

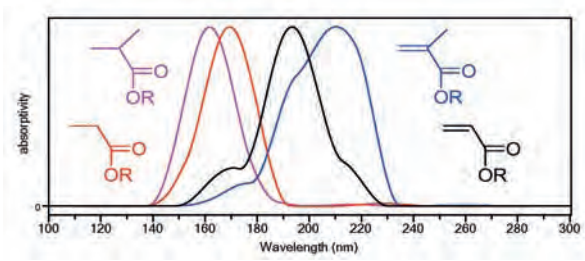

Figure 2: Calculated UV-spectra of model esters.

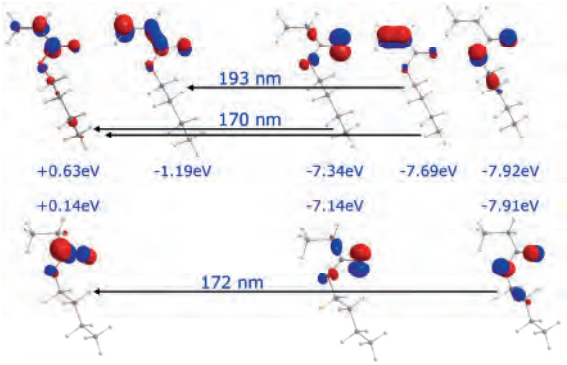

Figure 3: Molecular orbitals of unsaturated (top, butyl acrylate) and saturated (bottom, butyl propionate) esters.

at complete conversion of C=C bonds (exposure < 10^{-7} einstein/cm^2), a 7% decay of C=O occurs. However, continued irradiation leads to a further decay of both the C-O-C and C=O vibrations, the latter remaining longest (not shown). This correlates well with (i) further α-scission of the carboxyl bond leaving carbonyl groups and (ii) final consumption of remaining C=O bonds.

QC calculations reveal that the typical absorption bands in (meth)acrylates at ~ 200 nm (Fig. 2) are due to low-laying π–π* transitions involving orbitals on the conjugated C=C-C=O system (Fig. 3, top). Polymeriation leads to a loss of this conjugation and the main absorption bands are shifted to ~ 160-180 nm, reflecting excitation of the -C(=O)OC- group alone. Thus, only 172 nm light will excite the remaining carboxyl groups, leading to further crosslinking (wanted effect) and/or photoablation (unwanted). Thus, exposure must be carefully optimised.

Literature

[1] T. Scherzer, Macromol. Chem. Phys 213 (2012) 324-334.

Aspects of photochemical-based fabrication of gas barriers

L. Prager, L. Wennrich, H. Heller, U. Trimper

The successful realization of flexible organic light emitting diodes and flexible organic or inorganic photovoltaic cells is highly dependent on the existence of suitable barrier foils which protect these materials against oxygen and moisture. Therefore, the demand on **w**ater **v**apour and **o**xygen **t**ransmission **r**ates is very strong: WVTR ≤ 10^{-5} g (m^2 d)$^{-1}$ and OTR ≤ 10^{-5} cm^3 (m^2 d bar)$^{-1}$. Furthermore, encapsulation front sheets must feature high transparency, long-term stability and should be produced cost-efficiently. Some aspects of a photochemically based path for the development of such composites are presented here.

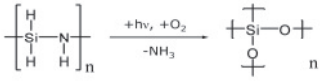

(1)

Using energy-rich vacuum UV irradiation (VUV), thin layers (100 nm) of the inorganic polysilazane oligomer perhydropolysilazane (PHPS) can be converted into dense silica layers (eq. 1). Based on the results of the research on kinetics and mechanism of the conversion process [1], a pilot plant had been designed and equipped to produce PHPS-based barrier layers on polymer foils, 20 cm wide, from roll to roll at process speeds up to 10 m/min. Typical oxygen and water vapour transmission rates (OTR and WVTR resp.) of such monolayer barrier foils are OTR ≤ 0.5 cm^3 (m^2 d bar)$^{-1}$ and WVTR ≤ 2 g (m^2 d)$^{-1}$. With the aim to enhance the barrier properties and to improve the above mentioned transmission rates, multilayers can be designed by alternating thin inorganic PHPS derived silica layers and organic interlayers, these latter being necessary for flexibility purpose and to decouple defects within the inorganic layer (Fig. 1).

An important problem during VUV triggered conversion of PHPS into silica is the fact that, in order to achieve a homogeneous conversion, the

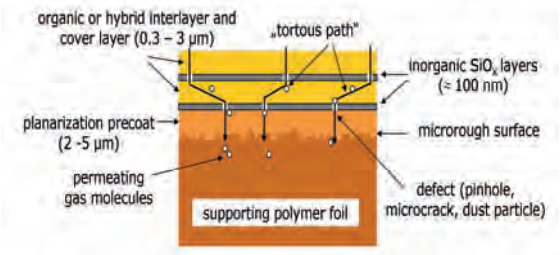

Figure 1: Scheme of an organic – inorganic bilayer on polymer foil.

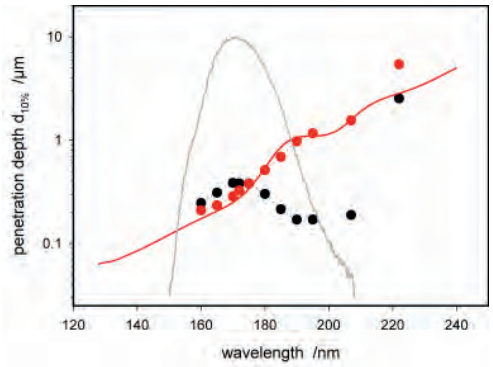

Figure 2: Penetration depth of VUV irradiation into hexanedioldiacrylate (HDDA): black – uncured layer, red – cured (polymerized) layer; grey line – emission spectrum of the Xe_2 excimer lamp.*

VUV irradiation should be uniformly absorbed within the whole PHPS layer. As a result, a considerable fraction of the radiation reaches the subjacent organic substrate causing there cleavage of covalent bindings, generation of radicals and finally crosslinking or damage [2]. For quantitative evaluation of the thickness of the affected layer the wavelength-dependent absorption coefficients and the penetration depths in the VUV range have been determined for some UV-curable resins (Fig. 2).

In the emission range of the Xe_2* excimer lamp the penetration depth changes from 200 nm to 1 µm for photons with wavelengths of 160 nm and of 195 nm, respectively. As a result, this irradiated fraction of the layer can be photochemically modified, in a beneficial or a detrimental way. In the course of the development of flexible high barrier foils using VUV irradiation, organic or hybrid interlayers have to be designed with irradiation resistance properties and enhanced adhesion properties to the SiO_x layer. By applying acrylate and epoxy based formulations, as well as hybrid organic-inorganic composites as interlayer and cover layer, oxygen barriers could be significantly improved reaching OTR ≤ 0.02 cm^3 (m^2 d bar)$^{-1}$.

Literature

[1] L. Prager, A. Dierdorf, H. Liebe, S. Naumov, S. Stojanović, R. Heller, L. Wennrich, M.R. Buchmeiser, Chem. Eur. J. 13 (2007) 8522.
[2] L. Prager, L. Wennrich, W. Knolle, S. Naumov, A. Prager, Mater. Chem. Phys. (2011) submitted.

Glycidol functionalization of plasma-treated polymer surfaces

A. Boulares-Pender, A. Prager, C. Elsner, S. Reichelt

The surface modification of polymers has evolved with the goal to suit various biological applications [1]. The optimization of the surface functionality for the covalent attachment of the bio-molecules is of primary interest. In order to limit protein adsorption at the surface, polyethylene glycol (PEG) is more often used as spacer than any other type of molecules [1, 2].

Polyglycerol are functional molecules with structure related to that of PEG and therefore can be used to distance biomolecules from the supporting surface, and also to reduce their adsorption [2]. Polyglycerols are generally prepared via cationic [3] or anionic polymerization of glycidol in the presence of initiators. Here we show that ionic species introduced at the surface of polymers, by a simple O_2-plasma treatment, are able to initiate the polymerization of glycidol in the absence of any initiator, producing a polyglycerol layer [4].

Upon oxygen plasma treatment (PS-1), PS samples were modified with glycidol, with an initial treatment of the initiator MeOK (PS-1.A) or without (PS-1.B). The modified PS samples were analyzed by XPS: samples not treated with the initiator (PS-1.B) also displayed high atomic oxygen content at their surface. The XPS C1s region (Fig. 1) clearly show peaks at 286.7 eV corresponding to the C-O bond of the glycidol ether segments on both modified samples.

SEM analysis shows interesting differences between the various surfaces (Fig. 2): both PS-1.A and PS-1.B surfaces present globular shapes, more pronounced with the MeOK-treated surfaces. These globular structures corresponding likely to nucleation sites at the plasma-treated polymer surface indicate that both treatments result in different glycidol polymerization processes; but, without differences in surface polarity or protein repulsion [4].

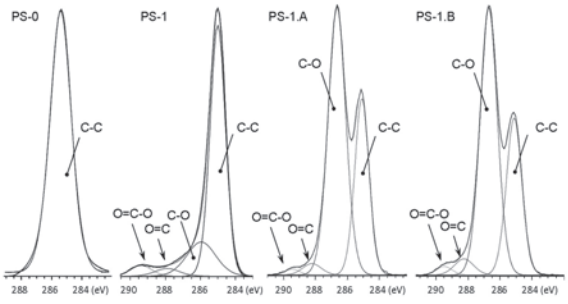

Figure 1: XPS-C1s of pristine (PS-0) and modified PS.

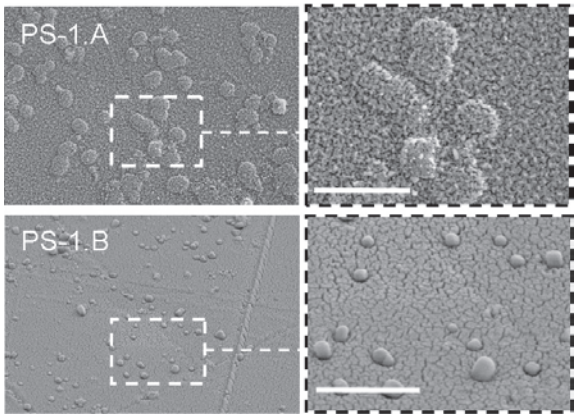

Figure 2: SEM of PS-1.A and PS-1.B. (Scale bar=1µm).

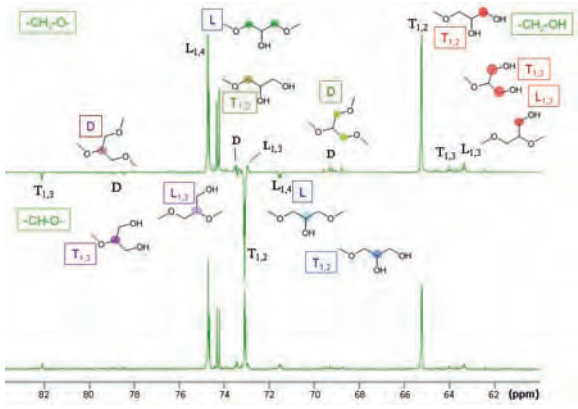

Figure 3: ^{13}C-NMR and DEPT spectra (up) (in D_2O) of polyglycerol recovered from PS-1.B.

^{13}C-NMR analysis of polyglycerol removed from the PS-1.B surface (Fig. 3) shows that the polymer formed at the surface is mainly linear: attested by linear segments (L) as well as corresponding terminal $T_{1,2}$ groups. Less prominent signals were assigned to the $T_{1,3}$, $L_{1,3}$ as well as to dendritic segments D.

The results of this work originated in collaboration with M. R. Buchmeiser, Universität Stuttgart, Germany.

Literature

[1] J.M. Goddard, J.H. Hotchkiss, Prog. Polym. Sci. 32 (2007) 698.
[2] J.G. Archambault, J.L. Brash, Colloids Surf. B 33 (2004) 111.
[3] A. Sunder et al., Macromolecules 33 (2000) 7682; A. Dworak et al., Macromol. Chem. Phys. 96 (1995) 1963.
[4] A. Boulares-Pender et al., J. Appl. Polym. Sci. 121 (2011) 2543.

Magnetic particles: A simple approach for the evaluation of surfaces for bio applications

S. Reichelt, C. Elsner

Magnetic microparticles are widely applied in separation technology. For instance biomarker labelled magnetic particles are used in cancer research. Their major advantage is the ease of separation from a liquid medium. In the framework of this project commercially available amine functionalized monosized, hydrophilic, spherical and superparamagnetitc PS-based microparticles (d ~ 2.5 µm) were used as model systems [1].

They constitute a tool for fast evaluation of the biocompatibility of polymeric surface modifications. The aim of our setup was to develop a system which enables the specific attachment of biomolecules via covalent linkage with simultaneously low unspecific protein adsorption.

Different amine containing polymers, as indicated in Figure 1, were immobilized via glutaraldehyde coupling based on an imine formation onto the NH_2-terminated pristine beads followed by covalent attachment of the enzyme trypsin. The bioactivity of the microparticles was evaluated using a biological test assay. The substrate N-benzoyl-L-arginin-p-nitroanilide was digested by the covalently immobilized trypsin and the corresponding release of p-nitroaniline was detected photometrically. Depending on the type of functionalization the bioactivity increased by a factor of 5.5 (Figure 1). A comparison of the adsorbed amount Γ of the best modification (4)

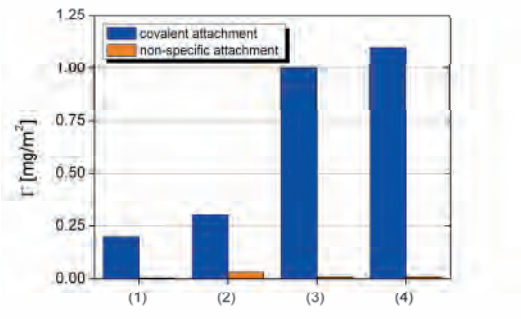

.Figure 1: Comparison of the covalently and non-specifically bound amount of trypsin attached to (1) pure beads and beads modified with (2) poly(ethylene imine) (PEI), (3) a 2-layer system of bovin serum albumin (BSA, for blocking of unspecific binding sites) and PEI, (4) poly(allyl amine) (PAAm). The modifiers were covalently attached to the amine-terminated beads via glutaraldehyde (GDA) linking.

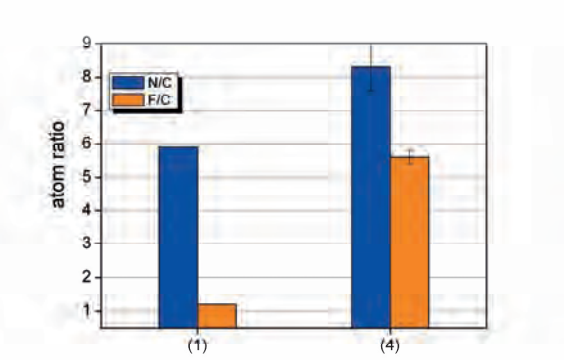

Figure 2: Atomic ratios of fluorine and nitrogen at the surface of pristine (1) and PAAm modified (4) beades determined by XPS using a labelling experiment with PFBA.

showed that although the non-porous beads have a comparable low surface area of 1.6 m²/g the adsorbed amount is comparable to high-surface (A=47 m²/g) porous polymeric particles (Γ = 1.8 mg/m²) [2]. The unspecific protein adsorption onto the modified beads remained unchanged.

Detailed XPS studies based on a labelling experiment with pentafluorobenzaldehyde (PFBA) showed that the amount of NH_2-groups and their accessibility to larger molecules was improved by functionalization with polyallylamine by a factor of 5 (figure 2).

Further evidence of the high bioactivity gave the digestion of the lectin concanavalin A. The peptide fragments were successfully detected with MALDI-mass spectrometry. Based on these results amine modified monoliths were developed for affinity chromatography [3].

The results of this work are based on a collaboration with M. R. Buchmeiser, Universität Stuttgart, Germany.

Literature

[1] Reichelt, S.; Elsner, C.; Pender, A.; Buchmeiser, M. R., J. Appl. Polym. Sci., 121, 2011, 3638.
[2] Malmsten, M., Larsson, A. Colloids Surf., B 2000, 18, 277.
[3] Reichelt, S., Elsner, C., Naumov, S. Prager A., Kuballa J., Buchmeiser, M., submitted to Analyst.

Synthesis and functionalization of porous polymeric materials

C. Elsner, C. Ernst, S. Reichelt

Porous polymeric, monolithic materials have gained a strong position in separation science. In particular, they are generally suited for small-scale separations of macromolecular compounds in capillaries or microfluidic devices (Fig 1, 2). Development of new methodologies for synthesis and modification of these materials provides the development of tailored applications and formats apart from the field of separation science. Thus, porous polymeric, monolithic materials are used as solid supports for catalysis and biocatalysis, responsive actuators and as scaffolds in regenerative medicine. During the last years novel thermal and radiation based techniques for synthesis and modification were developed. Thereby, radiation based spatially resolved functionalization-techniques of polymeric monolithic microdevices enables the construction of integrated fluidic systems and coupling of synthesis or transformation processes to separation and detection in one single unit. Based on previous studies according the modification of electron beam derived poly(acrylate)-monoliths by ring opening methatesis polymerization (ROMP) spatially resolved immobilization of the enzyme trypsin in a fluidic chip was accomplished (Fig. 3). The obtained device was successfully tested for the hydrolysis of Bz-Arg-OEt and proteins.

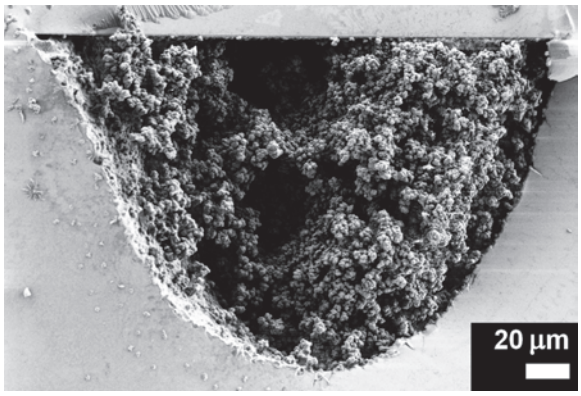

Figure 1: Monolithic polymer structure formed inside a fluidic chip by electron beam initiated polymerization.

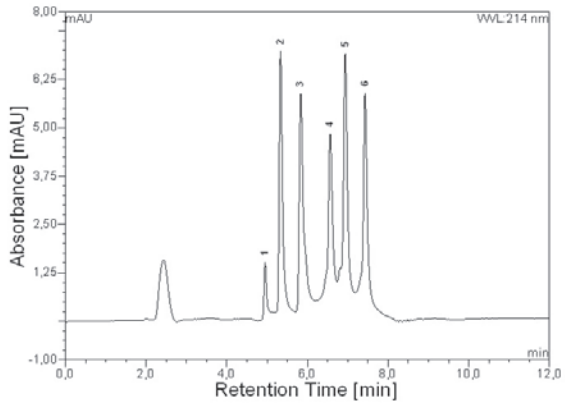

Figure 2: Separation of different proteins 1-6 on a chip integrated monolith.

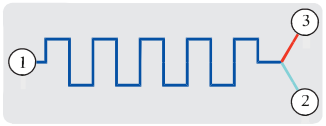

Figure 3: Schematic representation of a miniaturized monolithic chip device consisting of a separation channel (blue) and a channel with immobilized trypsin (red). During analysis substrates were loaded via inlet 3, eluents via inlet 2 and the UV-detection of hydrolysis products was performed via outlet 1.

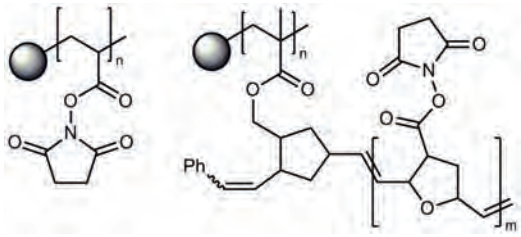

Figure 4: Activated monolithic supports with a poly-NHS-ester structure for the covalent immobilization of proteins generated via an electron beam assisted and a ROMP-based grafting approach.

Further investigations were performed according to the development of activated monolithic supports which enhance the immobilization of proteins on the one hand (Fig. 4) or reduce non-specific protein adsorption on the other hand. In the first case, the developed phases were tested for simple biotransformation processes, e.g. the trypsin catalyzed synthesis of dipeptides.

The results of this work originated in collaboration with M. R. Buchmeiser, Universität Stuttgart, Germany.

Literature

[1] C. Ernst, C. Elsner, A. Prager, et al. J. Appl. Polym. Sci. 121 (2011) 2551.
[2] C. Elsner, C. Ernst, M. R. Buchmeiser, J. Appl. Polym. Sci. 119 (2011) 1450.

Personal Activities

Doctoral Theses

Diploma and Master Theses

Bachelor Theses

Activities in Scientific Organisations

Honours and Awards

Doctoral Theses

Gjevori, Altin
Phase Formation of photoactive TiO_2 thin films by metal plasma immersion ion implantation and deposition
University of Tirana, Faculty of Natural Sciences, 2010

Khalil, Hazem
Preparation and Study of Some Novel Nanoparticle-Enforced Polymer Composites
Universität Leipzig, Fakultät für Chemie und Mineralogie, 2010

Lutz, Johanna
Diffusion Behaviour and Phase Formation for Ion Implanted Austenitic Metal Alloys
Universität Leipzig, Fakultät für Physik und Geowissenschaften, 2010

Pawar, Gjanan Manohar
Synthese Polymer-immobilisierter Katalysatoren und NHC-Metall Komplexe für die Organo- und Organometallkatalyse
Universität Leipzig, Fakultät für Chemie und Mineralogie, 2010

Kumar, Podiyanachari Santhosh
Regioselective Cyclopolymerization of 1,6-heptadiynes by the Action of Novel RuIV-Based Metathesis Initiators
Universität Leipzig, Fakultät für Chemie und Mineralogie, 2010

Schmidt, Christian
Synthese Stickstoff- und schwefelhaltiger konjugierter Polymere mittels Cyclopolymerisation von 1,6-Heptadiinen
Universität Leipzig, Fakultät für Chemie und Mineralogie, 2010

Weichelt, Franziska
Synthesis, Characterization and Application of Functional Nanocomposites and Monolithic Hybrid Materials
Universität Leipzig, Fakultät für Chemie und Mineralogie, 2010

Zou, Yuanlin
Synthesis of Group IV Transition Metal Catalysts for the Simultaneous Vinyl Insertion and Ring-Opening Metathesis (Co-)Polymerisation of Cyclic Olefins with Ethylene
Universität Leipzig, Fakultät für Chemie und Mineralogie, 2010

Cornejo, Marina
Pattern formation on Si surfaces by low-energy ion beam erosion
Universität des Saarlandes, Naturwiss.-Techn. Fakultät, 2011

Zachmann, Hendrik
Elektrische Defekte bei der ionenstrahlgestützten Abscheidung von $Cu(In,Ga)Se_2$
Universität Leipzig, Fakultät für Physik und Geowissenschaften, 2011

Diploma and Master Theses

Bergmann, Artjom, master thesis
In-situ XRD characterization of austenitic stainless steel during nitrogen low energy ion implantation
Universität Leipzig, Fakultät für Physik und Geowissenschaften, 2010

Fischer, Kristina, master thesis
Optimierung von Titandioxid-Nanoröhren zur Messung der mechanischen Dämpfungseigenschaften
Universität Leipzig, Fakultät für Chemie und Mineralogie, 2010

Rueppell, André, master thesis
Oberflächenmodifizierung von Dentalmaterial mittels eines atmosphärischen Plasmajets
Fachhochschule Osnabrück, Fakultät Ingenieurwissenschaften und Informatik, 2010

Schulte-Huxel, Henning, master thesis
Weiterentwicklung der fs-Lasertechnik zur Mikrostrukturierung von CIGS-Dünnschichtsolarzellen
Universität Leipzig, Fakultät für Physik und Geowissenschaften, 2010

Weise, Michael, diploma thesis
Dreidimensionale Germanium- und Silizium-Strukturen: Erzeugung mittels Glanzwinkeldeposition und Beeinflussung der Strukturmorphologie durch Depositionsparameter und geeignete Substratvorstrukturierung
Universität Leipzig, Fakultät für Physik und Geowissenschaften, 2010

Benke, Julia, master thesis
Characterization of thin $Ge_2Sb_2Te_5$ films produced via ultra-short pulsed laser deposition
Universität Leipzig, Fakultät für Physik und Geowissenschaften, 2011

Fichtner, Susanne, master thesis
Relaxation and Crystallisation of Amorphous Metallic Nanoparticles: A Molecular Dynamics Study
Universität Leipzig, Fakultät für Physik und Geowissenschaften, 2011

Starke, Sandra, master thesis
Immobilisierung von Trypsin an Polyethersulfon- und Polyvinylidenfluorid-Membranen mittels Elektronenbestrahlung
Hochschule Lausitz (FH), Fakultät für Naturwissenschaften, 2011

Fricke, Eike, master thesis
Dynamik und Reversibilität von Schertransformationszonen
Universität Leipzig, Fakultät für Physik und Geowissenschaften, 2011

Bachelor Theses

Huth, Steve
Herstellung von nanostrukturierten Substraten für medizinische Anwendungen
Universität Leipzig, Fakultät für Physik und Geowissenschaften, 2011

Activities in Scientific Organisations

W. Knolle

- Member of Editorial Board “Radiation Physics and Chemistry”

S. Mändl

- Member of the International Committee of the International Workshop “Plasma-Based Ion Implantation & Deposition”
- Guest editor, IEEE Transactions on Plasma Science, Special Issue on Plasma-Based Surface Modification and Treatment Technologies 2011, Volume 39.

H. Neumann

- Leader of the group „Electric Propulsion“ in technical committee "Chemische und Elektrische Raketenantriebe" of the DGLR

B. Rauschenbach

- Member of the Editional Board "Material Sciences”
- Member of the Steering Committee of Leipzig School of Natural Sciences – Building with Molecules and Nano-objects
- Member of the Curatorship “Innovation and Science”
- Member of the Coordination Board 'Plasma Surface Technologies'
- Member of the Advisory Board of the International Conference on Plasma Surface Engineering, Garmisch-Patenkirchen
- Member of the Advisory Board of the International Conference on Ion, Electron and Laser Physics (Bulgaria)
- Speaker of the DFG research group 845 "Selbstorganisierte Nanostrukturen durch niederenergetische Ionenstrahlerosion"
- Member of Internal Advisory Committee of the Translational Centre for Regenerative Medicine (TRM)
- Member of the Scientific Committee of the International Conference of Surface Modification of Materials

T. Scherzer

- Advisory Board des European Symposium of Photopolymer Science, 2010, Mulhouse, France
- Scientific Committee des 15th International Conference on Near Infrared Spectroscopy, 2011, Cap Town, South Africa

Honours and Awards

Thomas Arnold

- Wissenschafts- und Technologiepreis des IOM Leipzig 2010

Rajendar Bandari

- Preis für den besten Nachwuchswissenschaftler 2010

Marisa Mäder

- Preis für die beste Nachwuchswissenschaftlerin 2010

Sergej Naumov

- Wissenschafts- und Technologiepreis des IOM Leipzig 2011

Johanna Lutz

- Preis für die beste Nachwuchswissenschaftlerin 2011

Scientific Events

Scientific Meetings

Institute Colloquia

Lectures

Seminars

Scientific Meetings

XVII. Workshop „Oberflächentechnologien mit Plasma- und Ionenstrahlprozessen"
02.-05.03.2010, Mühlleithen, Dipl.-Phys. H. Neumann (organisation)

DFG-Begutachtung der Forschergruppe 845 "Selbstorganisierte Nanostrukturen"
15.05.-16.05.2010, Leipzig, Prof. Dr. B. Rauschenbach (organisation)

E-MRS Spring Meeting, Advanced Laser and Photon Processing of Materials
02.-06.06.2010, Straßbourg, Dr. K. Zimmer (co-organisation)

Interne Evaluation „Oberflächenultrapräzisionsbearbeitung"
16.09.2010, Leipzig, Prof. Dr. B. Rauschenbach (organisation)

V. Deutscher Workshop „Electric Propulsion" der Deutschen Gesellschaft für Luft- und Raumfahrt, Arbeitsgruppe Electric propulsion,
02.-03.11.2010, Leipzig, Dipl.-Phys. H. Neumann (organisation)

XVIII. Workshop „Oberflächentechnologien mit Plasma- und Ionenstrahlprozessen"
08.-10.03.2011, Mühlleithen, Dipl.-Phys. H. Neumann (Organisation)

Scientific Symposium "Hot nanoparticles and Nanostructures"
10.-11.10.2011, Leipzig, Prof. Dr. B. Rauschenbach

Scientific Symposium "Self-organized structure formation" Meeting of Material Research Society (MRS),
27.11.-02.12.2011 Boston, MA, USA, Prof. Dr. S.G. Mayr (co-organisation)

Institute Colloquia

Dr. Nico Scharnagl (14.01.2010)
Charité - Universitätsmedizin Berlin BCRT, Germany
Characterisation of Polymer Based Biomaterials

Prof. Dr. M. Stutzmann (21.01.2010)
Walter-Schottky-Institut München, Germany
Extreme Heterostrukturen: Biomoleküle auf Halbleitern

Prof. Dr. Cerwiec (04.02.2010)
INPL Nancy, France
Plasma assisted thermochemical treatments in Institut Jean Lamour: low temperature nitriding, carburizing of stainless steel and nickel base alloys

Prof. Dr. M. Kittler (08.04.2010)
Leibniz-Institut für Innovative Mikroelektronik & BTU Joint Lab Cottbus, Germany
Versetzungen in Si: Elektrische und optische Eigenschaften sowie ihre Nutzung als aktive Komponenten in neuartigen Bauelementen

Prof. Dr. M. Ulbricht (16.04.2010)
Universität Duisburg-Essen, Germany
Funktionalisierte Polymermembranen für selektive und effektive Trennverfahren

Prof. Dr. H. Hahn (22.04.2010)
FZ Karlsruhe, Germany
Electronically turnable nanostructures

Dr. M. Knez (29.04.2010)
MPI für Mikrostrukturphysik Halle/S., Germany
Atomic Layer Deposition - A View Beyond Thin Film Coating

Dipl.-Ing. H. Zimmermann (06.05.2010)
neoplas control GmbH, Germany
Q-MACS - Laserabsorptionsspektroskopie zur Überwachung
und -steuerung von Plasmaprozessen

Prof. Dr. U. Herr (27.05.2010)
Universität Ulm, Germany
Magnetic anisotropies in thin films and nanoparticles under large
mechanical stress

Dr. K. Dietliker (24.06.2010)
BASF Basel /Switzerland, Germany
Strahlenhärtung - Neue Möglichkeiten durch neue Photoinitiatoren

Prof. Dr. S. Simison and Prof. Dr. S. Brühl (30.09.2010)
University of Mar del Plata and Universidad Tecnológica Nacional, Argentinia
Corrosion behaviour of plasma nitrided and duplex treated stainless steel

Prof. Dr. J. Greene (05.10.2010)
University of Illinois, USA
Nucleation and growth of self-assembled nanostructures (the materials science of small things)

Dr. Th. Weitz (11.11.2010)
Harvard University Cambridge, USA & MPI für Festkörperforschung Stuttgart,
Germany
Field-effect transistors based on organic molecules

Prof. Dr. U. Krebs (18.11.2010)
Universität Göttingen, Institut für Metallphysik, Germany
Pulsed laser deposition of nanostructured materials

Dipl.-Phys. U. Preckwinkel (13.01.2011)
Bruker AXS GmbH, Karlsruhe, Germany
Aktuelle Röntgenbeugungstechnologie und neuartige Anwendungen

Prof. Dr. W. Arnold (18.01.2011)
Fraunhofer IZFP, Saarbrücken, Germany
Messung elastischer, anelastischer und nichtlinearer Eigenschaften von Werkstoffen mittels Nahfeldverfahren und Ultraschallkraftmikroskopie

Prof. Dr. S.G. Mayr (20.01.2011)
Translationszentrum für Regenerative Medizin & IOM Leipzig, Germany
Ferromagnetic shape memory alloys - fundamentals and miniaturization

Prof. Dr. P. Ziemann (27.01.2011)
Universität Ulm, Institut für Festkörperphysik, Germany
Nanolithografie auf Basis von Mizellen und Kolloiden: Ausgangspunkt für neue Eigenschaften

Prof. Dr. P. Böni (07.04.2011)
TU München, Germany & SwissNeutronics AG, Switzerland
Superspiegelbeschichtungen für die Neutronenoptik

Prof. Dr. J. Vienken (14.04.2011)
Fresenius Medical Care Bad Homburg, Germany
Gibt es Rahmenbedingungen für den Einsatz von Membranen in künstlichen Organen?

Prof. Dr. K. Wandelt (05.05.2011)
Universität Bonn, Germany
Spontane Nanostrukturbildung an Oberflächen

Prof. Dr. D. Falkenhagen (12.05.2011)
Universität Krems, Austria
Suspensionsgestützte extrakorporale Membran - Adsorptionstechnologien für die Blutreinigung als effiziente Therapieoption für das akute Leberversagen bzw. Sepsis

Prof. Dr. C. Croutxé-Barghorn (26.05.2011)
Université de Haute Alsace, Mulhouse, France
Recent Developments in UV Curing

Prof. Dr.-Ing. habil. Eberhard Manske (09.06.2011)
Technische Universität Ilmenau, Germany
Entwicklungstendenzen in der Nanopositionier- und Nanomesstechnik

Prof. Dr. M. Bradley (20.06.2011)
Department of Physics, Colorado State University, USA
Spontaneous nanoscale pattern formation induced by ion bombardment of binary compounds

Prof. Dr. T. Wichert (23.06.2011)
Universität des Saarlandes, Saarbrücken, Germany
Uphill-Diffusion in Halbleitern: Neuigkeiten zum Transport von Materie im Festkörper

Prof. Dr. V. Abetz (30.06.2011)
Helmholtz-Zentrum Geesthacht, Germany
Nanostrukturierung durch Selbstorganisation von Blockcopolymeren

Dr. G. Scherer (07.07.2011)
Paul Scherrer Institut Villigen, Switzerland
Protonen leitende Polymere Festelektrolyte für Brennstoffzellen

Prof. Dr. F. Otto (14.07.2011)
Max-Planck-Institut für Mathematik in den Naturwissenschaften Leipzig, Germany
Musterbildung und Mathematische Modelle

Prof. Dr. B. Abel (19.08.2011)
Wilhelm-Ostwald-Institut, Universität Leipzig, Germany
Analyse von Grenz- und Oberflächen mit Licht

Prof. Dr. A. Ostendorf (13.10.2011)
Universität Bochum, Germany
Dünnschichtbearbeitung mit ultrakurzen Laserpulsen

Prof. Dr. K. Samwer (27.10.2011)
Universität Göttingen, Germany
Glass – from an old material to modern physics

Dr. D. Duday (10.11.2011)
Centre de Recherche Public Belvaux, Luxemburg
Plasma surface treatment of wires

Prof. Dr. O.G. Schmidt (17.11.2011)
Leibniz-Institut für Werkstoffforschung, Dresden, Germany
Flexible nanomembranes

Prof. Dr. H. Kersten (08.12.2011)
Universität Kiel, Germany
Micro-particles as plasma probes

Lectures

J.W. Gerlach

- *Strukturaufklärung*
  Universität Leipzig, Fakultät für Physik und Geowissenschaften
  winter 10/11

T. Höche

- *Transmissionselektronenmikroskopie*
  Universität Leipzig, Fakultät für Physik und Geowissenschaften
  summer 10

- *Abbildung und Analyse mit Elektronen*
  Universität Leipzig, Fakultät für Physik und Geowissenschaften
  winter 10/11

S. Mändl

- *Quantenphysikalische Grundlagen der Nanotechnologie*
  Westsächsische Hochschule Zwickau
  winter 10/11

- *Plasmaphysik*
  Universität Leipzig, Fakultät für Physik und Geowissenschaften
  winter 10/11

- *Plasmaphysik*
  Universität Leipzig, Fakultät für Physik und Geowissenschaften
  winter 11/12

D. Manova

- *Plasma Immersion Ion Implantation*
  Universidad Technologica National, Uruguay
  two days short course

S.G. Mayr

- *Materialphysik*
  Universität Leipzig, Fakultät für Physik und Geowissenschaften
  summer 10

- *Strukturdefekte und Unordnung*
  Universität Leipzig, Fakultät für Physik und Geowissenschaften
  winter 10/11

- *Festkörperphysik*
  Universität Leipzig, Fakultät für Physik und Geowissenschaften
  summer 11

- *Defekte und Unordnung in Festkörpern*
  Universität Leipzig, Fakultät für Physik und Geowissenschaften
  winter 11/12

B. Rauschenbach

- *Introduction in Nanotechnology and Nanophysics*
  Universität Leipzig, Fakultät für Physik und Geowissenschaften
  summer 10

- *Strukturaufklärung*
  Universität Leipzig, Fakultät für Physik und Geowissenschaften
  winter 10/11

- *Ion-Solid Interaction*
  Universität Leipzig, Fakultät für Physik und Geowissenschaften
  summer 11

- *Physics of Thin Films*
  Universität Leipzig, Fakultät für Physik und Geowissenschaften
  winter 11/12

K. Zimmer

- *Mikro- und Nanotechnologie*
  Fachhochschule Mittweida
  winter 11/12

Seminars

S.G. Mayr

- *Materialwissenschaftliches Seminar*
  Universität Leipzig, Fakultät für Physik und Geowissenschaften
  summer 10, winter 10/11, summer 11, winter 11/12

B. Rauschenbach

- *Materialwissenschaftliches Seminar*
  Universität Leipzig, Fakultät für Physik und Geowissenschaften
  summer 10, winter 10/11, summer 11, winter 11/12

K. Zimmer

- *Mikro- und Nanotechnologie*
  Fachhochschule Mittweida
  winter 11/12

Publications and Presentations

Publications in Journals and Books

Conference Proceedings

Talks

Posters

Patents

Publications in Journals and Books

O. Albrecht, R. Zierold, S. Allende, J. Escrig, C. Patzig, B. Rauschenbach, K. Nielsch, D. Görlitz
Experimental evidence for an angular dependent transition of magnetization reversal modes in magnetic nanotubes
J. of Applied Physics **109** (2011) 093910

O. Albrecht, R. Zierold, C. Patzig, J. Bachmann, C. Sturm, B. Rheinländer, M. Grundmann, D. Görlitz, B. Rauschenbach, K. Nielsch
Tubular magnetic nanostructures based on glancing angle deposited templates and atomic layer deposition
Phys. Status Solidi B **247** (2010) 1365-1371

T. Arnold, G. Böhm, R. Fechner, J. Meister, A. Nickel, F. Frost, T. Haensel, A. Schindler
Ultra-precision surface finishing by ion beam and plasma jet techniques_status and outlook
Nucl. Instrum. Meth. A **616** (2010) 147-156

R. Bandari, T. Höche, A. Prager, K. Dirnberger, M. R. Buchmeiser
Ring-opening Mmtathesis polymerization-based pore size-selective functionalization of glycidyl methacrylate-based monolithic media: Access to size-stable nanoparticles for ligand-free metal catalysis
Chem. Eur. J. **16** (2010) 4650-4658

R. Bandari, A. Prager, T. Höche, M. R. Buchmeiser
Formation of Pd-nanoparticles within the pores of ring-opening metathesis polymerization-drived polymeric monoliths for use in organometallic catalysis
Arkivoc (2011) 54-70

A. Barkleit, S. Tsushima, O. Savchuk, J. Philipp, K. Heim, M. Acker, S. Taut, K. Fahmy
Eu(3+)-mediated polymerization of benzenetetracarboxylic acid studied by spectroscopy, temperature-dependent calorimetry, and density functional theory
Inorg. Chem **50** (2011) 5451-5459

F. Bauer, U. Decker, S. Naumov, C. Riedel
UV curing and matting of acrylate nanocomposite coatings by 172 nm excimer irradiation, Part 2
Prog. Org. Coat. **69** (2010) 287-293

M. Beyer, R. Flyunt, F. Weichelt, R. Emmler
Witterungsbeständige Beschichtungen von Holz und WPC auf der Basis von lösemittelarmen transparenten Acrylat-Silica-ZnO-Nanokompositen
Holztechnologie **6** (2010) 18-22

S. Bhattacharyya; T. Höche; J. Jinschek; I. Avramov; R. Wurth; M. Müller; C. Rüssel
Direct evidence of Al-rich layers around nanosized $ZrTiO_4$ in glass: Putting the role of nucleation agents in perspective
Crystal Growth & Design **10** (2010) 379-385

A. Boulares-Pender, A. Prager, S. Reichelt, C. Elsner, M. R. Buchmeiser
Functionalization of plasma-treated polymer surfaces with glycidol
J. Appl. Polym. Sci. **121** (2011) 2543-2550

O. Brede, S. Naumov
Femtosecond events in bimolecular free electron transfer
World Sci. Books (2010) 411-431

O. Brede, S. Naumov
Reactivity of radical cations in nonpolar condensed matter
In Charged Particle and Photon Interactions with Matter - Recent Advances, Applications and Interfaces (Taylor & Francis) **10** (2010) 237-264

O. Brede, S. Naumov
Free electron transfer - relations between molecule dynamics and reaction kinetics
Chem. Soc. Rev. **39** (2010) 3057-3071

M. R. Buchmeiser, R. Bandari, A. Prager-Duschke, A. Löber, W. Knolle
Polymeric Monolithic Media: Synthesis, Pore Size Selective Functionalization and Applications
Macromol. Symp. **287** (2010) 107-110

M. R. Buchmeiser, I. Ahmad, V. Gurram, P. S. Kumar
Pseudo-Halide and Nitrate Derivatives of Grubbs- and Grubbs-Hoveyda Initiators: Structural Features Related to the Alternating Ring Opening Metathesis Copolymerization of Norborn-2-ene with Cyclic Olefins
Macromolecules **44** (2011) 4098-4106

M. R. Buchmeiser, S. Camadanli, D. Wang, Y. Zou, U. Decker, C. Kühnel, I. Reinhardt
A Catalyst for the Simultaneous Ring-Opening Metathesis/Vinyl Insertion Polymerization
Angew. Chem. Int. Ed. **50** (2011) 3566-3571

C. Bundesmann, M. Tartz, F. Scholze, H. Neumann, H. J. Leiter, F. Scortecci
In Situ Thermal Characterization of the Accelerator Grid of an Ion Thruster
J. Propul. Power **27** (2011) 532-537

C. Bundesmann, M. Tartz, F. Scholze, H. J. Leiter, F. Scortecci, R. Y. Gnizdor, H. Neumann
An advanced in situ diagnostic system for characterization of electric propulsion thrusters and ion beam sources
Rev. Sci. Instrum. **81** (2010) 046106

S. Camadanli, U. Decker, C. Kühnel, I. Reinhardt, M. R. Buchmeiser
Homopolymerization of Ethylene, 1-Hexene, Styrene and Copolymerization of Styrene With 1,3-Cyclohexadiene Using (·5-Tetramethylcyclopentadienyl)dimethylsilyl(N-Ar_)amido-TiCl2/MAO (Ar_=6-(2-(Diethylboryl)phenyl)pyrid-2-yl, Biphen-3-yl)
Molecules **16** (2011) 567-582

I. Claussen, R.A. Brand, H. Hahn, S.G. Mayr
Relaxation scenarios in Fe_Pd and Fe_Pd_Cu ferromagnetic shape memory splats: Short range order and microstructure
Scripta Mater. **66** (2011) 163-166

I. Claussen, S.G. Mayr
Mechanical properties and twin boundary drag in Fe_Pd ferromagnetic shape memory foils_experiments and ab initio modeling
New J. Phys **13** (2011) 063034

M. Cornejo, B. Ziberi, C. Meinecke, F. Frost
Formation of two ripple modes on Si by ion erosion with simultaneous Fe incorporation
Appl. Surf. Sci. **257** (2011) 8659-8664

M. Cornejo, J. Völlner, B. Ziberi, F. Frost, B. Rauschenbach
Ion beam sputtering: A route for fabrication of highly ordered nanopattern
'Fabrication and Characterization in the Micro-Nano Range', Eds. A. Fernando Lasagni und A. F. Lasagni (Springer Berlin Heidelberg, 2011) **10** (2011) 69-94

M. Cornejo, B. Ziberi, Ch. Meinecke, D. Hirsch, J.W. Gerlach, T. Höche, F. Frost, B. Rauschenbach
Self-organized patterning on Si(001) by ion sputtering with simultaneous metal incorporation
Appl. Phys. A **102** (2011) 593-599

J. Dadda, E. Müller, S.Perlt, T. Höche, P. Bauer Pereira, R. Hermann
Microstructures and nanostructures in long-term annealed $AgPb_{18}SbTe_{20}$ (LAST-18) compounds and their influence on the thermoelectric properties
J Mater. Res. **26** (2011) 1800-1812

C. Díaz, J. A. García, S. Mändl, R. J. Rodríguez
Plasma immersion ion implantation for preventing metal ion releasing from CoCrMo alloys
IEEE Plasma Sci. **39** (2011) 3045-3048

T. Edler, S. Hamann, A. Ludwig, S.G. Mayr
Reversible fcc <--> bcc transformation in freestanding epitaxially grown Fe_Pd ferromagnetic shape memory films
SCRIPTA MATER **64** (2011) 89-92

M. Ehrhardt, K. Zimmer
Joining of Thin Films on Flexible Substrates with Nanosecond Laser Pulses
JLMN **6** (2011) 110-112

T. Edler, S.G. Mayr
Film Lift_Off from MgO: Freestanding Single Crystalline Fe_Pd Films Suitable for Magnetic Shape Memory Actuation _ and Beyond
Advanced Materials **22** (2010) 4969

M. Ehrhardt, K. Zimmer, G. Raciukaitis, P. Gecys
Laser-induced backside wet etching of fluoride and sapphire using picosecond laser pulses
Appl. Phys. A **101** (2010) 399-404

M. Ehrhardt, G. Raciukaitis, P. Gecys, K. Zimmer
Microstructuring of fused silica by laser-induced backside wet etching using picosecond laser pulses
Appl. Surf. Sci. **256** (2010) 7222-7227

I.-M. Eichentopf, G. Böhm, T. Arnold
Etching mechanisms during plasma jet machining of silicon carbide
Surf. Coat. Tech. **205** (2011) 430-434

C. Elsner, C. Ernst, M. R. Buchmeiser
Miniaturized Biocatalysis on Polyacrylate-Based Capillary Monoliths
J. Appl. Polym. Sci. **119** (2011) 1450-1458

C. Elsner, J. Zajadacz, K. Zimmer
Replication of 3D-microstructures with undercuts by UV-moulding
Microelectron. Eng. **88** (1) (2011) 60-63

C. Ernst, C. Elsner, A. Prager, B. Scheibitz, M. R. Buchmeiser
UV-and Thermally-Triggered Ring-Opening Metathesis Polymerization for the Spatially Resolved Functionalization of Polymeric Monolithic Devices
J. Appl. Polym. Sci. **121** (2011) 2551-2558

K. Fischer, S.G. Mayr
In-Plane Mechanical Response of TiO_2 Nanotube Arrays _ Intrinsic Properties and Impact of Adsorbates for Sensor Applications
Adv. Mater. **23** (2011) 3838-3841

P. Gaikwad, K. I. Priyadarsini, S. Naumov, B. S. M. Rao
Radiation and Quantum Chemical Studies of Chalcone Derivatives
J. Phys. Chem. **114** (30) (2010) 7877-7885

J. A. García, C. Díaz, S. Mändl, J. Lutz, R. Martínez, R. J. Rodríguez
Tribological Improvements of Plasma Immersion Implanted CoCr Alloys
Surf. Coat. Tech. **204** (2010) 2932

P. Gecys, G. Raciukaitis, M. Ehrhardt, K. Zimmer
ps-laser scribing of CIGS films at different wavelengths
Appl. Phys. A **101** (2010) 373-378

G. P. H. Gubbels, C. van Drunen, G. Böhm, T. Arnold, F. Kamphues, W. L. M. Gielesen
Fabrication of strongly curved aspheric silicon carbide mirrors
Paper Nr. O5B.1, euspen 10th International Conference, Delft, 31.05.-04.06. (2010)

A. Gjevori, J.W. Gerlach, D. Manova, W. Assmann, E. Valcheva, S. Mändl
Influence of Auxiliary Plasma Source and Ion Bombardment on Growth of TiO_2 Thin Films
Surf. Coat. Tech. **205** (2011) 232-234

M. Häberlen, J.W. Gerlach, B. Murphy, J. K. N. Lindner, B. Stritzker
Structural characterization of cubic and hexagonal GaN thin films grown by IBAMBE on SiC/Si
J. Cryst. Growth **312** (2010) 762-769

S. Hamann, M. E. Gruner, S. Irsen, J. Buschbeck, C. Bechtold, I. Kock, S.G. Mayr, A. Savan, S. Thienhaus, E. Quandt, S. Fähler, P. Entel, A. Ludwig
The ferromagnetic shape memory system Fe_Pd_Cu
Acta Materialia **58** (2010) 5949

K. Heymann, G. Mirschel, T. Scherzer
Monitoring of the Thickness of Ultraviolet-Cured Pigmented Coatings and Printed Layers by Near-Infrared Spectroscopy
Appl. Spectrosc. **64** (2010) 419-424

D. Hiller, R. Zierold, J. Bachmann, M. Alexe, Y. Yang, J.W. Gerlach, A. Stesmans, M. Jivanescu, U. Müller, J. Vogt, H. Hilmer, P. Löper, M. Künle, F. Munnik, K. Nielsch, M. Zacharias
Low temperature silicon dioxide by thermal atomic layer deposition: Investigation of materials properties
J. Appl. Phys. **107** (2010) 064314

D. Hiller, S. Götze, F. Munnik, M. Jivanescu, J.W. Gerlach, J. Vogt, E. Pippel, N. Zakharov, A. Stesmans, M. Zacharias
Nitrogen at the Si-nanocrystal/SiO_2 interface and its influence on luminescence and interface defects
Phys. Rev. B **82** (2010) 195401

T. Höche
Crystallization in Glass - Elucidating a Realm of Diversity by Transmission Electron Microscopy
J. Mater. Sci. **45** (2010) 3683-3696

A. Jenichen, C. Engler
Stability and band gaps of InGaP, BGaP, and BInGaP alloys: Density-functional supercell calculations
Phys. Status Solidi B **247** (2010) 59-66

J. A. Jacob, S. Naumov, T. Mukherjee, S. Kapoor
Preparation, characterization, surface modification and redox reactions of silver nanoparticles in the presence of tryptophan
COLLOID SURFACE B: Biointerfaces **87** (2011) 498-504

M. Janietz, T. Arnold
Surface figuring of glass substrates by local deposition of silicon oxide with atmospheric pressure plasma jet
Surf. Coat. Tech. **205** (2011) S351-S354

A. Jenichen, C. Engler
Metal-organic chemical vapour deposition of (BInGa)P: Density-functional calculations to the mechanisms
J. Cryst. Growth **312** (2011) 10-15

E. Kesters, Q. T. Le, M. Lux, L. Prager, G. Vereecke
Removal of post-etch 193 nm photoresist in porous low-k dielectric patterning using UV irradiation and ozonated water
Microelectr. Eng. **87** (2010) 1674-1679

H. Khalil, H.-J. Gläsel, L. Wennrich, A. Prager, M. R. Buchmeiser
Dihydroxyaluminum Carbocylate Nanoparticles with narrow size Distribution: Synthesis, Characterization and use for high Optical Transparency Protective Polymeric Coatings
Macromol. Mater. Eng. **295** (2010) 170-177

C. Khare, C. Patzig, J.W. Gerlach, B. Rauschenbach, B. Fuhrmann
Influence of substrate temperature on glancing angle deposited Ag nanorods
J. Vac. Sci. Technol. A **28** (4) (2010) 1002-1009

C. Khare, R. Fechner, J. Bauer, M. Weise, B. Rauschenbach
Glancing angle deposition of Ge nanorod arrays on Si patterend substrates
J. Vac. Sci. Technol. A **29** (2011) 041503

C. Khare, B. Fuhrmann, H. S. Leipner, J. Bauer, B. Rauschenbach
Optimized growth of Ge nanorod arrays on Si patterns
J. Vac. Sci. Technol. A **29** (2011) 051501

C. Khare, J.W. Gerlach, M. Weise, J. Bauer, T. Höche, B. Rauschenbach
Growth temperature altered morphology of Ge nanocolumns
Phys. Status Solidi A **208** (2011) 851–856

C. Khare, R. Fechner, J. Bauer, M. Weise, B. Rauschenbach
Glancing angle deposition of Ge nanorod arrays on Si patterned substrates
J. Vac. Sci. Technol. A **29** (4) (2011) 041503

H. Khesbak, O. Savchuk, S. Tsushima, K. Fahmy
The role of water H-bond imbalances in B-DNA substate transitions and peptide recognition revealed by time-resolved FTIR spectroscopy
J AM CHEM SOC **133** (15) (2011) 5834-5842

W. Knolle, L. Wennrich, S. Naumov, K. Czihal, L. Prager, D. Decker, M. R. Buchmeiser
222 nm Photo-Induced Radical Reactions in Silazanes. A combined Laser Photolysis, EPR, GC-MS and QC Study
Phys. Chem. Chem. Phys. **12** (2010) 2380-2391

I. Kock, S. Hamann, H. Bruken, T. Edler, S.G. Mayr, A. Ludwig
Development and characterization of $Fe_{70}Pd_{30}$ ferromagnetic shape memory splats
Intermetallics **18** (2010) 877

A. Lejars, D. Manova, S. Mändl, D. Duday, T. Wirtz
Simulated Plasma Immersion Ion Implantation Processing of Thin Wires
J. Appl. Phys. **108** (2010)

A. Löber, B. Scheibitz, B. Frerich, M. R. Buchmeiser
Ring-Opening Metathesis Polymerization-Derived Monolithic Materials: Novel Syntheses and Applications
Macromol. Symp. **293** (2010) 48-52

S. H. Lubbad, M. R. Buchmeiser
Fast separation of low molecular weight analytes on structurally optimized polymeric capillary monoliths
J. Chromatogr. A **1217** (2010) 3223-3230

J. Lutz, S. Mändl
Reduced Tribocorrosion of CoCr Alloys in Simulated Body Fluid after Nitrogen PIII
Surf. Coat. Tech. **204** (2010) 3043-3046

J. Lutz, C. Díaz, J. A. García, C. Blawert, S. Mändl
Corrosion Behaviour of Medical CoCr Alloy After Nitrogen Plasma Immersion Ion Implantation
Surf. Coat. Tech. **205** (2011) 3043-3049

J. Lutz, D. Manova, J.W. Gerlach, M. Störmer, S. Mändl
Interpretation of Glancing Angle and Bragg-Brentano XRD Measurements for CoCr Alloy and Austenitic Stainless Steel after PIII Nitriding
IEEE T PLASMA SCI **39** (2011) 3056-3060

Y. Ma, M. Zink, S.G. Mayr
Biocompatibility of single crystalline $Fe_{70}Pd_{30}$ ferromagnetic shape memory films
Appl. Phys. Lett. **96** (2010) 213703

S. Macko, F. Frost, B. Ziberi, D. Förster, T. Michely
Is keV ion induced pattern formation on Si(001) caused by metal impurities?
Nanotechnology **21** (2010) 085301

S. Macko, F. Frost, M. Engler, D. Hirsch, T. Höche, J. Grenzer, T. Michely
Phenomenology of iron-assisted ion beam pattern formation on Si(001)
New J. Phys **13** (2011) 073017

M. Mäder; T. Höche; J.W. Gerlach; S. Perlt; J. Dorfmüller; R. Vogelgesang; K. Kern; B. Rauschenbach
Plasmonic Activity of Large-Area Gold-Nanodot Arrays on Arbitrary Substrates
Nano Letters **10** (2010) 47-51

M. Mäder, S. Perlt, T. Höche, H. Hilmer, M. Grundmann, B. Rauschenbach
Gold nanostructure matrices by diffraction mask-projection laser ablation: extension to previously inaccessible substrates
Nanotechnology **21** (2010) 175304

M. Mäder, T. Höche, J.W. Gerlach, R. Böhme, B. Rauschenbach
Nanostructures by diffraction mask projection laser ablation
Phys. Status Solidi B **247** (2010) 1372-1383

D. Manova, J.W. Gerlach, F. Scholze, S. Mändl, H. Neumann
Nitriding of austenitic stainless steel by pulsed low energy ion implantation
Surf. Coat. Tech. **204** (2010) 2919-2922

D. Manova, J. Lutz, S. Mändl
Sputtering Effects During Plasma Immersion Ion Implantation of Metals
Surf. Coat. Tech. **204** (2010) 2875-2880

D. Manova, J.W. Gerlach, S. Mändl
Thin Film Deposition Using Energetic Ions
Materials **3** (2010) 4141

D. Manova, F. Scholze, S. Mändl, H. Neumann
Nitriding of Austenitic Stainless Steel Using Pulsed Low Energy Ion Implantation
Surf. Coat. Tech. **205** (2011) 286-289

D. Manova, J. Lutz, J.W. Gerlach, H. Neumann, S. Mändl
Relation between Lattice Expansion and Nitrogen Content in Expanded Phase after Nitrogen Insertion in Austenitic Stainless Steel and CoCr Alloys
Surf. Coat. Tech. **205** (2011) 290-293

S. Mändl
Ionenbeschuss von Polymeren für die Medizintechnik
Vakuum in Forschung und Praxis **22** (2010) 36-40

G. Mark, S. Naumov, C. von Sonntag
The Reaction of Ozone with Bisulfide (HS-) in Aqueous Solution -Mechanistic Aspects
OZONE-SCI ENG **33** (2011) 37-41

J. Meister, T. Arnold
New Process Simulation Procedure for High-Rate Plasma Jet Machining
Plasma Chem Plasma Process **31** (2011) 91-107

G. Merenyi, J. Lind, S. Naumov, C. von Sonntag
Reaction of Ozone with Hydrogen Peroxide (Peroxone Process): A Revision of Current Mechanistic Concepts based on Thermokinetic and Quantum-Chemical Considerations
Environ. Sci. Technol. **44** (2010) 3505-3507

G. Merényi, J. Lind, S. Naumov, C. von Sonntag
The reaction of ozone with the hydroxide ion. Mechanistic considerations based on thermokinetic and quantum-chemical calculations. The role of HO4 in superoxide dismutation
Chem. Eur. J. **10** (2010) 1372-1377

P.-E. Millard, L. Barner, J. Reinhardt, M. R. Buchmeiser, C. Barner-Kowollik, A. H.E. Müller
Synthesis of water-soluble homo-and block-copolymeres by RAFT polymerization under g-irradiation in aqueous media
Polym. J. **51** (2010) 4319-4328

G. Mirschel, K. Heymann, T. Scherzer
Simultaneous In-Line Monitoring of the Conversion and the Coating Thickness in UV-Cured Acrylate Coatings by Near-Infrared Reflection Spectroscopy
Anal Chem **82** (2010) 8088-8094

G. Mirschel, K. Heymann, T. Scherzer
Simultaneous Measurement of Coating Thickness and Conversion of UV-Cured Acrylate Coatings by In-line NIR Spectroscopy
Near Infrared Spectroscopy: Proceedings of the 14th International Conference, ed. by S. Saranwong, S. Kasemsumran, W. Thanapase, P. Williams, IM Publications, Chichester (2010) 1157-1159

R. Nagar, C. Patzig, B. Rauschenbach, B. R. Metha, J. P. Singh
Mechanical characteristics of Silicon nanostructures using force distance spectroscopy
J. Nanosci. Nanotechnol. **10** (2010) 2994-3000

R. Nagar, B. R. Metha, J. P. Singh, C. Patzig, B. Rauschenbach, D. Kanjilal
Enhancement of stiffness of vertically standing Si nanosprings by energetic ions
J. Appl. Phys. **107** (2010) 094315

S. Naumov, G. Mark, A. Jarocki, C. von Sonntag
The Reactions of Nitrite Ion with Ozone in Aqueous Solution - New Experimental Data and Quantum-Chemical Considerations
Ozone-Sci. Eng. **32** (2010) 430-434

S. Naumov, C. von Sonntag
Quantum Chemical Studies on the Formation of Ozone Adducts to Aromatic Compounds in Aqueous Solution
Ozone-Sci. Eng. **32** (2010) 61-65

S. Naumov, C. von Sonntag
Gibbs Free Energies of Reactions of Ozone with Free Radicals in Aqueous Solution Quantum-chemical Calculations
Environ. Sci. Technol. **45** (2011) 9165-9204

S. Naumov, C. von Sonntag
On the reaction of the hydroxyl radical with oxygen in aqueous solution 1 and the pKa of HO3
J. Phys. Org. Chem. **24** (2011) 600-602

C. Patzig, A. Miessler, T. Karabacak, B. Rauschenbach
Arbitrarily shaped Si nanostructures by glancing angle ion beam deposition
Phys. Status Solidi B **247** (2010) 1310-1321

C. Patzig, C. Khare, B. Fuhrmann, B. Rauschenbach
periodically arranged Si nanostructures by glancing angle deposition on patterend substrates
Phys. Status Solidi B **247** (2010) 1322-1334

G. M. Pawar, M. R. Buchmeiser
Polymer-Supported, Carbon Dioxide-Protected N-Heterocyclic Carbenes: Synthesis and Application in Organo- and Organometallic Catalysis
Adv. Synth. Catal. **352** (2010) 917-928

G. M. Pawar, J. Weckesser, S. Blechert, M. R. Buchmeiser
Ring-Opening Metathesis Polymerization-Derived Block Copolymers Bearing Chelating Ligands: Synthesis, Metal Immobilization and Use in Hydroformylation under Micellar Conditions
Beilstein J. Org. Chem. **6** (2010) 1199-1205

S. D. Phadatare, K. K. K. Sharma, B. S. M. Rao, S. Naumov, G. K. Sharma
Spectral Characterization of the Guanine C4-OH adduct in Aqueous Medium: A Radiation Chemical Study
J. Phys. Chem. **115** (2011) 13650-13658

J. P. Pocostales, M. M. Sein, W. Knolle, T. C. Schmidt, C. von Sonntag
Degradation of Ozone-Refractory Organic Phosphates in Wastewater by Ozone and Ozone/Hydrogen Peroxide (Peroxone): The Role of Ozone Consumption by Dissolved Organic Matter
Environ. Sci. Technol. **44** (2010) 8248-8253

B. Rauschenbach, C. Patzig
Dünne Schichten durch Deposition unter streifenden Einfall
Vakuum in Forschung und Praxis **22** (2010) 14-19

S. Reichelt, C. Elsner, A. Pender, M. Buchmeiser
Tailoring the surface of magnetic microparticles for protein immobilization
J. Appl. Polym. Sci. **121** (2011) 3628-3634

Y. M. Riyad, S. Naumov, B. Abel, R. Hermann
Shedding Light into the Detailed Excited State Relaxation Pathways and Reaction Mechanisms of Thionaphthol Isomers
J. Phys. Chem. **115** (2011) 718-725

S. Rupf, A. Lehmann, M. Hannig, B. Schäfer, A. Schubert, U. Feldmann, A. Schindler
Killing of adherent oral microbes by a non-thermal atmospheric plasma jet
Journal of Medical Microbiology **59** (2010) 206-212

C. Schmidt, D. Wang, M. R. Buchmeiser
Cyclopolymerization of N,N-Dipropargyl-3,4-dialkoxyanilines Using Schrock and Grubbs-Hoveyda Initiators: Influence of Initiator Structure on the Mode of Insertion
Macromol. Chem. Phys. **212** (2011) 1999-2008

K. Schmid, A. Manhard, Ch. Linsmeier, A. Wiltner, T. Schwarz-Seliger, W. Jacob, S. Mändl
Interaction of Nitrogen Plasmas with Tungsten
Nucl. Fusion **50** (2010) 025006

A. Schulze, B. Marquardt, S. Kaczmarek, R. Schubert, A. Prager, M. R. Buchmeiser
Electron Beam-Based Functionalization of Poly(ethersulfone) Membranes
Macromol. Rapid Comm. **31** (2010) 467-472

A. Shalabney, C. Khare, B. Rauschenbach, I. Abdulhalim
Sensitivity of surface plasmon resonancesensors based on metallic columnar thin films in the spectral and angular interrogations
Sensors and Actuators B: Chemical **159** (2011) 201-212

Z. Shen, Y. Xiong, T. Höche, D. Salamon, Z. Fu, L. Belova
Ordered Coalescence of Nanocrystals: a Path to Strong Macroporous Nanoceramics
Nanotechnology **21** (2010) 205602

P. Siffalovic, K. Vegso, M. Jergel, E. Majkova, J. Keckes, G. A. Maier, M. Cornejo, B. Ziberi, F. Frost, B. Hase, J. Wiesmann
Measurement of nanopatterned surfaces by real and reciprocal space techniques
Meas. Sci. Rev **10** (2010) 153-156

A. Sobottka, L. Drößler, M. Lenk, L. Prager, M. R. Buchmeiser
An Open Argon Dielectric Barrier Discharge VUV-Source
Plasma Process. Polym. **7** (8) (2010) 650-656

F. Szillat, S.G. Mayr
Self-organized pattern formation at organic-inorganic interfaces during deposition: Experiment versus modeling
Phys. Rev. B **84** (2011) 115462

M. Tartz, T. Heyn, C. Bundesmann, C. Zimmermann, H. Neumann
Sputter yields of Mo, Ti, W, Al, Ag under xenon ion incidence
Eur. Phys. J. D **61** (2011) 587-592

X. Tian, S. Mändl, D. T.-K. Kwok, P. K. Chu
Applications and Numerical Simulation of Plasma-Based Surface Modification
IEEE T Plasma Sci. **39** (2011) 3026-3027

T. Tobien, M. Bonifacic, S. Naumov, K.-D. Asmus
Time-resolved study on the reactions of organic selenides with hydroxyl and oxide radicals, hydrated electrons, and H-atoms in aqueous solution and DFT calculations of transients in comparison with sulfur analogues
Phys. Chem. Chem. Phys. **12** (2010) 6750-6758

A. Ulyanenkov, J. Chrost, P. Siffalovic, L. Chitu, E. Majkova, E. Majkova, H. Guerault, G. Maier, M. Cornejo, B. Ziberi, F. Frost
GISAXS and AFM study of self-assembled Fe_2O_3 nanoparticles and Si nanodots
Phys. Status Solidi A **208** (2011) 2619

C. Vree, S.G. Mayr
Dynamics and diffusive_conformational coupling in polymer bulk samples and surfaces: a molecular dynamics study
New J. Phys **12** (2010) 023001

J. Völlner, B. Ziberi, F. Frost, B. Rauschenbach
Topography evolution mechanism on fused silica during low-energy ion beam sputtering
J. Appl. Phys. **109** (2011) 043501

D. Wang, U. Decker, C. Kühnel, M. R. Buchmeiser
Latent Ruthenium (II)-based Photocatalysts for Ring-opening Metathtesis Polymerization
Polym. Preprints **51** (2010) 384-385

F. Weichelt, R. Emmler, R. Flyunt, E. Beyer, M. R. Buchmeiser, M. Beyer
ZnO-Based UV Nanocomposites for Wood Coatings in Outdoor Applications
Macromol. Mater. Eng. **295** (2010) 130-136

F. Weichelt, B. Frerich, S. Lenz, S. Tiede, M. R. Buchmeiser
Ring-Opening Metathesis Polymerization-Based Synthesis of $CaC0_3$ Nanoparticle-Reinforced Polymeric Monoliths for Tissue Engineering
Macromol. Rapid Comm. **31** (2010) 1540-1545

F. Weichelt, S. Lenz, S. Tiede, I. Reinhardt, B. Frerich, M. R. Buchmeiser
ROMP-Derived Cyclooctene-Based Monolithic Polymeric Materials Reinforced with Inorganic Nanoparticles for Applications in Tissue Engineering
Beilstein J. Org. Chem. **6** (2010) 1199-1205

F. Weichelt, M. Beyer, R. Emmler, R. Flyunt, E. Beyer, M. R. Buchmeiser
Zinc Oxide Based Coatings for the UV-Protection of Wood for Outdoor Applications
Macromol. Symp. **301** (1) (2011) 23-30

T. Welzel, S. Naumov, K. Ellmera
Ion distribution measurements to probe target and plasma processes in electronegative magnetron discharges: I. Negative Ions
J. Appl. Phys. **109** (2011) 073302.

T. Welzel, S. Naumov, K. Ellmera
Ion distribution measurements to probe target and plasma processes in electronegative magnetron discharges: II. Positive Ions
J. Appl. Phys. **109** (2011) 073303

R. Werner, T. Höche, S.G. Mayr
Synthesis of shape, size and structure controlled nanocrystals by pre-seeded inert gas condensation
Cryst. Eng. Comm. **13** (2011) 3046-3050

Zado, E. Tschumak, J.W. Gerlach, K. Lischka, D. J. As
Carbon as an acceptor in cubic GaN/3C-SiC
J. Cryst. Growth **323** (2011) 88-90

Conference Proceedings

T. Arnold, G. Böhm, I.-M. Eichentopf, M. Janietz, J. Meister, A. Schindler
Plasma Jet Machining- A novel technology for precision machining of optical elements
Vakuum in Forschung und Praxis 22 (2010) 10

T. Arnold, G. Böhm
Plasma Jet Machining - Fertigung von off-axis Parabolspiegeln aus Siliziumkarbid
111. Jahrestagung der DGaO, Paper Nr. A4, Wetzlar, (2010)

J. Bauer, M. Weise, Ch. Grüner, Ch. Khare, B. Rauschenbach, N. Geyer, B. Fuhrmann
Glanzwinkeldeposition von geordneten Si/Ge-Nanostrukturen
Jahresbericht IZM/ MLU Halle (2010) 31

A. Boulares-Pender, I. Thomas, A. Schulze
Surface Modification of Polyamide and Polyvinylidene Fluoride Membranes
6th IWA Specialist Conference on Membrane Technology for Water & Wastewater Treatment, Aachen, Germany, (2011) 433

A. Boulares-Pender, I. Thomas, A. Schulze
Surface modification of polyamide and polyvinylidene fluoride membranes
ICOM 2011 - International Congress on Membranes and Membrane Processes, Paper Nr. ICOM1053, Amsterdam, The Netherlands, (2011)

S. Camadanli, Y. Zou, V. N. Gurram, D. Wang, M. R. Buchmeiser
Catalysts for the Simultaneous Ring-Opening Metathesis and Vinyl Insertion Copolymerization of Ethylene With Cyclic Olefins
Polym. Prep. (Div. Polym. Chem., Am. Chem. Soc.) 52 (2011) 217-218

S. Camadanli, Y. Zou, V. N. Gurram, M. R. Buchmeiser
Tandem Catalysts for Olefin Polymerization
Stuttgarter Kunststoffkolloquium, ISBN 978-3-00034152-6 1V2 (2011) 1-7

M. Ehrhardt, K. Zimmer
Laser micro joining of thin metal films on flexible substrates for mechanical and electrical connections
Photonic West, Paper Nr. 792109, San Francisco, CA, USA, (2011)

C. Elsner
Plasma-induzierte Polymerisation von Acrylaten
Vakuum in Forschung und Praxis 22(4) (2010) 6-9

A. Gjevori, K. Nonnenmacher, D. Manova, B. Ziberi, D. Hirsch, J.W. Gerlach, S. Mändl
Phase Formation of Photocatalytically Active TiO_2 Thin Films By MPIIID
Proc. IVth International Meeting of the Institute Alb-Science, AKTET-Journal of Institute Alb-Science, International Annual Meetings, Vol. III Nr. 2, ISSN 2073-2244, Tetovo, Albania, (2010) 157-161

R. Mehnert, E. Mai, C. Riedel, R. Schubert T. Scherzer
Surface Micro-Structuring of Acrylate Nanocomposite Coatings by 172 nm Excimer Irradiation
Proc. European Coatings Congress, Nürnberg, (2011)

H. Neumann, F. Scholze, M. Tartz, H. Leiter
A cathodeless radio frequency plasma bridge neutralizer and results of the first coupled test with the RIT 22 ion thruster
Space Propulsion 2010, Paper Nr. SP2010_1853118, San Sebastian, Spain, (2010)

L. Prager, L. Wennrich, W. Knolle, R. Heller, A. Prager, U. Decker
Creation of organic-inorganic multilayer systems: aspects of photochemical-based fabrication of gas barriers
2nd International Conference on Thermosets 2011, Berlin, Germany, (2011) 26

L. Prager, L. Wennrich, M. Dubiel, R. Heller
Aspekte der Herstellung und Charakterisierung von organisch/anorganischen Schichtsystemen am Beispiel von Barriereverbunden
9. Neues Dresdner Vakuumtechnisches Kolloquium, Dresden, Germany, (2011) 50-54

S. Reichelt, C. Elsner, W. Knolle, A. Prager, K. Umnus, J. Kuballa, M. R. Buchmeiser
Electron beam derived polymeric monoliths for affinity separation
Polymer Materials, Halle, Germany, (2010) 46

S. Reichelt, C. Elsner
Elektronenstrahl-initiierte 'Ein-Topf'-Synthese von polymerbasierten Enzymreaktoren
14. Problemseminar 'Polymermischungen', Paper Nr. OP12, Halle, Germany, (2011)

S. Reichelt, C. Elsner, K. Umnus J. Kuballa, M. R. Buchmeiser
Electronbeam-initiated synthesis and functionalization of polymeric monoliths and their application in affinity chromatography
Biomater 12 (2011) 158

T. Scherzer, G. Mirschel, O. Savchuk, K. Heymann, B. Genest
Control of UV Offset Printing Processes by In-line NIR Spectroscopy
RadTech Europe 2011, Basel, Switzerland, (2011)

T. Scherzer, M. W. Schröder
Monitoring of the Development of Viscoeleastic Parameters and Conversion during UV Curing of Acrylate Formulations by Hyphenated Photorheometry and NIR Spectroscopy
Near Infrared Spectroscopy: Proceedings of the 14th International Conference, ed. by S. Saranwong, S. Kasemsumran, W. Thanapase, P. Williams, IM Publications, Chichester (2010) 1161-1165

T. Scherzer, G. Mirschel, K. Heymann, L. Prager
In-line Monitoring of the Thickness of Silica and Silazane Layers in the Submicron Range by NIR Reflection Spectroscopy
Near Infrared Spectroscopy: Proceedings of the 14th International Conference, ed. by S. Saranwong, S. Kasemsumran, W. Thanapase, P. Williams, IM Publications, Chichester (2010) 803-807

T. Scherzer, G. Mirschel, K. Heymann, M. R. Buchmeiser
Continuous Monitoring of Process Parameters in UV Curing Processes
RadTech Report 24(2) (2010) 40-48

F. Scholze, M. Tartz, H. Neumann
Modelling of a Radio Frequency Plasma Bridge Neutraliser
Space Propulsion 2010, San Sebastian, Spain, (2010)

R. Schubert, K. Barucki, M. Hinkefuss, B. Marquart, R. Mehnert, J. Peuker, L. Prager, C. Riedel, A. Schulze, J. Vogel
Using excimer UV radiation to produce folded, matted surfaces
Farbe + Lack 117 (2011) 21-22

A. Schulze, B. Marquardt, S. Kaczmarek, R. Schubert, A. Prager, M. R. Buchmeiser
Electron Beam-Based Modification of Polymer Membranes
13th Aachener Membrankolloquium, Paper Nr. L 11.3, Aachen, Germany, (2011) 241

A. Schulze, B. Marquardt, S. Kaczmarek, R. Schubert, A. Prager, M. R. Buchmeiser
Electron Beam-Based Functionalization of Polymer Membranes
AMS6/IMSTEC10, Paper Nr. 166, Sydney, Australia, (2010)

A. Schulze, B. Marquardt, S. Kaczmarek, R. Schubert, A. Prager, M. R. Buchmeiser
Electron Beam-Based Functionalization of Polymer Membranes
IWA-MTWR 2010, Paper Nr. 106, Istanbul, Turkey, (2010) 218

A. Schulze, A. Boulares-Pender, M. Went, I. Thomas, B. Marquardt, A. Prager-Duschke
Membrane Hydrophilization using Electron Beam and Plasma Techniques
International Congress on Membranes and Membrane Processes (ICOM 2011), Paper Nr. ICOM888, Amsterdam, The Netherlands, (2011)

A. Schulze, A. Boulares-Pender, M. Went, I. Thomas, B. Marquardt, A. Prager
Plasma- und Elektronenstrahlbehandlung zur permanenten Hydrophilierung von Polymermembranen
7. Thüringer Grenz- und Oberflächentage, Zeulenroda, Germany, (2011) 75-80

A. Wehrmann, H. Schulte-Huxel, M. Ehrhardt, D. Ruthe, K. Zimmer, A. Braun, S. Ragnow
Change of electrical properties of CIGS thin-film solar cells after structuring with ultrashort laser pulses
Paper Nr. 79210T, Photonic West, San Francisco, CA, USA, (2011)

Presentations

Talks

I. Alig, S. Agarwal, D. Lellinger, H. Oehler, K. Heymann, G. Mirschel, T. Scherzer
Monitoring of Photopolymerization Kinetics and Network Formation by Ultrasound Reflectometry and Near-Infrared Spectroscopy
European Symposium of Photopolymer Science, Mulhouse, France, 28.11.-01.12.2010

T. Arnold, G. Böhm, M. Janietz, I.M. Eichentopf, H. Paetzelt
Precision machining of optical surfaces with small plasma jet tools
2nd EOS Conference on Manufacturing of Optical Components, München, Germany 23-25.05.2011

T. Arnold
Technologie der Ultrapräzisions-bearbeitung mit Atmosphären-Plasmajets
EFDS-Workshop 'Plasmaquellen und Anlagentechnik der Atmosphärendruck-Plasmatechnologien', Wörlitz, Germany, 07.06.2011

T. Arnold, G. Böhm
Plasma Jet Machining - Fertigung von off-axis Parabolspiegeln aus Siliziumkarbid
111. Jahrestagung der DGaO, Wetzlar, Germany, 25.-29.5.2010

T. Arnold
Ultra-precision Surface Finishing by Ion Beam and Plasma Jet Techniques-Status and Outlook
Kolloquium Precision Engineering Centre, Cranfield University, Cranfield, UK, 20.10.2010

T. Arnold
Process simulation for ultra-precision surface finishing with ion beams and plasma jets
Precision Engineering Centre Colloquium, Cranfield University, UK, 20.10.2010

J. Bauer, M. Weise, C. Khare, C. Grüner, B. Rauschenbach
Herstellung von Si/Ge-Nanostrukturen mittels Glanzwinkeldeposition
Workshop Oberflächentechnologie mit Plasma- und Ionenstrahlprozessen, Mühlleithen, Germany, 08.-10.03.2011

J. Bauer, M. Weise, C. Khare, C. Grüner, B. Rauschenbach
Ordered Si-Ge nanostructures by glancing angle deposition via ion beam sputtering
MRS spring meeting, San Francisco, CA, USA, 25.-29.04.2011

J. Bauer, M. Weise, C. Grüner, B. Rauschenbach
Nanostructured Thin Films by Glancing Angle Deposition
Leibniz-Institut für Neue Materialien, Saarbrücken, Germany, 08.-09.11.2011

G. Böhm, T. Arnold
Plasma Jet Machining Used in High Precision Free Form Fabrication
EOS Conference on Manufacturing of Optical Components - Precise Optics Fabrication, ICC Munich, Germany, 15.-17.06.2010

C. Bundesmann, M. Tartz, F. Scholze, H. Neumann
AEPD - Eine interessante EP-Diagnostikplattform
4. Deutscher Workshop 'Electric Propulsion', Leipzig, Germany, 02.-03.11.2010

C. Bundesmann, M. Tartz, F. Scholze, F. Scortecci, R.Y. Gnizdor, H. Neumann
Ein Stationary Plasma Thruster (SPT) in situ betrachtet
Workshop Oberflächentechnologie mit Plasma- und Ionenstrahlprozessen, Mühlleithen, Germany, 02.-04.03.2010

C. Bundesmann
Optical in-situ characterization techniques for thin film growth processes
Workshop Oberflächentechnologie mit Plasma- und Ionenstrahlprozessen, Mühlleithen, Germany, 08.-10.03.2011

M. Cornejo, B. Ziberi, F. Frost, B. Rauschenbach
Self-organized pattern formation on Si by low-energy ion beam erosion with simultaneous Fe incorporation
DPG Frühjahrstagung der Sektion Kondensierte Materie, Regensburg, Germany, 21.-26.03.2010

J. Dadda, E. Müller, S. Perlt, T. Höche, P. Bauer, R. P. Hermann
Thermoelectric and Microstructural Characteristics of Quenched and Annealed $AgPb_{18}SbTe_{20}$ (LAST-18) Compounds
8th European Conference on Thermoelectrics, Como, Italien, 22.-25.09.2010

J. Dadda, E. Müller, S.Perlt, T. Höche, P. Bauer Pereira, R. Hermann
Selection of annealing temperature and composition for the optimization of TE properties in LAST
ICT 2011 International Conference on Thermoelectrics, Traverse City, MI, USA 17.-21.07.2011

M. Ehrhardt, A. Wehrmann, K. Zimmer
Laser micro joining of thin metal films on flexible substrates for mechanical and electrical connections
Photonic West, San Francisco, CA, USA, 22.-27.01.2011

M. Ehrhardt, K. Zimmer, P. Lorenz
Studies on the material erosion mechanism at Laser-Induced Back side Wet Etching (LIBWE) of fused silica
11th International Conference on Laser Ablation, Playa del Carmen, Mexico, 13.-19.11.2011

M. Ehrhardt, K. Zimmer, C. Scheit
Laser micro joining of thin films on flexible substrates for electrical connection
11th International *Symposium* on Laser Precision Microfabrication, München, Germany, 07.-10.06.2010

I.-M. Eichentopf, G. Böhm, T. Arnold
Untersuchungen zur Plasma-Oberflächenwechselwirkung während Plasmajet-gestützter Bearbeitung von SiC
Workshop Oberflächentechnologie mit Plasma- und Ionenstrahlprozessen, Mühlleithen, Germany, 02.-04.03.2010

I.-M. Eichentopf, T. Arnold
Ätzmechanismen bei der Bearbeitung von SiC mittels atmosphärischer Plasmajets
DPG Frühjahrstagung der Sektion AMOP (SAMOP), Hannover, Germany, 08.-12.03.2010

I.-M. Eichentopf, G. Böhm, T. Arnold
Untersuchungen zu Ätzmechanismen bei der Plasmajetbearbeitung von Siliziumkarbid
DPG Frühjahrstagung, Kiel, Germany, 28.03.-31.03.2011

I.-M. Eichentopf, T. Arnold
Untersuchungen zu Ätzmechanismen bei der Plasmajetbearbeitung von Siliziumkarbid
Workshop Oberflächentechnologie mit Plasma- und Ionenstrahlprozessen, Mühlleithen, Germany, 08.03.-10.03.2011

M. Engler, S. Macko, F. Frost, T. Michely
Evolution of surface topography of Si(100) during ion beam erosion
DPG Frühjahrstagung, Dresden, Germany, 14.-18.03.2011

C. Ernst, C. Elsner, S. Reichelt, B. Schlemmer, R. Bandari, A. Prager, M. Buchmeiser
Herstellung monolithischer Trennmedien durch strahleninduzierte Polymerisation und deren Anwendung
3. Workshop: Möglichkeiten und Grenzen der HPLC in den Lebenswissenschaften, Forschungszentrum Rossendorf, Germany, 29.01.2010

L. Fricke, S.G. Mayr
Dynamics of shear transformation zones during mechanical cycling of glassy CuTi - a molecular dynamics study
DPG Frühjahrstagung, Dresden, Germany, 14.-18.03.2011

F. Frost, J. Völlner
Mechanismen der Musterbildung auf Quarzglasoberflächen bei der Ionenstrahlerosion
Workshop Oberflächentechnologie mit Plasma- und Ionenstrahlprozessen, Mühlleithen, Germany, 08.-10.03.2011

F. Frost, J. Völlner, J. Lorbeer, M. Teichmann, M. Cornejo, B. Ziberi, B. Rauschenbach
Ion Induced Ripple Pattern on Fused Silica Surfaces: Genesis Coarsening and Faceting
MRS Fall Meeting, Boston, MA, USA, 28.11.-02.12.2011

F. Frost, B. Ziberi, M. Cornejo, J. Völlner, A. Schindler, B. Rauschenbach
Surface engineering with low-energy ion beams: from ultra-smooth surfaces to hierarchical nanostructures
18th International Vacuum Congress, Beijing, China, 23.-27.08.2010

F. Frost, J. Völlner, B. Ziberi, B. Rauschenbach
Stabilization and destabilization of ion beam eroded quartz glass surfaces by gradient dependent sputtering: From topographic defects towards ordered ripple pattern
Workshop Oberflächentechnologie mit Plasma- und Ionenstrahlprozessen, Mühlleithen, Germany, 02.-04.03.2010

J. A. Garcia, C. Diaz, R. Pereiro, B. Fernández, S. Mändl, D. Manova
Metal Ion Release of Implanted CoCrMo Alloys
11th Int. Workshop on Plasma Based Ion Implantation & Deposition, Harbin, China, 08.-12.09.2011

J.W. Gerlach, L. Neumann, B. Rauschenbach
Hyperthermal ion assisted nitride film epitaxy
20th International Conference on Ion-Surface Interactions, Zvenigorod, Russia, 25.-29.08.2011

J.W. Gerlach, W. Assmann, B. Rauschenbach
Origin of oxygen contamination during epitaxy of GdN films on YSZ(100) substrates
European Conference on Applications of Surface and Interface Analysis, Cardiff, UK, 04.-09.09.2011

J.W. Gerlach, C. Patzig, B. Rauschenbach
Ion-beam assisted droplet epitaxy of thin wurtzitic gallium nitride films with polar and non-polar orientation
15th International Conference on Thin Films, Kyoto, Japan, 08.-11.11.2011

J.W. Gerlach
Application of accelerated ions in thin film epitaxy and analysis
Graduiertenvorlesung 'Optoelectronics and Photonics', Universität Paderborn, Germany, 03.02.2010

J.W. Gerlach, L. Neumann, M. Abd El Khair, B. Rauschenbach
Early stages of ion beam assisted epitaxial growth of GaN films on 6H-SiC(0001)
18th International Vacuum Congress, Beijing, China, 23.-27.08.2010

J.W. Gerlach, A. Hofmann, T. Höche, F. Frost, G. Benndorf, B. Rauschenbach
m-plane oriented GaN films by ion beam assisted molecular beam epitaxy
Kolloquium der School of Physics and Technology der Universität Wuhan, Wuhan, China, 31.08.2010

G. P. H. Gubbels, C. van Drunen, G. Böhm, T. Arnold, F. Kamphues, W.L.M. Gielesen
Fabrication of Strongly Curved Aspheric Silicon Carbide Mirrors
10th International Conference of the European Society for Precision Engineering & Nanotechnology, Delft, Netherland, 31.05.-04.06.2010

D. Hirsch
Sekundärionenmassenspektroskopie
Seminar Institut für Physik, Technische Universität Chemnitz, Germany, 14.12.2010

A. M. Jakob, S.G. Mayr
Probing nanomechanics with contact resonance atomic force microscopy (CR-AFM) - Fundamentals, applications, challenges
Euro AFM Forum 2011, ETH Zürich, Switzerland, 07. -09.09.2011

M. Janietz, T. Arnold
Untersuchung verschiedener Precursoren zur lokalen Plasmajetbeschichtung
DPG Frühjahrstagung, Kiel, Germany, 28.-31.03.2011

M. Janietz, T. Arnold
Precursoren für die Plasmajetbeschichtung
Workshop Oberflächentechnologie mit Plasma- und Ionenstrahlprozessen, Mühlleithen, Germany, 08. -10.03.2011

M. Janietz, G. Böhm, T. Arnold
Formgebung mittels lokaler Plasmajet-Abscheidung von Siliziumoxid
Workshop Oberflächentechnologie mit Plasma- und Ionenstrahlprozessen, Mühlleithen, Germany, 02.-04.03.2010

M. Janietz, G. Böhm, T. Arnold
Lokale Abscheidung dünner Oxidschichten mittels atmosphärischen Plasmajets
4. Workshop des AK-ADP: 'Abscheidung funktioneller Beschichtungen', Jena, Germany, 18.03.2010

M. Janietz, G. Böhm, T. Arnold
Lokale Abscheidung von Siliziumoxidschichten mittels atmosphärischen Plasmajets
DPG Frühjahrstagung, Hannover, Germany, 08.-12.03.2010

C. Khare, J. Bauer, J.W. Gerlach, B. Fuhrmann, T. Höche, B. Rauschenbach
Growth Temperature Controlled Morphology of Ge Nanocolumns
AVS 57th International Symposium and Exhibition, Albuquerque, NM, USA, 17.-22.10.2010

C. Khare, J. Bauer, M. Weise, B. Rauschenbach
Glancing angle deposited Ge nanorod arrays: Growth optimization on self-elevated Si patterns
3rd BuildMoNa workshop, Lutherstadt Wittenberg, Germany, 04.-05.10.2010

W. Knolle, H. Oppermann, S. Naumov, L. Prager, U. Decker, T. Scherzer, K. Czihal, L. Wennrich
Photochemistry of (Meth)Acrylates Following 172 - 222 nm Excitation
European Symposium of Photopolymer Science, Mulhouse, France, 28.11.-01.12.2010

I. Kock, T. Edler, L. Kühnemund, G. Mahnke, S.G. Mayr
Single crystalline freestanding ferromagnetic shape memory alloy thin films
Symposium of the SPP 1239, Dresden, Germany, 04.03.2010

A. Lehmann, A. Rueppell, M. Volkmer, S. Rupf, T. Arnold, A. Schindler
Plasmajet-Modifizierung von Materialoberflächen in der Zahnmedizin
10. Workshop des ak-adp, Plasmamedizin, Erfurt, Germany, 02.-03.12.2011

Y. Ma, F. Szillat, D. Manova, S. Mändl, J.W. Gerlach, S.G. Mayr
Phase transformations and mechanical properties of freestanding single crystalline $Fe_{70}Pd_{30}$ thin films
DPG Frühjahrstagung, Dresden, Germany, 14.-18.03.2011

Y. Ma, A. Setzer, P. Esquinazi, S.G. Mayr
Martensitic phase transformation in freestanding single crystalline $Fe_{70}Pd_{30}$ thin films
4th BuildMoNa workshop for doctoral candidates, Dresden, Germany, 26.-27.09.2011

S. Macko, M. Engler, F. Frost, T. Michely
Shadowing in metal assisted ion beam patterning on Si(100)
DPG Frühjahrstagung, Dresden, Germany, 14.-18.03.2011

S. Macko, F. Frost, B. Ziberi, D. F. Foerster, T. Michely
Conditions for ion beam induced pattern formation on Si(001)
17th International Conference on Ion Beam Modification of Materials, Montrèal, Canada, 22.-27.08.2010

S. Macko, F. Frost, B. Ziberi, D. Förster, T. Michely
Factors influencing metal impurity induced ion beam patterning of Si(001)
DPG Frühjahrstagung, Regensburg, Germany, 21.-26.03.2010

S. Mändl, D. Manova, J. Lutz
Oberflächenaufrauhung bei Nitrierprozessen und Tiefenprofilierungen
Workshop Oberflächentechnologie mit Plasma- und Ionenstrahlprozessen, Mühlleithen, Germany, 02.-04.03.2010

S. Mändl
Surface Functionalization by Energetic Plasmas
Centre de Recherche Public - Gabriel Lippmann, Belvaux, Luxembourg, 18.02.2011

S. Mändl
Nutzung von Plasma-Immersions-Ionenimplantation zur Verbesserung der Biokompatibilität von Metalloberflächen, Materials Valley Workshop Wechselwirkung Material/Zelle - Oberflächeneigenschaften beeinflussen die Zelldifferenzierung, Hanau, Germany, 24.02.2011

S. Mändl
Surface Functionalisation by Energetic Plasma Particles
Institute for Plasma Physics (INFIP), Departamento de Fisica, Universidad de Buenos Aires, Buenos Aires, Argentina, 02.03.2011

S. Mändl
Biocompatibility of Cobalt Chromium alloys after PIII treatment
11th Int. Workshop on Plasma Based Ion Implantation & Deposition, Harbin, China, 08.-12.09.2011

S. Mändl
Surface Modification by Energetic Particles from a Plasma _ Applications for Advanced Biomaterials
Departamento de Ingeniería Electromecánica, Facultad Regional Concepción del Uruguay, Universidad Tecnológica Nacioncal, Concepción del Uruguay, Argentina, 09.03.2011

S. Mändl
Surface Modification for Advanced Biomaterials
Seminario Física de la Materia Condensada, Pontificia Universidad Católica de Chile, Santiago, Chile, 18.03.2011

S. Mändl
Energetic Particles from a Plasma for Surface Functionalisation
Coloquio del Departamento de Física, Pontificia Universidad Católica de Chile, Santiago, Chile, 17.03.2011

S. Mändl
Surface Modification by Energetic Particles Fundamentals and Applications for Advanced Biomaterials
Brazilian Physics Meeting, Foz do Iguaçu, Brazil, 06.-09.06.2011

S. Mändl
Surface Sputtering by Energetic Ions: From Self-Organisation for Bioactive Surfaces Towards Secondary Ion Mass Spectrometry
División Corrosión, Instituto de Investigaciones en Ciencia y Tecnología de Materiales. Facultad de Ingeniería, Universidad Nacional de Mar del Plata, Mar del Plata, Argentina, 04.03.2011

D. Manova, S. Mändl
Plasma Immersion Ion Implantation for Surface Functionalization
Shanghai Institute of Microsystem and Information Technology, Chinese Academy of Sciences, Shanghai, China, 06.09.2011

D. Manova, A. Bergmann, S. Mändl, H. Neumann, B. Rauschenbach
In situ XRD observation of phase formation
Workshop Oberflächentechnologie mit Plasma- und Ionenstrahlprozessen, Mühlleithen, Germany, 08.-10.03.2011

D. Manova, J.W. Gerlach, S. Mändl, H. Neumann
Phase formation after nitriding of austenitic stainless steel by pulsed low energy ion implantation
Workshop Oberflächentechnologie mit Plasma- und Ionenstrahlprozessen, Mühlleithen, Germany, 02.-04.03.2010

D. Manova
Metal plasma immersion ion implantation and deposition
Institutsseminar, Universidad Technologica Nacional, Facultad Regional Cencepcion del Uruguay, Concepcion del Uruguay, Argentina, 17.07.2010

D. Manova
Plasma immersion ion implantation
Institutsseminar, Facultad Regional Concepcion del Uruguay, Universidad Technologica Nacional, Concepcion del Uruguay, Argentina, 16.07.2010

S.G. Mayr
Miniaturization of functional materials
German/Spanish meeting at the EU representation of Spain, Brussels, Belgium, 04.07.2010

S.G. Mayr
Mechanical properties of metallic glasses
DPG Frühjahrstagung, Regensburg, Germany, 21.-26.3.2010

S.G. Mayr
Nanomechanics of metallic glasses
Kalvi-Institute for theoretical Physics, University of California at Santa Barbara, CA, USA, May 2010

R. Mehnert, E. Mai, C. Riedel, R. Schubert, T. Scherzer
Surface Micro-Structuring of Acrylate Nanocomposite Coatings by 172 nm Excimer Irradiation
European Coatings Congress, Nürnberg, Germany, 29.-31.3.2011

J. Meister, T. Arnold
Neue Prozedur zur Prozesssimulation bei der Plasmajetbearbeitung
Workshop Oberflächentechnologie mit Plasma- und Ionenstrahlprozessen, Mühlleithen, Germany, 08.-10.03.2011

J. Meister, T. Arnold
Simulation des Plamajet-Hochratenätzens von massivem Quarzglas
DPG Frühjahrstagung, Hannover, Germany, 08.-12.03.2010

J. Meister, T. Arnold
Simulation of high-rate Plasma Jet Machining
12th International Conference on Plasma Surface Engineering, Garmisch-Partenkirchen, Germany, 13.-17.09.2010

J. Meister, T. Arnold
Simulation des Plamajet-Hochratenätzens von massivem Quarzglas
Workshop Oberflächentechnologie mit Plasma- und Ionenstrahlprozessen, Mühlleithen, Germany, 02.-4.03.2010

T. Michely, S. Macko, M. Engler, F. Frost, S. Müller, D. Förster, T. Höche, D. Hirsch, M. Fritzsche, J. Grenzer
Phenomenology of pattern formation on Si(001) with and without impurities
Workshop on Nanoscale Pattern Formation at Surfaces, El Escorial, Madrid, Spain, 18.09.-22.09.2011

T. Michely, S. Macko, M. Engler, D. Förster, F. Frost, B. Ziberi, T. Höche, D. Hirsch, J. Grenzer
Pattern formation on Si(001) with and without impurities
International Conference on Ion-Beam Induced Nanopatterning of Materials, Institute of Physics, Bhubaneswar, India, 06.-10.02.2011

A. Mießler, A. Mill, J.W. Gerlach, T. Arnold
Subapertur-Materialbearbeitung mit reaktiven Ionenstrahlen
Workshop Oberflächentechnologie mit Plasma- und Ionenstrahlprozessen, Mühlleithen, Germany, 08.-10.03.2011

A. Mießler, A. Mill, T. Arnold
Pattern transfer on large samples using a sub-aperture reactive ion beam
17. International Summer School on Vacuum, Electron and Ion Technologies, Sunny Beach, Bulgaria, 19.-23.09.2011

A. Mießler, A. Mill, J.W. Gerlach, T. Arnold
Pattern transfer on large samples using a sub-aperture reactive ion beam
DPG Frühjahrstagung, Dresden, Germany, 14.-18.03.2011

A. Mießler, C. Khare, T. Arnold
Grundlagenuntersuchen zur Subapertur-Oberflächenbearbeitung mit reaktiven Ionenstrahlen
Workshop Oberflächentechnologie mit Plasma- und Ionenstrahlprozessen, Mühlleithen, Germany, 02.-04.3.2010

A. Mießler, T. Arnold, B. Rauschenbach
Surface characterization after subaperture Reactive Ion Beam Etching
DPG Frühjahrstagung, Regensburg, Germany, 22.-26.03.2010

H. Neumann, F. Scholze, M. Tartz, H. Leiter
A cathodeless radio frequency plasma bridge neutralizer and results of the first coupled test with the RIT 22 ion thruster
4. Workshop -Electric Propulsion, Leipzig, Germany, 02.-03.11.2010

H. Neumann, F. Scholze, M. Tartz, H. Leiter
A cathodeless radio frequency plasma bridge neutralizer and results of the first coupled test with the RIT 22 ion thruster
Space Propulsion 2010, San Sebastian, Spain, 03.-06.05.2010

L. Neumann, J.W. Gerlach, T. Höche, B. Rauschenbach
Initial stages of the ion-beam assisted epitaxial GaN film growth on 6H-SiC(0001)
DPG Frühjahrstagung, Dresden, Germany, 14.-18.03.2011

H. Neumann
Ionenstrahlquellen für die Oberflächenbearbeitung und Satellitenantriebe
Tag der Raumfahrt, Brockhaus-Gymnasium, Leipzig, Germany, 12.04.2011

L. Neumann, J.W. Gerlach, T. Höche, B. Rauschenbach
Initial stages of the ion-beam assisted epitaxial GaN film growth on 6H-SiC(0001)
DPG Frühjahrstagung, Dresden, Germany, 13.-18.03.2011

S. Perlt, T. Höche, J. Dadda, E. Müller
Correlation Between Microstructure and Thermoelectric Properties of $AgPb_{18}SbTe_{20}$ (LAST-18)
European Conference on Thermoelectrics, Thessaloniki, Greece
28.-30.09.2011

S. Perlt, T. Höche, J. Dadda, E. Müller
Complex Chalcogenides for Thermoelectrics: Microstructure Analysis of $AgPb_{18}SbTe_{20}$ (LAST-18)
Microscopy Conference, Kiel, Germany, 28.08.-02.09.2011

S. Perlt, T. Höche, J. Dadda, E. Müller
Complex Chalcogenides for Thermoelectrics: Microstructure Analysis of $AgPb_{18}SbTe_{20}$,
DPG Frühjahrstagung, Dresden, Germany,13.-18.03.2011

L. Prager, L. Wennrich, W. Knolle, S. Naumov, M. Dubiel, J.W. Gerlach, R. Heller, A. Prager, U. Trimper
Aspekte der Herstellung und Charakterisierung von organisch/anorganischen Schichtsystemen am Beispiel von Barriereverbunden
19. Neues Dresdner Vakuumtechnisches Kolloquium, Dresden, Germany, 19.-20.10.2011

L. Prager, L. Wennrich, J.W. Gerlach, C. Bundesmann, A. Prager, D. Decker, M. Roth
Charakterisierung von mittels VUV-Strahlung unter Normaldruck und -temperatur auf Polymerfolien nasschemisch hergestellten polysilazanbasierten SiOx-Schichten als Gasbarrieren
Workshop Oberflächentechnologie mit Plasma- und Ionenstrahlprozessen, Mühlleithen, Germany, 02.-04.03.2010

L. Prager, L. Wennrich, D. Decker, W. Knolle, R. Heller, A. Prager, M. Roth, U. Trimper
UV-induzierte Umwandlung von Perhydropolysilazan- in SiOx- Schichten als transparente Gasbarrieren - Entwicklungsstand
11. Wörlitzer Workshop 'Anforderungen an Schichten auf flexiblen Sustraten für Barriereschutz', Wörlitz, Germany, 09.06 2010

B. Rauschenbach
Nanotechnologie an Oberflächen
WGL-Forschungsfelddiskussion, Berlin, Germany, 07.06.2011

B. Rauschenbach
Evolution of structures at surfaces by sputtering
Workshop Sputtering FhG Braunschweig, Braunschweig, Germany, 23.-24.02.2011

B. Rauschenbach
Low-energy ion beam induced nanostructures on surfaces
17th International Conference on Surface Modification of Materials by Ion Beams, Harbin, China, 13.09.-17.09.2011

B. Rauschenbach
Ionenstrahl induzierte Nanostrukturen - Grundlagen und Anwendung
Kolloquium des Instituts für Funktionswerkstoffe, Universität Saarbrücken, Saarbrücken, Germany, 17.05.2011

B. Rauschenbach
Nanotechnologie am IOM Leipzig
Deutsche Physikalische Gesellschaft (DPG), Leipzig, Germany, 12.05.2011

B. Rauschenbach
Selbstorganisierte Nanostrukturen - Grundlagen und Applikationen
Workshop 'Intelligente, ressourcenschonende Prozess-Technologien unter Nutzung von Selbstorganisationseffektem', Materials Valley Heraeus Hanau, Germany, 24.04.2011

B. Rauschenbach
Sculptured thin films by glancing angle deposition
Institutskolloquium, University Wuhan, School of Physical Science and Technology, Wuhan, China, 31.08.2010

B. Rauschenbach C. Khare, M. Weise, J. Bauer
Silicon and germanium sculptured thin films ba glancing angle deposition
18th International Vacuum Conference, Beijing, China, 27.08.2010

B. Rauschenbach
Physics of low-energy ion beam assisted deposition
Kolloquium, TU Berlin, Berlin, Germany, 12.07.2010

B. Rauschenbach
Analytische Elektronenmikroskopie und Nanotechnologie
Stiftung für Innovation und Technologietransfer Leipzig, Leipzig, Germany, 19.10.2010

B. Rauschenbach
Self-organisation of nanostructures by low-energy ion bombardment and sputtering
Institutskolloquium, Leibniz-Institut für innovative Mikroelektronik, Frankfurt/O., Germany, 28.06.2010

S. Reichelt, C. Elsner, W. Knolle, A. Prager, K. Umnus, J. Kuballa, M. R. Buchmeiser
Electron beam derived polymeric monoliths for affinity separation
Polymer Materials 2010, Halle, Germany, 15.-17.09.2010

S. Reichelt, C. Elsner
Elektronenstrahl-initiierte 'Ein-Topf'-Synthese von polymerbasierten Enzymreaktoren
14. Polymerseminar Polymermischungen, Halle, Germany, 14.-15.09.2011

S. Reichelt, C. Elsner
Current Issues of the working group “Biofunctional Surfaces” at the IOM Leipzig - Biofunctionalization of electronbeam-derived and plasma-modified surfaces
Kolloquium Abteilung Biomaterialien, Leibniz-Institut für Polymerforschung, Dresden, Germany, 28.06.2011

T. Scherzer, G. Mirschel, O. Savchuk, K. Heymann, B. Genest
Control of UV Offset Printing Processes by In-line NIR Spectroscopy
RadTech Europe 2011, Basel, Switzerland, 18.-20.10.2011

T. Scherzer, G. Mirschel, O. Savchuk, K. Heymann
In-line Monitoring of Process Parameters in UV Curing and Printing Processes
Kolloquiumsvortrag, Département de Photochimie Générale, Université de Haute Alsace, Mulhouse, France, 17.10.2011

T. Scherzer, O. Savchuk, S. Naumov, W. Knolle
Self-Initiation of Photopolymerization Reactions Using Halogenated (Meth)Acrylates
Photopolymerization Fundamentals, Breckenridge, CO, USA, 26.-29.06.2011

T. Scherzer, C. Schmidt, O. Savchuk
Aufbau eines gekoppelten Photorheometrie-NIR-Spektroskopie-Messplatzes und dessen Einsatz bei der Entwicklung innovativer UV-härtbarer Beschichtungen
2. Bayreuther Kompetenztage, Bayreuth, Germany, 28.-30.11.2011

T. Scherzer, G. Mirschel, K. Heymann
In-line Monitoring of UV Curing Processes by NIR Reflection Spectroscopy
18th European Symposium on Polymer Spectroscopy, Zadar, Croatia, 19.-22.9.2010

T. Scherzer, G. Mirschel, K. Heymann
In-line Monitoring von Prozessparametern in UV-Härtungsprozessen
2. Oberflächenseminar des Vereins der Ingenieure für Lacke & Farben (VILF), Würzburg, Germany, 06.-07.10.2010

T. Scherzer, G. Mirschel, K. Heymann
In-line-Monitoring von Beschichtungsprozessen mittels NIR-Spektroskopie
59. Sitzung des Arbeitskreises -Strahlenchemische Veredlung bahnförmiger Materialien', Hochschule München für Angewandte Wissenschaften, München, Germany, 11.6.2010

T. Scherzer
VUV-Induced Photopolymerization of Acrylates: A Study by Real-Time FTIR/ATR-Spectroscopy
European Symposium of Photopolymer Science, Mulhouse, France, 28.11.-01.12.2010

A. Schindler, T. Arnold
Surface Engineering with Ion Beams and Plasma Jets
EUSPEN Meeting: Manufacturing Technologies to Support Large Science Projects, Paris, France, 25.-26.11.2010

M. Schlegel, K. Barucki, S. Mändl, M. Kunert
PIIID von Silber auf Implantatschrauben aus $TiAl_6V_4$
Workshop Oberflächentechnologie mit Plasma- und Ionenstrahlprozessen, Mühlleithen, Germany, 02.-04.03.2010

F. Scholze, M. Tartz, H. Neumann
Modelling of a Radio Frequency Plasma Bridge Neutraliser
Space Propulsion 2010, San Sebastian, Spain, 03.-06.05.2010

F. Scholze
Simulationswerkzeuge für Plasmen am IOM
4. Deutscher Workshop 'Electric Propulsion', Leipzig, Germany, 02.-03.11.2010

F. Scholze, M. Tartz, H. Neumann
Simulation eines HF-PBN mit PIC
Workshop Oberflächentechnologie mit Plasma- und Ionenstrahlprozessen, Mühlleithen, Germany, 02.-04.03.2010

F. Scholze
Plasmasimulation für Triebwerke mittels PIC-Methode
ZARM Seminar, Bremen, Germany, 16.02.2011

F. Scholze, H. Neumann
Modellierung eines Radio-Frequenz Plasmabrückenneutralisators
DPG Frühjahrstagung, Kiel, Germany, 28.-31.03.2011

F. Scholze, D. Manova, H. Neumann
Veränderung der tribologischen Eigenschaften von Edelstahl durch Niederenergieionenstrahlbearbeitung
Workshop Oberflächentechnologie mit Plasma- und Ionenstrahlprozessen, Mühlleithen, Germany, 08.-10.03.2011

A. Schulze, A. Boulares-Pender, M. Went, I. Thomas, B. Marquardt, A. Prager
Membrane Hydrophilization Using Electron Beam and Plasma Techniques
International Congress on Membranes and Membrane Processes (ICOM 2011), Amsterdam, Netherlands, 23.-29.07.2011

A. Schulze, A. Boulares-Pender, S. Starke, B. Marquardt, M. Went, I. Thomas, A. Prager
Plasma and Electron Beam-Based Modification of Polymer Membranes
Seminarvortrag, Institut für Polymerforschung, Helmholtz-Zentrum Geesthacht, Germany, 09.12.2011

A. Schulze, A. Boulares-Pender, M. Went, I. Thomas, B. Marquardt, A. Prager
Plasma- und Elektronenstrahlbehandlung zur permanenten Hydrophilierung von Polymermembranen
7. Thüringer Grenz- und Oberflächentage, Zeulenroda, Germany, 13.-15.09.2011

A. Schulze, B. Marquardt, S. Kaczmarek, R. Schubert, A. Prager, M. R. Buchmeiser
Electron Beam-Based Functionalization of Polymer Membranes
6th Conference of the Aseanian Membrane Society in Conjunction with the 7th International Membrane Science and Technology Conference, Sydney, Australia, 22.-26.11.2010

A. Schulze, B. Marquardt, S. Kaczmarek, R. Schubert, A. Prager, M. R. Buchmeiser
Electron Beam-Based Functionalization of Polymer Membranes
13th Aachener Membrankolloquium, Aachen, Germany, 27.-28.10.2010

A. Schulze, B. Marquardt, S. Kaczmarek, R. Schubert, A. Prager, M.R. Buchmeiser
Electron Beam-Based Modification of Polymer Membranes
13th Aachener Membrankolloquium, Aachen, Germany, 27.-28.10.2010

F. Szillat, S.G. Mayr
Structure formation during deposition of organic films on inorganic substrates - experiments vs. modeling
DPG Frühjahrstagung, Dresden, Germany, 14.-18.03.2011

F. Szillat, S.G. Mayr
Self-Organized Pattern Formation at the Organic-Metal Interface during Deposition — Experiment vs. Modeling
MRS Fall Meeting, Boston, MA, USA, 28.11.-0.12.2011

A. Wehrmann, H. Schulte-Huxel, M. Ehrhardt, K. Zimmer, A. Braun, S. Ragnow
Change of electrical properties of CIGS thin-film solar cells after structuring with ultrashort laser pulses
Photonic West, San Francisco, CA, USA, 22.-27.01.2011

K. Zimmer, M. Ehrhardt, R. Böhme, P. Lorenz
Precise processing of transparent dielectrics by pulsed laser radiation
2nd European Optical Society Conference on Manufacturing of Optical Components, München, Germany, 23.-25.05.2011

K. Zimmer, M. Ehrhardt, A. Wehrmann, C. Scheit
Joining of thin metal films on flexible substrates by pulsed laser irradiation
3rd International Symposium on Laser-Micromachining, Chemnitz, Germany, 27.-28.10.2010

Posters

D. Abou-Ras, T. Rissom, B. Marsen, F. Frost, H. Schulz, F. Bauer, V. Efimova, V. Hofmann, A. Eicke
Cu agglomerate formation upon ion bombardment on Cu(In,Ga)(S,Se)$_2$ thin films for solar cells
Microscopy Conference 2011, Kiel, Germany, 28.08.-02.09.2011

D. Abou-Ras, T. Rissom, B. Marsen, F. Frost, H. Schulz, F. Bauer
Enhanced cross-section preparation for imaging and analysis of Cu(In,Ga)(S,Se)$_2$ thin-film solar cells
EMRS Spring Meeting, Strasbourg, France, 07.-11.06.2010

I. Assenova, K. Kirilov, D. Manova, S. Mändl, E. Valcheva
Annealing Behaviour of Photoactive TiO_2 Thin Films Deposited by PBIID at Room Temperature
11th Int. Workshop on Plasma Based Ion Implantation & Deposition, Harbin, China, 08.-12.09.2011

J. Bauer, M. Weise, Ch. Grüner, Ch. Khare, B. Rauschenbach
Customized arrangements of a-Ge nanocolumns by glancing angle deposition
DPG Frühjahrstagung, Dresden, Germany 13.-18.03.2011

J. Bauer, Ch. Khare, M. Weise, D. Hirsch, Ch. Patzig, B. Rauschenbach
Glancing angle deposition and annealing of a-Si and a-Ge nanostructures
DPG Frühjahrstagung, Regensburg, Germany 21.-26.03.2010

J. Bauer, Ch. Patzig, Ch. Khare, M. Weise, B. Rauschenbach
Glancing angle deposition of Si and Ge nanostructures for thermoelectrics
451. WE-Heraeus-Seminar - Nanostructured Thermoelectric Materials, Bad Honnef, Germany, 21.-24.02.2010

A. Boulares-Pender, I. Thomas, A. Schulze
Surface Modification of Polyamide and Polyvinylidene Fluoride Membranes
6th IWA Specialist Conference on Membrane Technology for Water & Wastewater Treatment, Aachen, Germany, 04.-07.10.2011

A. Boulares-Pender, I. Thomas, A. Schulze
Surface Modification of Polyamide and Polyvinylidene Fluoride Membranes
International Congress on Membranes and Membrane Processes, Amsterdam, Netherlands, 24.-29.07. 2011

A. Colak, H. Wormeester, F. Frost, H. J.W. Zandvliet, B. Poelsema
Surface adhesion modification by nanopatterning of Si(001)
Workshop on Nanoscale Pattern Formation at Surfaces, El Escorial, Madrid, Spain, 18.09.-22.09.2011

J. Dadda, E. Müller, S.Perlt, T. Höche, P. Bauer Pereira, R. Hermann, A. Neubrand
NanoKoCh Selbstorganisierende Nanostrukturen in komplexen Chalkogeniden
WING.DE, Berlin, Germany, 04.-06.10.2011

J. Dadda, E. Müller, S. Perlt, T. Höche
Thermoelectric and Microstructural Characterization of Segregated $AgPb_{18}SbTe_{20}$ (LAST-18) Compound
Thermoelectric Winter School, Bremen, Germany,15.-19.02.2010

M. L. Drob, F. Weichelt, B. Frerich, S. Lenz, M. R. Buchmeiser
Nanoparticles Reinforced Monolithic Materials based on Modified ²-cyclodextrin for Tissue Engineering Applications
Hierarchically Structured Polymers (EUPOC), Gargano, Italy, 30.05.-04.06.2010

M. Ehrhardt, K. Zimmer, S. Scheit
Characterization of the electrical and optical properties of backside opened thin metal films
International Conference Fundamentals of Laser Assisted Micro– & Nanotechnologies, St. Petersburg-Pushkin, Russia, 05.-08.07.2010

M. Ehrhardt, K. Zimmer, S. Scheit
Electrical properties of thin metal films after laser processing
EMRS Spring Meeting, Strasburg, France, 07.-11.06.2010

M. Ehrhardt, U. Löschner, P. Lorenz, A. Wehrmann, K. Zimmer
Joining of thin metal films with pulsed nanosecond laser radiation
EMRS Spring Meeting, Nice, France, 09.-13.05.2011

M. Ehrhardt, P. Lorenz, Ch. Scheit, A. Wehrmann, K. Zimmer, L. Gerlach
Low-damage micro-interconnection with nanosecond laser pulses for high-efficient GaAs solar cells
11th International Conference on Laser Ablation, Playa del Carmen, Mexico, 13.-19.11.2011

M. Ehrhardt, K. Zimmer
Characterization of the laser-induced absorbance due to etching with LESAL
DPG Frühjahrstagung, Dresden, Germany, 13.-18.03.2011

M. Engler, S. Macko, F. Frost, T. Michely
Fluence dependence of ion beam induced pattern morphology on Si(001)
Workshop on Nanoscale Pattern Formation at Surfaces, El Escorial, Madrid, Spain, 18.09.-22.09.2011

L. Escalada, E. Dalibon, S. Simison, S. Brühl D. Manova, H. Neumann, S. Mändl
Influence of Processing Conditions on Corrosion Results of Nitrided Stainless Steel AISI 316L
17th Int. Conf. on Surface Modification of Materials By Ion Beams, Harbin, China, 13.-17.09.2011

L. Escalada, J. Lutz, S. Mändl, S. Simison, D. Manova, H. Neumann
Corrosion Properties of Stainless Steel 316L after Energetic Nitrogen Insertion
EMRS Spring Meeting, Nice, France, 09.-13.05.2011

S. Fichtner, S.G. Mayr
Molecular dynamics studies on amorphous CuTi nanoparticles
DPG Frühjahrstagung, Dresden, Germany, 14.-18.03.2011

K. Fischer, S.G. Mayr
In-plane mechanical response of TiO_2 nanotube arrays-intrinsic properties and impact of adsorbates for sensor applications
MRS Fall Meeting, Boston, MA, USA, 28.11.-02.12.2011

K. Franke, H. Hildebrand, R. Mehnert, E. Mai, A. Freyer, E. Bilz, C. Isaacson, K. Schirmer, A. Ammann, L. Sigg
NanoTrack _ Untersuchung des Lebenszyklus von Nanopartikeln anhand von $[^{44}Ti]TiO_2$ und $[^{110m}Ag]Ag^0$
Wing.de 2011, Berlin, Germany, 04.-06.10.2011

A. Freyer, E. Bilz, A. Prager
Verfolgung des Abbaus von TiO_2-haltigen Nanokompositen _ NanoTRACK
1. Clustertreffen NanoCare/NanoNature, Frankfurt a.M., Germany, 10.-11.5.2011

J.W. Gerlach, M. Mäder, T. Höche, D. Hirsch, B. Rauschenbach
Local elemental and surface chemistry analysis of laser-nanostructured thin Au films
DPG Frühjahrstagung, Dresden, Germany, 14.-18.03.2011

J.W. Gerlach, M. Mäder, T. Höche, D. Hirsch, B. Rauschenbach
Local elemental and surface chemistry analysis of laser-nanostructured ultrathin gold films
European Conference on Applications of Surface and Interface Analysis, Cardiff, UK, 04.-09.09.2011

J.W. Gerlach, W. Assmann, B. Rauschenbach
Complementary ion beam analysis and photoelectron spectroscopy study of oxygen contamination in epitaxial GdN films on YSZ substrates
DPG Frühjahrstagung, Regensburg, Germany, 21.-26.03.2010

A. Gjevori, D. Hirsch, J.W. Gerlach, D. Manova, S. Mändl
Influence of Auxiliary Plasma Source on Properties of Photoactive TiO_2 Films by MePIII&D
Frühjahrstagung der Deutschen Physikalischen Gesellschaft, Regensburg, Germany, 21.-26.03.2010

A. Gjevori, D. Hirsch, J.W. Gerlach, D. Manova, S. Mändl
Influence of Auxiliary Plasma Source on Properties of Photoactive TiO_2 Films by MePIII&D
Vth International Meeting of the Institute Alb-Science, Tirana, Albania, 30.08.-02.09.2010

A. Gjevori, J.W. Gerlach, D. Manova, W. Assmann, E. Valcheva, S. Mändl
Influence of Auxiliary Plasma Source and Ion Bombardment on Stoichiometry of TiO_2 Thin Films
12th Int. Conf. on Plasma Surface Engineering, Garmisch-Partenkirchen, Germany, 13.-17.09.2010

Ch. Grüner, J. Bauer, Ch. Khare, B. Rauschenbach
Hydrogenated a-Si and a-Ge nanostructures
DPG Frühjahrstagung, Dresden, Germany, 13.-18.03.2011

F. Guzmán, H.M. Ruiz, M. Favre, S. Hevia, M. Flores, H. Bhuyan, B. Bora, H.Chuaqui, E. Wyndham, S. Mändl, D. Manova
Pulsed laser deposition of thin carbon films in argon background
11th International Conference on Laser Ablation, Playa del Carmen, Mexico, 13.-19.11.2011

F. Guzman, D. Manova, S. Mändl, H. Bhuyan, M. Walczak, M. Favre
Plasma Immersion Ion Implantation of Nitrogen into Steel 460LI-21Cr
EMRS Spring Meeting, Nice, France, 09.-13.05.2011

M. Hennes, T. Höche, S.G. Mayr
Synthesis of Magnetic Nanoparticles via Inert Gas Condensation (IGC)
World Conference on Regenerative Medicine, Leipzig, Germany, 02.-04.11.2011

A. Henriquez, D. Hirsch, D. Manova, H. Bhuyan, W. Assmann, S. Mändl, M. Favre
Formation of Nanostructured Surfaces by Plasma Focusing Device
17th Int. Conf. on Surface Modification of Materials By Ion Beams, Harbin, China, 13.-17.09.2011

A. Henriquez, H. Bhuyan, M. Favre, B. Bora, E. Wyndham, H. Chuaqui, S. Mändl, J.W. Gerlach, D. Manova
Nitriding of Ti substrate using energetic ions from plasma focus device
XIV Latin American Workshop on Plasma Physics, Mar del Plata, Argentina, 20.-25.11.2011

A. Henriquez, D. Manova, H. Bhuyan, S. Mändl, M. Favre
Investigation of Thin Film Deposition by Plasma Focusing Device
XXX Int. Conf. on Phenomena in Ionized Gases, Belfast, UK, 28.08.-02.09.2011

K. Heymann, G. Mirschel, L. Prager, T. Scherzer
In-line Determination of the Thickness of Thin Polysilazane-Based SiO_x Layers by NIR Reflection Spectroscopy
18th European Symposium on Polymer Spectroscopy, Zadar, Croatia, 19.-22.9.2010

H. Hilmer, C. Sturm, R. Schmidt-Grund, J. Zuniga-Perez, H. Hochmuth, M. Cornejo, F. Frost, M. Grundmann
Fabrication of ZnO cavities for planar microresonators
DPG Frühjahrstagung, Regensburg, Germany, 21.-26.03.2010

H. Hilmer, C. Sturm, R. Schmidt-Grund, J. Zúñiga-Pérez, M. Lange, A. Meißner, J. Lenzner, G. Zimmermann, M. Cornejo, R. Fechner, F. Frost, H. Hochmuth, M. Lorenz and M. Grundmann
PLD growth of ZnO-based planar and cylindrical microresonators
11th International Conference on Physics of Light-Matter Coupling in Nanostructures, Berlin, Germany,04.-08.04.2011

H. Hilmer, T. Michalsky, C. Sturm, R. Schmidt-Grund, J. Zuninga-Perez, R. Fechner, F. Frost, M. Grundmann
Combinatorial growth of ZnO resonators
DPG Frühjahrstagung, Dresden, Germany, 14.-18.03.2011

H. Hilmer, C. Sturm, R. Schmidt-Grund, M. Cornejo, R. Fechner, F. Frost, M. Grundmann
Towards BEC in ZnO-based microresonators
4th Scientific Symposium of the Graduate School BuildMoNa, Leipzig, Germany, 21.03.2011

D. Hirsch, M. Cornejo, B. Ziberi, C. Meinecke, J.W. Gerlach, and F. Frost
ToF-SIMS depth profiling of low energy implanted metals in silicon
SIMS Europe 2010, Münster, Germany, 19.-21.09.2010

M. Janietz, T. Arnold
Surface figuring of glass substrates by local deposition of silicon oxide with atmospheric pressure plasma jet
12th International Conference on Plasma Surface Engineering, Garmisch-Partenkirchen, Germany, 13.-17.09.2010

A.M. Jakob, S.G. Mayr
Nanoscale mechanical characterization of surfaces
DGP Frühjahrestagung 2011, Dresden, Germany, 13. -18.03.2011

A.M. Jakob, S.G. Mayr
Nanoscale mechanical characterization of surfaces
MRS Fall Meeting, Boston, MA, USA, 28.11.-02.12.2011

B. Khanbabaee, B. Arezki, A. Biermanns, M. Cornejo, F. Frost, U. Pietsch
X-ray investigation of the depth profile of ion beam induced nanopatterned Si surface after co-sputtering of Kr^+ and metal ions
Workshop on Nanoscale Pattern Formation at Surfaces, El Escorial, Madrid, Spain, 18.-22.09.2011

B. Khanbabaee, B. Arezki, A. Biermanns, M. Cornejo, F. Frost, U. Pietsch
Investigation of the depth profile of ion beam induced nanopattern on Si with simultaneous metal incorporation
DPG Frühjahrstagung, Dresden, Germany, 14.-18.03.2011

C. Khare, J. Bauer, M. Weise, C. Patzig, J.W. Gerlach, B. Rauschenbach, H.S. Leipner, B. Fuhrmann
Nano-sculptured thin film growth using glancing angle deposition
Third Scientific Symposium of the Graduate School BuildMoNa, Leipzig, Germany, 29.-30.03.2010

C. Khare, C. Patzig, J.W. Gerlach, B. Fuhrmann, H.S. Leipner, B. Rauschenbach
Growth of crystalline Ag nanorods by ion beam sputter glancing angle deposition
DPG Frühjahrstagung, Regensburg, Germany, 21.-26.03.2010

W. Knolle, S. Naumov, L. Prager, T. Scherzer, H. Oppermann, K. Czihal
Photochemistry of (Meth)Acrylates Following 172 - 222 nm Excitation
5th European Young Investigator Conference, Frankfurt/Oder, Germany and Slubice, Poland, 22.-26.06.2011

J. Kreith, J. Keckes, A. Ulyanenkov, L. Bruegemann, F. Frost, L. Chitu, P. Siffalovic, E. Majkova, G. A. Maier
Current Applications in Laboratory GISAXS
10th Biennial Conference on High Resolution X-Ray Diffraction and Imaging
University of Warwick, UK, 20.-23.09.2010

J. Lorbeer, J. Völlner, M. Teichmann, M. Cornejo, F. Frost, B. Rauschenbach
Faceting and coarsening of ion induced ripple pattern on fused silica surfaces
Workshop on Nanoscale Pattern Formation at Surfaces, El Escorial, Madrid, Spain, 18.-22.09.2011

P. Lorenz, M. Ehrhardt, A. Wehrmann, K. Zimmer
Laser-induced front side etching of fused silica with XeF excimer laser using thin metal layers
EMRS Spring Meeting, Nice, France, 09.-13.05.2011

P. Lorenz, M. Ehrhardt, A. Wehrmann, K. Zimmer
Laser-induced front side and back side etching of fused silica with KrF and XeF excimer lasers using metallic absorber layers: A comparison
2nd EOS Conference on Manufacturing of Optical Components, München, Germany,23.-25.05.2011

P. Lorenz, M. Ehrhardt, A. Wehrmann, K. Zimmer
Laser-induced front side etching of commercial glasses with KrF- and XeF excimer lasers
11th International Conference on Laser Ablation, Playa del Carmen, Mexico, 13.-19.11.2011

P. Lorenz, K. Zimmer
Laser-induced front side etching of fused silica with KrF excimer laser using thin metal layers
DPG Frühjahrstagung, Dresden, Germany, 13.-18.03.2011

J. Lutz, S. Mändl
Wear Rates of CoCr Alloys Crucially Depend on Counter Body in Ball-on-Disc Tests
12th Int. Conf. on Plasma Surface Engineering, Garmisch-Partenkirchen, Germany, 13.-17.09.2010

J. Lutz, J.W. Gerlach, S. Mändl
XPS Analysis of Phase Formation after Nitrogen Insertion in CoCr and FeCrNi Alloys
DPG Frühjahrstagung, Regensburg, Germany, 21.-26.03.2010

J. Lutz, J.W. Gerlach, S. Mändl
XPS Analysis of Phase Formation after Nitrogen Insertion in CoCr and FeCrNi Alloys
3rd Scientific Symposium of BuildMoNa, Leipzig, Germany, 29.-30.03.2010

Y. Ma, M. Zink, S.G. Mayr
Biocompatibility of Fe-Pd magentic shape memory alloys
DPG Frühjahrstagung, Regensburg, Germany, 21.-26.03.2010

Y. Ma, A. Setzer, A. Arabi-Hashemi, P. Esquinazi, S.G. Mayr
Martensitic transformation and magnetic properties of freestanding single crystalline $Fe_{70}Pd_{30}$ thin films
10th Research Festival for Life Sciences, Leipzig, Germany, 16.12.2011

Y. Ma, A. Setzer, A. Arabi-Hashemi, P. Esquinazi, S.G. Mayr
Martensitic transformation and magnetic properties of freestanding single crystalline $Fe_{70}Pd_{30}$ thin films
World Conference on Regenerative Medicine, Leipzig, Germany, 02.-04.11.2011

Y. Ma, A. Setzer, P. Esquinazi, S.G. Mayr
Martensitic transformation and magnetic properties of freestanding single crystalline $Fe_{70}Pd_{30}$ thin films
4th Scientific Symposium of the Graduate School BuildMoNa, Dresden, Germany, 21.03.2011

S. Macko, F. Frost, M. Engler, T. Michely
Ion beam pattern formation on Si(001) by addition of Fe impurities: mechanism and processes
17th International Conference on Ion Beam Modification of Materials, Montrèal, Canada, 22.-27.08.2010

D. Manova, F. Scholze, S. Mändl, H. Neumann
Development of Pulsed Low Energy Ion Implantation for Nitriding of Austenitic Stainless Steel
12th Int. Conf. on Plasma Surface Engineering, Garmisch-Partenkirchen, Germany, 13.-17.09.2010

D. Manova, J. Lutz, J.W. Gerlach, H. Neumann, S. Mändl
No Direct Correlation between Lattice Expansion and Nitrogen Content in Expanded Phase after Nitrogen Insertion in Austenitic Stainless Steel and CoCr Alloys
12th Int. Conf. on Plasma Surface Engineering, Garmisch-Partenkirchen, Germany, 13.-17.09.2010

D. Manova, J.W. Gerlach, S. Mändl, H. Neumann
Correlation between Ion Bombardment, Lattice Expansion and Nitrogen Content After Nitriding of Austenitic Stainless Steel
Frühjahrstagung der Deutschen Physikalischen Gesellschaft, Regensburg, Germany, 21.-26.03.2010

D. Manova, A. Bergman, S. Mändl, H. Neumann, B. Rauschenbach
In-situ X-ray Diffraction during Low Energy Nitriding of Austenitic Stainless Steel
EMRS Spring Meeting, Nice, France, 09.-13.05.2011

D. Manova, I. Assenova, K. Kirilov, J.W. Gerlach, W. Assmann, E. Valcheva, S. Mändl
Correlation between Deposition Rate and Photoactivity of TiO_2 Thin Films
EMRS Spring Meeting, Nice, France, 09.-13.05.2011

D. Manova, S. Mändl
Influence of Surface Roughening on Depth Profiling of Nitrided Stainless Steel
11th Int. Workshop on Plasma Based Ion Implantation & Deposition, Harbin, China, 08.08.-12.09.2011

J. Meister, T. Arnold
Neue Prozedur zur Prozesssimulation bei der Plasmajetbearbeitung
DPG Frühjahrstagung, Kiel, Germany, 28.-31.03.2011

A. Mießler, T. Arnold
Surface characterization after subaperture Reactive Ion Beam Etching
12th International Conference on Plasma Surface Engineering, Garmisch-Partenkirchen, Germany, 13.-17.09.2010

G. Mirschel, K. Heymann, T. Scherzer
Simultaneous Monitoring of Conversion and Coating Thickness during UV Curing of Acrylate Coatings by In-line NIR Spectroscopy
18th European Symposium on Polymer Spectroscopy, Zadar, Croatia, 19.-22.9.2010

G. Mirschel, K. Heymann, O. Savchuk, T. Scherzer
Monitoring of Photopolymerization Reactions by Near-Infrared Spectroscopy
European Symposium of Photopolymer Science, Mulhouse, France, 28.11.-1.12.2010

M. Müller, S.G. Mayr
Epitaxy, lift-off and surface treatment of NiMnGa magnetic shape memory alloy films
DPG Frühjahrstagung, Dresden, 13.-18.03.2011

S. Naumov, W. Knolle
On the mechanism of the Transformations of the Radiolytically Generated Cyclic Cation Radicals in Inert Matrix
10th International Symposium on Functional pi-Electron Systems (F-pi-10), Beijing, China, 13.-17.10 2011

S. Naumov, M. Bonifa, T. Tobien, R. S. Glass and K.-D. Asmus
Sulfur vs. Selenium. Theoretical calculations and experimental data on S- and Se-centered radicals
XIIth EUCHEM Conference on Free Radicals, Bologna, Italy, 28.06.-02.07.2010

L. Neumann, J.W. Gerlach, M. Abd El Khair, B. Rauschenbach
SPM characterization of GaN formed by ion-beam assisted epitaxy
DPG Frühjahrstagung, Regensburg, Germany, 21.-26.03.2010

S. Perlt, T. Höche, J. Dadda, E. Müller
Complex Chalcogenides for Thermoelectrics: Microstructure-Property Relationship
DPG Frühjahrstagung 2010, Regensburg, Germany, 22.-26.03.2010

S. Perlt, T. Höche, J. Dadda, and E. Müller
Complex Chalcogenides for Thermoelectrics: Microstructure Analysis of $AgPb_{18}SbTe_{20}$
17th International Microscopy Congress, Rio de Janeiro, Brazil, 19.-24.09.2010

S. Perlt, T. Höche, J. Dadda, E. Müller
Complex Chalcogenides for Thermoelectrics: Microstructure Analysis of $AgPb_{18}SbTe_{20}$
Frühjahrsschule Thermoelektrik, Köln, Germany, 28.03.-01.04.2011

S. Reichelt, C. Elsner, W. Knolle, A. Prager, K. Umnus, J. Kuballa, M. Buchmeiser
Preparation of electron beam derived polymeric monoliths and their application for affinity separation
1st International Symposium on POLYmer modification With High Energy ELectrons, Dresden, Germany, 24.-26.11.2010

S. Reichelt, C. Elsner
Electron-beam Induced Fabrication and Functionalization of Porous Monolithic Polymers
Biomaterialkolloquium Zeulenroda, Zeulenroda, Germany, 15.09.2011

S. Reichelt, C. Elsner, K. Umnus, J. Kuballa, M. Buchmeiser
Electronbeam-initiated synthesis and functionalization of polymeric monoliths and their application in affinity chromatography
Jahrestagung der Deutschen Gesellschaft für Biomaterialien, Gießen, Germany, 10.-12.11.2011

L. Prager, L. Wennrich, W. Knolle, R. Heller, A. Prager, U. Decker
Creation of organic-inorganic multilayer systems: aspects of photochemical-based fabrication of gas barriers
Thermosets 2011 From Monomers to Components, Berlin, Germany, 21.-23.09.2011

O. Savchuk, K. Fahmy
Polymorphism of bio-polymers studied by CD spectroscopy
18th European Symposium on Polymer Spectroscopy, Zadar, Croatia, 19.-22.9.2010

T. Scherzer
Kinetic Investigations on the VUV-Induced Photopolymerization of Acrylates by Real-Time FTIR/ATR-Spectroscopy
18th European Symposium on Polymer Spectroscopy, Zadar, Croatia, 19.-22.9.2010

T. Scherzer, G. Mirschel, K. Heymann, O. Savchuk
In-line Monitoring von Umsatz und Schichtdicke
European Coatings Congress, Nürnberg, Germany, 29.-31.3.2011

C. Schmidt, O. Savchuk, I. Reinhardt, T. Scherzer
Photorheometry - An Easy Method for the Determination of Shrinkage in Dependence on Conversion
RadTech Europe 2011, Basel, Switzerland, 18.-20.10.2011

T. Scherzer
Kinetic Investigations on the VUV-Induced Photopolymerization of Acrylates by Real-Time FTIR/ATR-Spectroscopy
18th European Symposium on Polymer Spectroscopy, Zadar, Croatia, 19.-22.9.2010

H. Schneider, K. Schröck, J. Lutz, S. Mändl, M. Schulz-Siegmund, M. Kamprad
Biocompatibility testing of a wear-resistant Cobalt Chromium alloy
International Bone-Tissue-Engineering Congress, Hannover, Germany, 07.-10.10.2010

H. Schneider, K. Schröck, J. Lutz, S. Mändl, M. Schulz-Siegmund, M. Kamprad
Biocompatibility testing of a wear-resistant Cobalt Chromium alloy
23nd European Conference on Biomaterials, Tampere, Finland, 11.-15.09.2010

M. W. Schröder, O. Savchuk, T. Scherzer
Kinetic Investigations on the Photopolymerization of Acrylates by Simultaneous Photorheometry and Near-Infrared Spectroscopy
European Symposium of Photopolymer Science, Mulhouse, France, 28.11.-1.12.2010

M.W. Schröder, T. Scherzer
Investigation of Photopolymerization Reactions by Simultaneous Near-Infrared Spectroscopy and Dynamic Mechanical Analysis
18th European Symposium on Polymer Spectroscopy, Zadar, Croatia, 19.-22.9.2010

A. Schulze, M. Went, B. Marquardt
Electron Beam-Based Functionalization of Polymer Membranes with Small Molecules
6th IWA Specialist Conference on Membrane Technology for Water & Wastewater Treatment, Aachen, Germany, 04.-07.10.2011

F. Szillat, S.G. Mayr
Structure formation at inorganic/organic interaces
DPG Frühjahrstagung, Regensburg, Germany, 21.-26.03.2010

M. Teichmann, M. Cornejo, J. Lorbeer, J. Völlner, F. Frost, B. Rauschenbach
Pattern formation on Si by ion sputtering at high incidence angles
Workshop on Nanoscale Pattern Formation at Surfaces, El Escorial, Madrid, Spain, 18.09.-22.09.2011

A. Ulyanenkov, J. Chrost, P. Siffalovic, L. Chitu, E. Majkova, K. Erlacher, G. Maier, M. Cornejo, B. Ziberi, F. Frost
GISAXS and AFM Study of self-assembled FeO and Si Nanoparticles
10th Biennial Conference on High Resolution X-Ray Diffraction and Imaging, University of Warwick, UK, 20.-23.09.2010

A. Wehrmann, S. Puttnis, M. Ehrhardt, P. Lorenz, K. Zimmer
Optical and electrical investigations of laser-scribed flexible thin-film Cu(In,Ga)Se_2 solar cells by localized measurements
11th International Conference on Laser Ablation, Playa del Carmen, Mexico, 13.-19.11.2011

A. Wehrmann, S. Puttnins, L. Hartmann, M. Ehrhardt, P. Lorenz, K. Zimmer
Electrical and optical analysis of laser scribed CIGS thin-film solar cells by localized measurements
EMRS Spring Meeting, Nice, France, 09.-13.05.2011

A. Wehrmann, S. Puttnins, M. Ehrhardt, P. Lorenz, K. Zimmer
Optical and electrical investigations of laser-scribed flexible thin-film CIGS solar cells by localized measurements
11th International Conference on Laser Ablation, Playa del Carmen, Mexico, 13.-19.11.2011

F. Weichelt, M. L. Drob, B. Frerich, S. Lenz, M. R. Buchmeiser
Nanoparticle-Reinforced Monolithic Materials for Applications in Tissue Engineering
44. DGBMT Jahrestagung, Rostock, Germany, 06.-08.10.2010

F. Weichelt, M. L. Drob, B. Frerich, S. Lenz, M. R. Buchmeiser
Ring-Opening Metathesis Polymerization-Based Synthesis of Hydroxyapatite and $CaCO_3$ Nanoparticle-Reinforced Polymeric Monoliths for Tissue Engineering
Biannual Meeting of the GDCh-Division of Macromolecular Chemistry and Polydays 2010, Berlin-Dahlem, Germany, 03.-06.10.2010

M. Weise, Ch. Khare, B. Fuhrmann, J. Bauer, B. Rauschenbach
Definierte Variation der Nanostruktur in Ge-Schichten mittels Glanzwinkelabscheidung
DPG Frühjahrstagung, Regensburg, Germany, 21.-26.03.2010

J. Zajadacz, R.Fechner, K. Zimmer, C. Dhima, H.-C. Scheer
Fabrication of optimized 3D microstructures with undercuts in transparent fused silica for replication
37. International Conference of Micro and Nano Engineeering, Berlin, Germany, 19.-23.09.2011

J. Zajadacz, K. Zimmer, R. Fechner, A. Mayer, H.-C. Scheer
Sub-wavelength gratings for infrared optical filters and there fabrication by nano imprint lithography and reactive ion beam etching
37. International Conference of Micro and Nano Engineering, Berlin, Germany, 19.-23.09.2011

B. Ziberi, F. Frost, K. Zimmer, B. Rauschenbach
Multiscale nanostructuring of Si surfaces combining topdown and bottom-up techniques
DPG Frühjahrstagung der Sektion Kondensierte Materie, Regensburg, Germany, 21.-26.03.2010

M. Zink, U. Allenstein, A. Arabi-Hashemi, Y. Ma, S.G. Mayr
Biocompatibility of ferromagnetic shape memory alloys for cell actuation
2011 MRS Fall Meeting, Boston, MA, USA, 28.11.-02.12.2011

M. Zink, Y. Ma, S.G. Mayr
Biocompatibility of single crystalline $Fe_{70}Pd_{30}$ ferromagnetic shape memory films for cell actuation
DPG Frühjahrstagung, Dresden, Germany,
13.-18.03.2011

M. Zink, U. Allenstein, A. Arabi-Hashemi, Y. Ma, S.G. Mayr
Biocompatibility of ferromagnetic shape memory alloys for single cell actuation
Biophysical Society 55th Annual Meeting, Baltimore, MD, USA, 05.-09.03.2011

Patents

Y. Bohne, C. Elsner, B. Rauschenbach, C. Jahn
Verfahren zur Herstellung einer rotativen Druckform zum Einsatz in einem Rollenrotationsdruckverfahren
Patent granted Germany DE10 2008 035 203.9

R. Schubert, M. Hinkefuß, J. Vogel
Vorrichtung zur Ermittlung der Faltungskinetik und der Faltungsgeschwindigkeit strahlenhärtbarer Farben und Lacke während des Prozesses der photochemischen Mikrofaltung initiiert durch kurzwellige monochromatische Excimer-UV-Strahlung
Patent granted Germany DE 10 2008 024 149.0

T. Hänsel, P. Seidel, A. Schindler, A. Nickel, H.-J. Thomas, I. Bucsi
Verfahren zur Modifikation der Oberfläche einer Probe mittels eines gepulsten Ionenstrahls oder mittels eines ionenstrahlgenerierten Teilchenstrahls mit homogen oder gaußförmig verteilter Stromdichte
Patent granted Germany DE 10 2005 017 632.1